High-resolution spatial and temporal sensitivity of river hydrodynamics: Implications for walleye (*Sander vitreus*) and lake sturgeon (*Acipenser fulvescens*) spawning habitat use in a large regulated river

by

Jeffrey William Muirhead

A thesis
presented to the University of Waterloo
in fulfillment of the
thesis requirement for the degree of
Master of Applied Science
in
Civil Engineering

Waterloo, Ontario, Canada, 2014

Author's Declaration

This thesis consists of material all of which I authored or co-authored: see Statement of Contributions included in the thesis. This is a true copy of the thesis, including any required final revisions, as accepted by my examiners.

I understand that my thesis may be made electronically available to the public.

Statement of Contributions

Chapter 4.0, entitled "The role of spatial habitat heterogeneity in walleye (*Sander vitreus*) and lake sturgeon (*Acipenser fulvescens*) critical spawning habitat in a large, northwestern Ontario river" within this thesis was prepared in collaboration with Adrienne Smith and under the supervision of Dr. Michael Power in the Department of Biology, University of Waterloo. The insights and guidance of both Adrienne and Dr. Power were fundamental to collecting, processing, and analyzing the results presented in Chapter 4. I certify, with the above qualification, that this thesis, and the research to which it refers, is the product of my own work.

Abstract

A reach-scale, high-resolution investigation of the spatial and temporal characteristics and sensitivities of hydrodynamic metrics on a large, low-relief, hydroelectrically regulated river in northwestern Ontario was performed. Velocity profile transects using an acoustic Doppler current profiler (ADCP) and the moving-vessel method were obtained at 7 – 10 discrete discharge levels at 47 cross-section locations over a 21 km reach, for 427 transects in total. Eighty-three (83) commonly computed hydrodynamic metric expressions of 23 hydraulic parameters were computed for each transect, addressing channel geometry, velocity, and flow complexity.

Spearman correlations identified inter-dependencies between metric values, eliminating 61 parameters and resulting in a subset of 22 statistically independent and representative metrics. Visual and statistical examination of metric values revealed no consistent trend as a function of International Falls Dam (IFD) discharge. Uniform and featureless cross sections demonstrated low metric normalized variances ($\sigma^2{}_n$) indicating that channel homogeneity will result in aggregate hydraulic condition consistency and insensitivity. A smaller collection of cross sections possessing observable channel complexities producing large-scale turbulent structures displayed higher $\sigma^2{}_n$. Therefore, areas susceptible to macro-scale turbulence due to large roughness elements and complex morphology are likely to produce a broad range of hydraulic conditions under single-transect ADCP surveys.

Results of the hydrodynamic characterization were subsequently cross-examined with coupled walleye (*Sander vitreus*) and lake sturgeon (*Acipenser fulvescens*) spawning survey findings to investigate the role of spatial and temporal habitat heterogeneity in spawning site selection. Cross sections were categorized according to spawning utilization (high, moderate, low). Statistical analysis identified a higher fraction of spatial heterogeneity metrics within those demonstrating significant differences between spawning and non-significant spawning locations. The observed preference for habitat diversity in spawning site selection corresponds to locations possessing large roughness elements and macroturbulence. The identified eco-hydraulic linkages will be applied to optimize spawning habitat for walleye and lake sturgeon on the Rainy River.

Acknowledgements

I would like to thank my supervisor Dr. William Annable for his guidance, support, and mentorship in academic and personal pursuits over the past three years. Bill has provided the resources and opportunities for me to learn and succeed while also proving to be an inspiring and motivating figure both professionally and personally. The research Dr. Annable has allowed me to pursue could not have been better suited to my academic background and personal interests, and for this opportunity I am extremely grateful.

I would also like to thank Dr. Michael Power and my research partner Adrienne Smith in the University of Waterloo Department of Biology, whose insights were paramount in bridging the gap between the fields of hydraulic engineering and fisheries biology. I would also like to acknowledge the resources, both in equipment and personnel, provided by the Department of Fisheries and Oceans Canada (DFO) and the project manager there, Dr. Karen Smokorowski, for without these the project would not have been possible.

The research presented in this thesis considers data collected over countless hours of field work, for which the assistance of others must be recognized: Terry Ridgway, Adrienne Smith, and Emma Buckrell of the University of Waterloo as well as Bill Gardner and Evan Timusk of the Federal Department of Fisheries and Oceans (DFO). Subsequent post-processing, analysis, and countless revisions of document drafts would not have been completed without the support and advice of my fellow eco-hydraulics group researchers Ben Plumb, Cailey McCutcheon, and Lorenzo Brignoli. Significant thanks is also owed to Clint and Doris Barton, my hosts in Fort Frances, for their gracious hospitality and support during my field seasons.

I also would like to thank the Department of Civil and Environmental Engineering, the Natural Science and Engineering Council of Canada (NSERC) Discoveries Grant, the International Joint Commission (IJC) and the Federal Department of Fisheries and Oceans (DFO), Ontario Federation of Anglers and Hunters and the Oakville Rod and Gun Club for providing the funding and resources required for the completion of this research.

Dedication

I would like to dedicate this work to my grandfather, David Sandrock, who passed away in February of 2008. "Pops" inspired my passion for fishing and taught me to welcome and embrace challenges as opportunities for excellence, eventually leading me to where I am now both professionally and personally.

Table of Contents

List of Tables

List of Figures

List of Abbreviations and Symbols

σ^2	=	variance
σ^2_{max}	=	maximum variance
σ^2_{norm}	=	normalized variance
$\overline{\sigma^2}_{norm,XS}$	=	arithmetic average of cross section normalized variances
α	=	velocity head coefficient [-]
a	=	regression slope coefficient [-]
g	=	gravitational acceleration [LT^{-2}]
κ	=	von Karman's constant (assumed = 0.4) [-]
ρ	=	density of water [ML^{-3}]
μ	=	dynamic viscosity of water [$ML^{-1}T^{-1}$]
γ	=	specific weight of water [$ML^{-2}S^{-2}$]
ADCP	=	acoustic Doppler current profiler
ADV	=	acoustic Doppler velocimeter
$A_{j,k}$	=	cross sectional area for cell *j, k* [L^2]
AR	=	aspect ratio [-]
AWV	=	area weighted vorticity [T^{-1}]
A_{XS}	=	cross sectional area [L^2]
BS	=	boat speed [LT^{-1}]
C	=	cell
CPUE	=	catch per unit effort
D	=	flow depth [L]
D_{84}	=	84^{th} percentile of percent passing (by mass) for grain size distribution [L]
d_{avg}	=	average transect flow depth [L]
DCX	=	longitudinal dispersion coefficient [-]
DCY	=	lateral dispersion coefficient [-]
d_j	=	flow depth of profile *j* [L]
d_{max}	=	maximum transect flow depth [L]
DR	=	depth ratio [-]
ESF	=	elliptical shape factor [-]
EV	=	error velocity [LT^{-1}]
FR	=	Froude number [-]

FST	=	Fliess-Wasser-Stammtisch
h_d	=	hydraulic depth [L]
Het	=	heterogeneous pair
Hom	=	homogeneous pair
Hz	=	hertz [T^{-1}]
IQ	=	interquartile
j	=	transect profile index
k	=	transect cell index
KE	=	kinetic energy [M^2T^{-2}]
LRE	=	large roughness element
r	=	metric subscript
R^2	=	coefficient of determination
R_h	=	hydraulic radius [L]
RSF	=	rectangular shape factor [-]
R_{Sp}	=	Spearman correlation coefficient [-]
P	=	profile
P_w	=	wetted perimeter [L]
Q	=	discharge [L^3T^{-1}]
Q_{IFD}	=	International Falls Dam discharge [L^3T^{-1}]
RE	=	Reynolds number [-]
Δs_k	=	vertical distance between centroids of cells k and $k+1$ [L]
Δs_j	=	horizontal distance between profiles j and $j+1$ [L]
SHH	=	spatial habitat heterogeneity
SNR	=	signal-to-noise ratio [-]
SR	=	seasonal range
SV	=	single value
T	=	transect
u_*	=	shear velocity [LT^{-1}]
V	=	flow velocity [LT^{-1}]
$\bar{V}$	=	average cross sectional velocity [LT^{-1}]
V_{min}	=	minimum of V_{j+1} and V_j [LT^{-1}]
$VG1$	=	velocity gradient 1 [LT^{-2}]
$VG2$	=	velocity gradient 2 [T^{-1}]
W	=	transect top width [L]

WDR	=	width to depth ratio [-]
WS	=	water speed [LT^{-1}]
WSE	=	water surface elevation [L]
XS	=	cross section
z_0	=	independent estimate of bed roughness = $aD_p/30$ (a = 3 for P = 84)

1.0 Introduction

Historically, engineers, biologists, and geomorphologists worked separately in aquatic rehabilitation and ecological management. However, each discipline shared a common goal: to create a stable, self-supporting lotic environment which would function sustainably with respect to flow conveyance, sediment erosion/deposition, and ecological function. Research has highlighted the interrelatedness of biotic and abiotic river components in achieving this goal, emphasizing that hydraulics, aquatic ecology, and geography are not separate aspects of a river system but in fact work together to create a sustainably functioning lotic environment (Gilliam and Fraser, 2001; Peres-Neto, 2004; Roni and Beechie, 2012). Accordingly, efforts have been made to formulate comprehensive river classification and restoration methodologies which would satisfy all components of a thriving lotic system (e.g., Annable, 1995; Rosgen, 1996; Montgomery and Buffington, 1997; Roni and Beechie, 2012). Successes in restoration have resulted, however failures have also occurred, often due to a lack of understanding of how physical hydraulic, or abiotic, river characteristics impact organisms inhabiting the watercourse which has lead to failures (Kauffman et al., 1997). Identification of these eco-hydraulic linkages between discharge-dependent watercourse hydrodynamics and organism behaviour are crucial in the formulation of best management/restoration protocols, and are amplified where discharge regimes are anthropogenically controlled or altered (Poff, 1997; Milan et. al.. 2001; Brandt, 2000; Bowen et. al., 2003; Graf, 2006).

Flow velocities and associated hydraulic characterizations of physical habitat are considered most influential in determining ecological structure and function (Hynes 1970; Statzner et. al. 1988; Jowett and Duncan 1990). Identification of the relationship between ecology and hydraulics first requires a robust set of hydrodynamic metrics which effectively characterize the various elements of four-dimensional spatio-temporal fluid states. Countless theories and parameters have been proposed over the past centuries since the early contributions of Chézy (1775) and DuBoys (1879), with varying degrees of complexity (e.g., Keulegan, 1938; Einstein,1950; Chow, 1959; Graf, 1984; French, 1985; ;Yang, 1996; Jain, 2001; Parker, 2007). These numerical characterizations have been developed by engineers and geomorphologists for applications of sediment and contaminant transport and hydraulic/erosion considerations surrounding human infrastructure (e.g., Keulegan, 1938; Chow, 1959). Technological advances have given rise to more complex quantifications of hydrodynamics (Shields et. al., 2003; Muste et. al., 2004, Shen et. al., 2010), and in recent years have been preliminarily applied in aquatic ecology (Lamouroux et. al., 1999; Crowder and Diplas, 2000a, 2000b, 2002, 2006; Shields and Rigby, 2005). Nevertheless, the extensive and variable potential approaches for hydraulic habitat characterization

presented in literature makes selection of an appropriate set of characterizing hydraulic parameters a difficult task (Milan et. al., 2001).

As noted above, recent work has attempted to link hydrodynamics with ecological function. However, many such efforts consider single point-measurement velocities at a micro-habitat scale corresponding to an organism's instantaneously observed location (e.g., Hayes and Jowett, 1994). These approaches do not recognize proximal velocities and any resulting hydraulic complexities which may encourage organism activities in the near vicinity. These factors often correspond to increased values of biotic community indices such as species richness, diversity, and biomass (Booker et. al. 2004; Rhoads et. al. 2003; Crowder and Diplas 2000a, 2002; Shields et. al. 1998, 1995; Freeman and Grossman 1993; Statzner et. al. 1988). Indeed, studies have demonstrated that it is the macro-scale heterogeneity of micro- and meso-scale physical characteristics which is more important than site-specific values (Lancaster and Hildrew, 1993; Hayes and Jowett, 1994).

Quantification of physical habitat heterogeneity requires measurement of velocities at high cross sectional and planform resolutions, which is inherently problematic in large rivers not amenable to wading. Geomorphic sub-units such as pools, riffles, chutes, glides, bars and other bed forms (Kellerhals et al., 1972; Rosgen, 1996; Buffington, 1998; Montgomery and Buffington, 1997; Brierley and Fryirs, 2000) are not as readily apparent, nor definable, as they are in smaller watercourses (O'Neill and Abrahams, 1984; Lisle, 1987; Madej, 2000; Wooldridge and Hickin, 2002). Logistical challenges of field methods have resulted in the preferential survey of hydraulic data at bridge crossings or cableways not fully representative of the comprehensive suite of habitat niches available to organisms in the river. Practitioners have obtained increased planform resolutions of velocities using one- and two-dimensional hydraulic modelling approaches. However, these approaches induce spatial and temporal averaging which render them inapplicable for heterogenetic habitat investigations.

Recent advancements in acoustic Doppler current profiler (ADCP) technology have offered a relatively efficient method of acquiring high-resolution field discharge data under non-wadable flow conditions at locations throughout a river reach by means of the moving-vessel method (Muste et. al., 2004). Well documented as an effective and efficient technology for discharge measurement (e.g., Gordon 1989; Simpson, 2001; Oberg et. al., 2005; Rennie and Rainville, 2006; Oberg and Mueller, 2007;) the increased sampling speed and cell resolution of moving-vessel ADCP surveys combined with Real-Time Kinematic GPS (RTK-GPS) ADCP system integration affords researchers and practitioners the ability to rapidly obtain spatially accurate detailed velocity and depth characteristics throughout large river systems.

The main objectives of this work are as follows, and pertain to the cross-section scale analysis of a 21 km reach of a large, low-gradient river where discharges are regulated by a hydroelectric generating facility:

i) Determine if and how inter-dependencies and correlations exist within a broad collection of published hydrodynamic metrics which may be applicable for physical habitat characterization,

ii) Determine the discharge-related spatial characteristics of the set of statistically independent, representative hydrodynamic metrics from i), and

iii) Determine if and how walleye (*Sander vitreus*) and lake sturgeon (*Acipenser fulvescens*) spawning habitats are correlated with temporal patterns in terms of central tendency and/or spatial heterogeneity of the hydrodynamic conditions.

1.1 Organization of Thesis

The format of this thesis follows a multi-part structure whereby Chapters 2, 3,and 4 are organized into three distinct topics with respective introductions, methods, results, discussions, and conclusions, also known as manuscript format. Chapter 2 examines the vertical precision and accuracy of geospatial coordinates collected by a nongeorectified real-time kinematic (RTK) GPS acoustic Doppler current profiler (ADCP) system and compares them to those simultaneously acquired using a georectified RTK differential GPS (RTK-DGPS) system. While not a focal objective of this research, Chapter 2 presents useful findings as an ancillary product of the main analysis. Chapter 3 investigates the inter-dependencies and spatio-temporal sensitivities of a wide range of hydrodynamic parameters on a 21 km stretch of a large, low-relief river with flows regulated by a hydroelectric generating facility using high-resolution velocity profiles obtained with an ADCP. Chapter 4 examines whether walleye and lake sturgeon spawning habitats are correlated with discharge-related patterns in terms of the central tendency and spatial heterogeneity of the hydrodynamic conditions at a cross-section scale for the river reach considered in Chapter 3. Chapter 5 presents summary conclusions of the above three research chapters, along with recommendations for future investigation.

Four technical appendices (A, B, C, and D) present methods and results of hydrological, water temperature, substrate, and bathymetric characterizations (respectively) for the study reach.

The compendium of works presented herein is considered appropriate for the awarding of the degree of Master of Applied Science (M.ASc.) from the University of Waterloo.

2.0 Limitations in Extraction of Survey Data from Real-Time Kinematic GPS ADCP Systems*

2.1 Introduction

Acoustic Doppler current profiler (ADCP) technology offers an effective and efficient tool for river discharge measurement at a range of scales (Oberg and Mueller 2007; Rennie and Rainville, 2006; Oberg et. al., 2005; Mueller, 2002; Simpson, 2001). Extended applications include the rapid acquisition of velocity profiles from moving vessels in hydraulic analyses (Jamieson et. al., 2011; Shields et. al., 2003), bathymetry data acquisition (Dinehart and Burau, 2005), calibration of hydraulic models (Guerrero et. al., 2013; Czuba and Barton, 2011; Conaway and Moran, 2004), sediment transport analysis (Rennie and Church, 2010), aquatic habitat evaluation (Shields and Rigby, 2005), contaminant dispersion investigations (Shen et. al., 2010), and zooplankton abundance inventories (Flagg and Smith, 1989). Recent integration of real-time kinematic global positioning systems (RTK-GPS) into ADCP systems has provided an alternative to bottom-tracking methods in discharge measurements (Rennie and Rainville, 2006) by logging geospatial coordinates of ADCP profiles collected by built-in (SonTek, 2011) or independent (Teledyne, 2013) RTK-GPS systems. The improved technology precision has afforded ancillary applications beyond discharge measurement, which are contemporaneously being employed, such as the extraction of bathymetry data—historically a costly and time consuming endeavor.

RTK-GPS ADCP systems operate using triangulation algorithms between satellites, a stationary base station unit, and a mobile rover unit (located at the ADCP transducer position) to acquire geospatial coordinates. Where base stations are erected over established survey control benchmarks (which are georectified), horizontal and vertical accuracy of rover/ADCP survey data may be considered accurate within ±0.01 m and ±0.03 m, respectively (USACE, 2007). Conversely, where a base station is not referenced to established control benchmarks (nongeorectified), ADCP measurements are acquired relative to an arbitrary vertical datum. This accuracy limitation is well disseminated within the field of geomatics and poses no accuracy concerns when employing nongeorectified RTK-GPS ADCP systems for discharge measurements as the intertransect ping coordinates are accurate relative to one another.

*The chapter appears as published in the ASCE Journal of Hydraulic Engineering as follows:
Muirhead, J. and Annable, W. 2014. Limitations in Extraction of Survey Data from Real-Time Kinematic GPS ADCP Systems. *Journal of Hydraulic Engineering* **140**(8), 06014012.

However, concerns arise where the extraction of geospatial ADCP data coordinates [specifically water surface elevation (WSE)] are employed in bathymetry mapping and hydraulic modeling studies which is a growing practice amongst practitioners and researchers. This study examines the vertical precision and accuracy of geospatial coordinates (represented by WSEs) collected by a nongeorectified RTK-GPS ADCP system and compares them to WSEs simultaneously acquired using a georectified RTK differential GPS (RTK-DGPS) system.

2.2 Methods

During the period of April–July 2012, ADCP river surveys were completed along a 21-km reach of the Rainy River immediately downstream from Fort Frances, Ontario. The study reach is a border water separating northwestern Ontario and northern Minnesota and is predominantly straight and wide (typically 200–300 m) with a low WSE gradient (<0.5%). Forty-seven cross sections were repeatedly measured over the large seasonal fluctuation in WSE [327–330 metres above sea level (masl)] producing a suite of 595 discrete ADCP transects.

Two different RTK systems were simultaneously employed to obtain paired WSEs at each transect at the time of measurement. The first was a Sokkia GRX1, which is an L1/L2 receiver global navigation satellite system (GNSS) capable of obtaining first-order RTK-DGPS positions at horizontal and vertical accuracies of ±0.01 m and ±0.015 m, respectively (Topcon 2010). In this study, the GRX1 base station unit was georectified to two globally accurate permanent geodetic benchmarks along the study reach and transmitted RTK corrections to the mobile rover unit (Topcon, 2010). The rover's reception range was enhanced using a Pacific Crest positioning data link (PDL) high power antenna with a coverage extent of 10 km (Pacific Crest Corporation, 2005). However, the field application observed shorter distances dictated by lines of sight.

A series of quality control (QC) benchmarks were established along the study reach and georectified to the same permanent benchmarks using the Sokkia GRX1 system to ensure RTK-level survey control along the longitudinal traverse. Repeated surveys of QC benchmarks during the field season using the Sokkia GRX1 verified global accuracy of the georectified system using the root-mean-square-error method (RMSE) as defined by Marriott (1990):

$$RMSE = \sqrt{\frac{\sum_{i=1}^{n}(\chi)^2}{n}} \quad (2.1)$$

where n is the total number of QC benchmarks surveyed (40); $\chi = X_{Sokkia;i} - X_i$, where $X_{Sokkia;i}$ is the spatial coordinate acquired by the Sokkia GRX1 rover; and X_i is the known coordinate of the QC benchmark. The RMSE for northings, eastings, and elevations were 0.031, 0.047, and 0.033 m, respectively. Although RMSE were sometimes greater than cited specifications, they were considered acceptable for river surveys, confirming global accuracy of Sokkia surveyed coordinates. The Sokkia GRX1 rover obtained a single WSE (∇_{Sokkia}) at each ADCP transect as an independent comparison of WSEs surveyed using the nongeorectified system as discussed below.

The second RTK system employed was a SonTek M9 ADCP— a nine-beam ADCP, which obtains velocity profiles (pings) at a frequency of 1 Hz for depths between 0.2–30 m utilizing two sets of four profiling beams (3.0 MHz and 1.0 MHz, respectively) and one depth-measuring vertical beam (0.5 MHz) (SonTek, 2011). For this study, the M9 was integrated with a SonTek base station furnishing geospatial coordinates of ADCP data to RTK-level precision (±0.03 m) (SonTek, 2011). The SonTek base station and RiverSurveyor recording software do not currently have the ability to be georectified to geodetic benchmarks. The SonTek base station is established on shore and communicates to the M9 ADCP transducer on a moving vessel via an onboard power and communications module (PCM) using a spread spectrum radio connection (2-km maximum distance; SonTek, 2011). The base station was erected in open areas and was allowed to interpolate with satellites until an RTK lock was established. The base station was moved when required throughout the study reach to ensure that an RTK level of survey control was maintained. Since the system has no ability to georectify to geodetic benchmarks, setup positions were not constrained to the QC benchmarks, rather they were located to optimize lines of sight in order to best maintain an RTK lock.

Vertical corrections for the offset between the SonTek M9 ADCP GPS antenna head and ADCP transducer bottom of 1.0 and 0.37 m for boat-mounted and kayak-mounted configurations were applied, respectively, to reconcile vertical antenna elevations to WSEs. Discharge (and WSE) was assumed to remain constant during the period of each transect. Each SonTek transect was measured within a 15-min duration at a frequency of 1 Hz, resulting in 60–900 pings (each with a WSE) for each transect. The average standard deviation of ping WSEs measured within each of the 595 transects was 0.028 m and fell within the manufacturer's precision tolerances of ±0.03 m (SonTek, 2011). Therefore, at each transect, a

single SonTek WSE (∇_{SonTek}) was considered representative of the nongeorectified WSEs and calculated as the arithmetic average of inclusive ping WSEs.

The accuracy of ∇_{SonTek} was evaluated against ∇_{Sokkia} acquired at identical transect locations based upon a threshold of the combined manufacturer's vertical tolerances (±0.063 m) corresponding to the SonTek (±0.03 m; SonTek 2011) and Sokkia GRX1 (±0.033 m) systems. Establishment of setup-specific arbitrary vertical datum at each SonTek base station initialization was first confirmed using the standard deviation (σ_b) (Marriott, 1990) of field observed errors in ∇_{SonTek} as

$$\Delta_i = \Delta_{SonTek,i} - \Delta_{Sokkia,i} \tag{2.2}$$

$$\sigma_b = \sqrt{\frac{\sum_{i=1}^{n}(\Delta_i - \bar{\Delta}_b)^2}{n-1}} \tag{2.3}$$

$$\bar{\Delta}_b = \frac{1}{n}\sum_{i=1}^{n}\Delta_i \tag{2.4}$$

where b is the base station setup and n is the total number of paired ∇_{SonTek} and ∇_{Sokkia} obtained within a given SonTek base station setup. Values of $\sigma < 0.063$ m (corresponding to combined manufacturer's tolerances) were present in 77% of base station setups. This intersetup consistency in field observed error confirmed the relative accuracy of ∇_{SonTek} to an established setup-specific arbitrary vertical datum.

The global accuracy/inaccuracy of the setup-specific arbitrary vertical datum is of great importance for practitioners wishing to integrate WSE data and/or dependent properties obtained using nongeorectified RTK-GPS ADCP systems (e.g., bathymetry, hydraulics) with other geospatial globally rectified datasets, such as digital elevation models (DEMs), airborne light detection and ranging (LiDAR), land surveys, and ADCP transects in adjacent base station setups. River surveys for the above purposes are commonly deployed using one of two scenarios. Scenario 1 considers the situation where all desired transects are acquired using a single RTK-GPS ADCP base station setup. Scenario 2 is analogous to a longitudinal survey traverse and occurs when a base station must be moved along the river survey due to loss of the spread spectrum communication/RTK-lock. Each SonTek base station setup for Scenario 2 operates as individual occurrences of Scenario 1 with arbitrary vertical datum established at each setup initialization.

The $RMSE$ method was employed to assess the global accuracy of ∇_{SonTek} relative to the confirmed globally accurate ∇_{Sokkia}. Global accuracy was considered to occur when $RMSE \leq 0.063$ m

(corresponding to the combined manufacturer's tolerances). The $RMSE$ was first calculated for the entire population of ∇_{SonTek} and ∇_{Sokkia} irrespective of base station setup where Equation (2.1) is here defined by: $\chi = \nabla_{SonTek;i} - \nabla_{Sokkia;i}$ and n is the total number of ∇_{SonTek} and ∇_{Sokkia} pairs (n = 595).

To evaluate global accuracy of setup-specific arbitrary vertical datum, the $RMSE$'s (referred to here as $RMSE_b$) were calculated for each base station setup using Equation (2.1) where $\chi = \nabla_{SonTek;i} - \nabla_{Sokkia;i}$ and n is the number of paired WSE observed within each discrete SonTek base station setup. $RMSE$'s were subsequently recalculated for each SonTek base station setup (referred to here as $RMSE_{*b}$), considering the setup-specific average vertical datum differences of the nongeorectified system from the georectified system. Thus, $RMSE_{*b}$ was calculated using Equation (2.1), where $\chi = (\nabla_{SonTek;i} - \bar{\Delta}_b) - \nabla_{Sokkia;i}$, and n is the number of paired WSEs observed within each discrete SonTek base station setup.

2.3 Results

Figure 2.1 illustrates ∇_{SonTek} versus ∇_{Sokkia} at corresponding spatial locations, regardless of base station setup. ∇_{SonTek} is not globally accurate ($RMSE$ = 0.741 m) and displays an overall tendency to underestimate ∇_{Sokkia}. Separate analyses, not shown, identified no influence of geographic location along the study reach or distance away from the base station provided that spread spectrum connections to the SonTek base station were maintained in RTK lock.

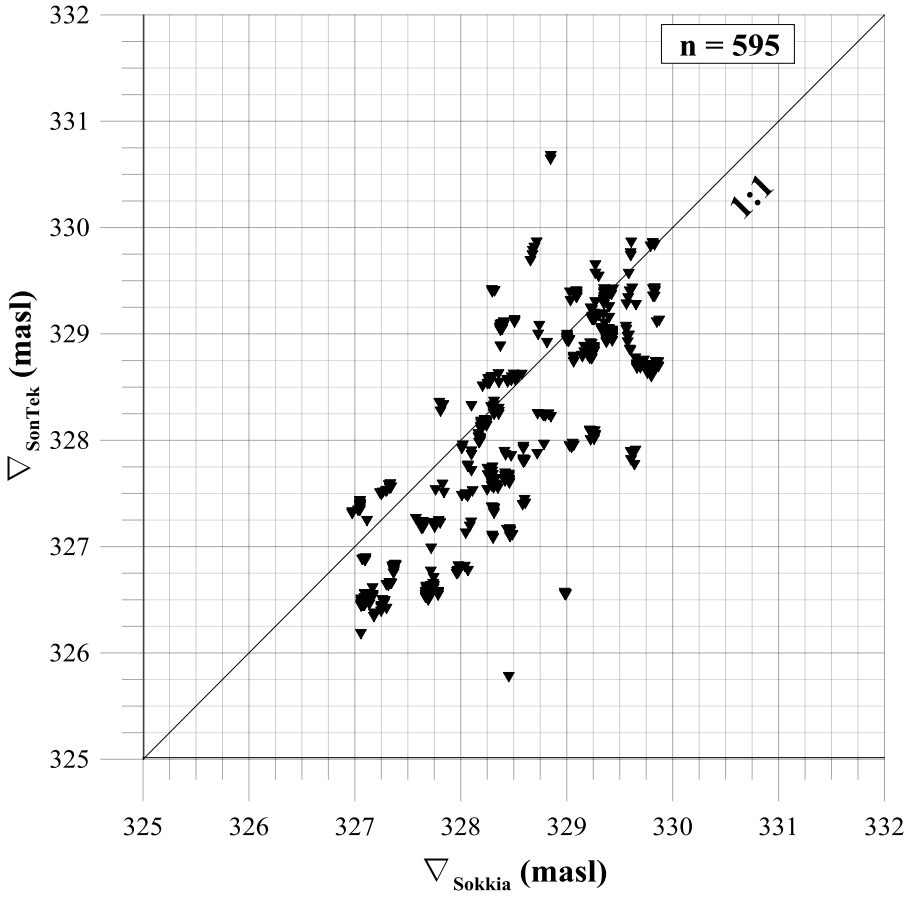

Figure 2.1: Georectified (∇_{Sokkia}) versus nongeorectified (∇_{SonTek}) WSE

Figure 2.2(a) illustrates a histogram of $RMSE_b$ for the 81 base station setups acquired in this study. Only five of the 81 (7%) SonTek base station setups resulted in$RMSE_b \leq 0.063$ m, identifying poor global accuracy in the initialization of the arbitrary vertical datum. A broad range in nongeorectified base station vertical datum corrections were observed (−2.43 m to +1.80 m).

Upon adjustment of using setup-specific arbitrary vertical datum correction values, 65 of the 81 (80%) SonTek base station setups resulted in $RMSE_{*b} \leq 0.063$ m [Figure 2.2(b)]. Thus, WSE from nongeorectified RTK-GPS systems are not and should not be considered globally accurate until corrected by setup-specific datum corrections acquired via a georectified RTK-DGPS system. Results here reinforce application concerns when directly employing vertical data acquired from nongeorectified RTK-GPS ADCP systems for purposes other than discharge measurement.

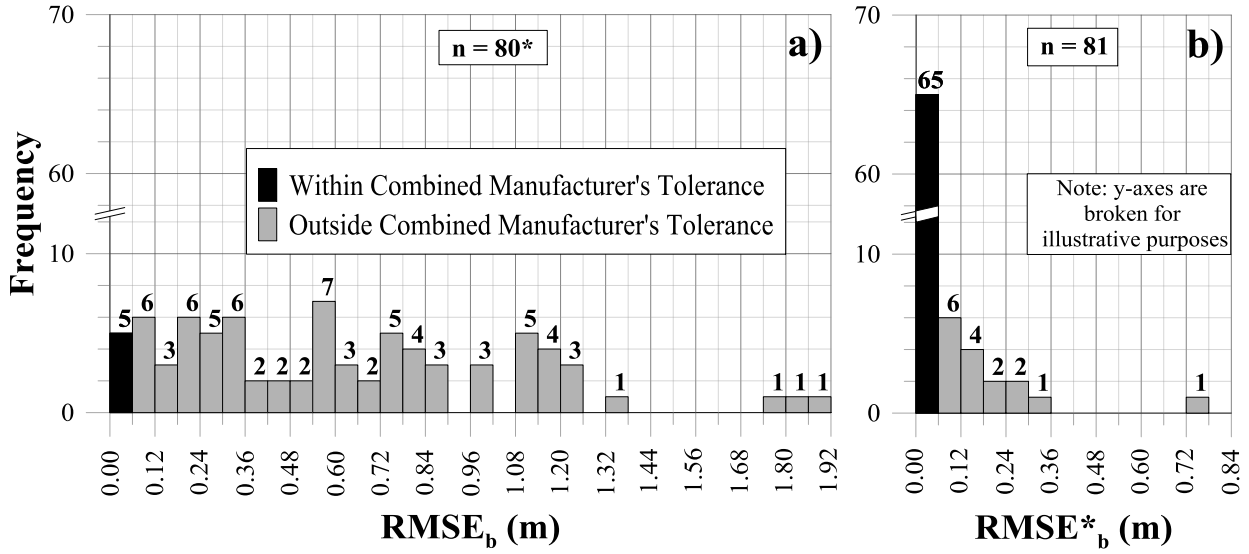

Figure 2.2: Histogram of root-mean-square error of ∇_{SonTek} compared to ∇_{Sokkia} for each base station setup: a) $RMSE_b$ before; (b) $RMSE_{*b}$ after georectified vertical datum corrections. [Note: * = single instance of RMSE = 2.44 m not shown for illustrative purposes in a)]

This study evaluated the performance of a nongeorectified RTK-GPS ADCP system to a georectified RTK-GPS system by comparing surveyed WSEs. Figure 2.3 illustrates the potential error in using a nongeorectified RTK-GPS ADCP system for bathymetric mapping purposes along the 21-km study reach if the assumption was made that the nongeorectified system was globally accurate. Thalweg elevations, represented by the solid line, were produced from maximum water depths (relative to the WSEs) obtained from repeated discharge transect surveys using the nongeorectified system and corrected to the corresponding WSEs obtained from the georectified Sokkia system (globally accurate). The thickness of the solid line (±0.05 m) represents a commonly applied WSE error threshold in one-dimensional (1D) model calibrations applied by the USGS (Czuba and Barton, 2011) projected onto the thalweg profile—although it is recognized that threshold methodologies may vary between studies (Guerrero et al., 2013; Conaway and Moran, 2004). The shaded region and dashed lines depict the thalweg elevations projected from the WSEs, which would result from applying the average and maximum errors observed at each given transect location. Representing the WSE along the longitudinal profile would have provided further insight. However, as multiple transects were conducted at each cross section over the range in annual flows, the longitudinal thalweg profile portrayed a clearer representation of the possible bathymetry errors that may arise.

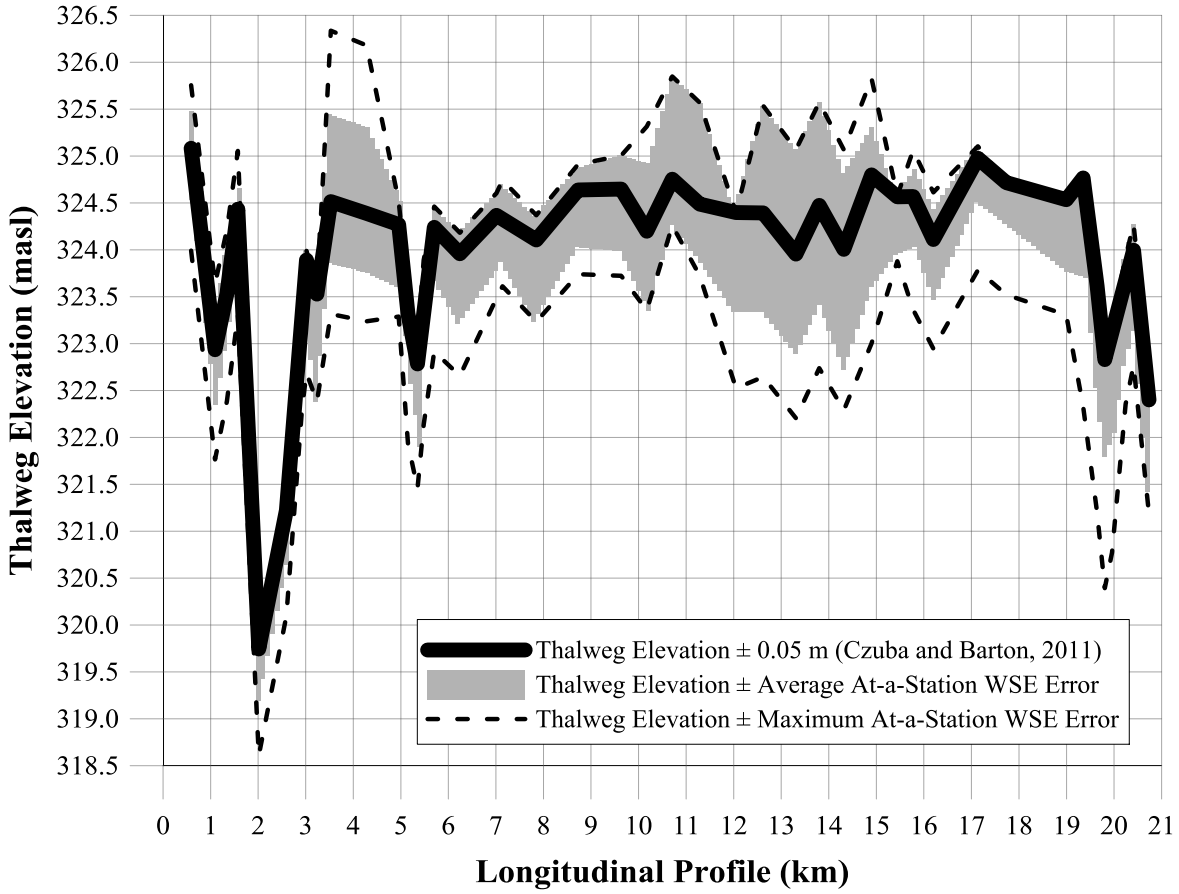

Figure 2.3: Survey error implications along a longitudinal profile of the Rainy River comparing georectified and nongeorectified datum

2.4 Conclusions

RTK-level WSEs (n = 595) were compared at the same spatial locations using nongeorectified (SonTek RTK-GPS ADCP) and georectified (Sokkia) survey systems. Vertical global accuracy was confirmed for the georectified Sokkia survey system ($RMSE$ = 0.033 m). The average vertical precision of the ping WSEs within each given discharge transect using the nongeorectified SonTek RTK-GPS ADCP was found to be σ = 0.028 m, occurring within manufacturer's precision specifications (SonTek, 2011). A vertical $RMSE$ = 0.741 m was obtained for 595 nongeorectified RTK-GPS ADCP WSE measurements when compared with georectified WSEs at the same spatial locations. Standard deviation of field-observed errors in ∇_{SonTek} within respective base station setups were within combined manufacturer's tolerances, confirming establishment of setup-specific arbitrary vertical datum. However, the global accuracy of setup-specific arbitrary vertical datum demonstrated $RMSE_b \leq 0.063$ m (combined

manufacturer's tolerance) in only 7% of base station setup cases. Upon applying setup-specific vertical datum corrections to ∇_{SonTek}, using the globally accurate georectified system, 80% of the base station setups produced $RMSE_{*b} \leq 0.063$ m. Vertical datum corrections varied broadly between setups ranging between −2.43 and +1.80 m.

Findings here support commonly accepted practices in the field of geomatics that nongeorectified RTK-GPS ADCP base stations assign arbitrary vertical datums upon base station initialization, and subsequently acquired geospatial data are accurate relative to the assumed datum but cannot be considered globally accurate. This is of particular concern where hydraulic modeling or bathymetry analyses may be employed using WSEs and bathymetry data extracted from nongeorectifed RTK-GPS ADCP systems. Great care must be exercised in verifying WSEs from RTK-GPS ADCP systems if they do not have explicit benchmark georeferencing capabilities and are used for purposes other than discharge measurement (i.e., WSEs or bathymetry data extraction). In this study, WSEs obtained from the nongeorectified RTK-GPS ADCP system were independently corrected using a parallel georectified RTK-DGPS system. This proved to be the most amenable way of accurately correcting WSE elevations.

3.0 Evaluation of hydraulic aquatic habitat metrics using a high-resolution spatial and temporal dataset measured in a large, hydroelectrically regulated, low-relief river in northwestern Ontario

3.1 Introduction

Since the early contributions of Chézy (1775) and DuBoys (1879), an array of metrics and theories have been advanced to characterize the four-dimensional spatio-temporal fluid states, conditions and sediment movement within rivers at varying degrees of complexity (e.g., Keulegan, 1938; Chow, 1959; Cunge et al., 1980; Graf, 1984; Julien, 2002). Juxtaposed, the characterization and quantification of lotic habitats have also evolved and are strongly reliant upon hydraulic and sedimentological metrics (e.g., Hobbs, 1937; Hynes 1970; Statzner et al. 1988; Jowett and Duncan 1990; Jowett, 1997; Crowder and Diplas, 2000a, 2000b; Kozarek et al., 2010; Harrison et al. 2011; Marchildon et al., 2011). Verification and validation of aquatic habitat metrics, however, remain formidable tasks which are further complicated when considering seasonal variability in flow regimes and river scale (Milhous, 1989; Crowder and Diplas 2000b; Milan et al., 2001; Bowen et al., 2003).

Large, low gradient rivers pose additional challenges in the measurement of physical and biological aquatic habitat metrics as they are not amenable to wading, resulting in the preponderance of data being collected at bridge crossings, cableways or moving vessel cross-sectional and longitudinal surveys. Geomorphic sub-units such as pools, riffles, chutes, glides, bars and other bed forms (Kellerhals, 1972; Rosgen, 1996; Buffington, 1998; Montgomery and Buffington, 1998; Brierley and Fryirs, 2000) are not as readily apparent or definable as they are in smaller or steeper watercourses (O'Neill and Abrahams, 1984; Lisle, 1987; Wooldridge and Hickin, 2002). Anthropogenically altered and/or controlled water courses, such as hydroelectric power scheme operations, present further challenges where managed flow releases cause more rapid variations in flow depth gradients and other hydraulic responses relative to uncontrolled and more natural hydrologic regimes (Poff, 1997; Brandt, 2000; Bowen et al., 2003; Graf, 2006). Characterizing and quantifying habitat characteristics under such varied flow regimes and scales has been noted as important for identifying and mitigating long-term aquatic impacts (e.g., Milhous, 1989; Milan et al., 2001).

Recognizing the disparate spatial and temporal scales of aquatic habitat inventories and associated costs of data acquisition, many investigations have employed one- and two-dimensional hydraulic models to supplement limited field observations and to enhance assessments and interpretations under seasonal and anthropogenically altered flow regimes (Milhous, 1989; Lamouroux et al., 1999; Crowder and Diplas, 2000a, 2002, 2006; Bowen et al., 2003). However, spatial and temporal numerical simplifications are also common place in the forms of ill-conditioned linkages and empiricisms as a dearth of high-resolution field investigations currently exists to validate and calibrate numerical models (Statzner et al. 1988; Jowett and Duncan 1990; Jowett, 1997; Crowder and Diplas, 2000a, 2000b, 2002, 2006; Shields et al., 2003). Recent studies have advocated for the computation of more complex hydrodynamic metrics to represent the spatio-temporal heterogeneity of macro-scale and meso-scale flow fields (Crowder and Diplas, 2000a, 2000b ; Kozarek et al., 2010; Harrison et al. 2011; Marchildon et al., 2011). However it remains unclear how transferable or what relations may exists for the various aquatic habitat metrics in larger scale river systems, relative to smaller more accessible and wadable watercourses.

Recent advancements in acoustic Doppler current profiler (ADCP) technology have offered a relatively efficient method of acquiring high-resolution field discharge data under non-wadable flow conditions by means of the moving-vessel method (Muste et al., 2004). Well documented as an effective and efficient technology for discharge measurement (e.g., Gordon 1989; Simpson, 2001; Oberg et al., 2005; Rennie and Rainville, 2006; Oberg and Mueller, 2007) the increased sampling speed and cell resolution of moving-vessel ADCP surveys combined with Real-Time Kinematic GPS (RTK-GPS) affords researchers and practitioners the ability to rapidly obtain spatially accurate detailed velocity and depth characteristics throughout large river systems.

Employing high-resolution velocity profiles from an RTK-GPS ADCP system, this study investigates the spatio-temporal hydrodynamic characteristics of a large low-gradient river at the cross-section scale along a 21 km reach where tailwater flows are regulated by a hydroelectric generating facility. A series of 47 cross-sections were repeatedly measured for velocities and depth over a two year period to characterize the hydraulic habitat niches over the seasonal range in flows. A broad contemporaneous suite of physical aquatic habitat metrics were evaluated in a larger-scale river system and to identify correlations which would allow for hydraulic representation using a more rudimentary subset.

3.2 Background

Efficient and spatially accurate data acquisition on large-scale river hydraulic conditions only became possible for non-wadable conditions in the late 1990's with the integration of depth-sounders with geographic positioning systems (GPSs) (Christilaw, 1996; Marceau et al., 1997; Monroe and Betteridge, 2000; Levec and Skinner, 2004). The obtained cross-sectional channel topographies were subsequently applied in one-dimensional (1-D) hydraulic models (e.g., HEC-RAS – Dyhouse et al., 2003; USACE, 2010) producing cross-section depth and average velocity. The method did not, however, produce location-specific or nose-running velocities which are frequently of more interest in aquatic habitat considerations (Ottaway et al., 1981; Witzel and MacCrimmon, 1983). The method also did not produce component velocity vectors, and field methods employed in smaller rivers for obtaining such data were unsuitable in larger systems. With advancement of computational abilities and adequate bathymetric mapping, two-dimensional (2-D) and even three-dimensional (3-D) hydraulic simulations were able to fill the void producing high intra- and inter-cross-section resolution of velocities over a range of user-defined discharges (e.g., Ghanem et al., 1996; Crowder and Diplas, 2000a, 2000b, 2002; Booker, 2003; Hilldale and Mooney, 2007; Harrison et al., 2011).

While 2-D and 3-D hydraulic models avoid the gross generalization of fluid parcel interaction inherent to conventional 1-D applications, a dearth of knowledge exists regarding the ability of these simulations to produce accurate and ecologically meaningful hydraulics around natural features (e.g., boulders, logs, etc.). The limited research which has been completed on the topic specifies that models require high-resolution surveys of habitat-forming features, accompanied by explicit modelling of the features themselves to produce velocity patterns at spatial scales of consequence for aquatic habitat analysis (Crowder and Diplas, 2000b). Adopting the technique therefore necessitates detailed field survey of micro- and meso-scale channel features and limits its applicability to micro-habitat investigations for short reaches of wadable systems (Crowder and Diplas 2000a, 2000b, 2002, 2006; Shields et al., 2003). The limitations render 2-D and 3-D hydraulic models ineffective for reach scale studies of large rivers where survey of detailed channel features is largely implausible.

These limitations have led to the increasing popularity of ADCP technology in hydraulic characterizations, as this tool observes micro- and meso-scale hydraulic phenomena. ADCP's are downward looking velocity profilers that utilize the Doppler shift in emitted soundwave frequencies resulting from sediment suspended in flowing water to obtain 3-D velocity measurements at variable vertical increments down the water column (Simpson, 2001; Oberg et al., 2005). Where the moving-

vessel method (Muste et al., 2004) is applied, velocity profiles across the channel are obtained producing cross-sectional arrays of each component velocity.

Just as methods for acquiring channel velocities are extensive, a proportionate number of hydrodynamic parameters have been introduced and advocated for by researchers in hydraulics, geomorphology, and ecology (Milan et al, 2001). The most common and easily obtained parameters are flow depth (D) and either streamwise velocity (V_x) or resultant current speed (V_{mag}), due to their ease of measurement and/or computation. Depths have often reported as mean cross-sectional depth or thalweg depth, and velocities are predominantly considered in the form of streamwise velocity or current speed, corresponding to output formats of the frequently applied field methods (e.g., current meters) and 1-D hydraulic models (e.g., HEC-RAS – Dyhouse et al., 2003; USACE, 2010).

Utilizing detailed bathymetry mapping capabilities, past works have also calculated a wide variety of channel geometry characterizations for application in river classification, restoration, and aquatic habitat enhancement. Hydraulic radius (R_h) and width to depth ratio (WDR) are commonly computed parameters representing the hydraulic efficiency of the channel (less flow resistance from riverbed grains/forms). Other bathymetric characterizations include depth ratio (DR) (Fahnestock, 1963) and aspect ratio AR (Mosley, 2006), each aiming to quantify bathymetric variation for a given cross-section. In fact, virtually any ratio of cross-sectional geometries are possible, including rectangular and elliptical shape factors (RSF and ESF, respectively). RSF may be computed as the ratio of cross-sectional area to that of an idealized rectangle considering D_{max}; ESF is analogous to RSF however it makes the comparison to an idealized half-ellipse considering D_{max}. Where the resolution of vertical profiles permits, irregularity of riverbed bathymetry has also been characterized by depth gradient (DG) that expresses the slope in riverbed elevation between two adjacent vertical profiles (Wang et al., 2013).

Researchers have also computed more complex hydraulic parameters characterizing the flow field, utilizing high resolution intra- and inter-cross-section velocities. Some, such as V_x, lateral velocity (V_y), vertical velocity (V_z), and V_{mag}, can be directly extracted from 2-D/3-D hydraulic models or ADCP surveys. Others are calculated considering various elements of the high resolution velocity dataset Examples include characterization of flow condition such as kinetic energy (KE), Reynolds number (RE), and Froude number (FR) (Lamouroux et al., 1999; Kemp et al., 2000; Shamloo et al., 2001; Marchildon et al., 2011). Various forms of kinetic energy have been of particular interest in characterizing the non-uniformity of velocities present in the flow field by considering turbulent kinetic energy (requires time-series data) and velocity head, or Coriolis, coefficient (α) (Hulsing, 1966; Kim and Muste 2012; Silva et

al. 2012). Near-bed hydraulic conditions have been quantified by velocities occurring at a distance 0.5 m above the bed (Kieffer and Kynard, 1996; Kynard et al. 2000), and have also been represented by substrate conditions and shear velocity (u_*) (Wilcock 1996; Sime et al. 2007; Wang et al., 2013).

More recent eco-hydraulic studies have advocated for hydrodynamic metrics representing spatial heterogeneity in the velocity field (energy gradients, vorticity, etc.) to characterize hydraulics and aquatic habitat conditions resulting at various geomorphologies (Crowder and Diplas, 2000a, 2000b; Shields et al., 2003; Shields and Rigby, 2005; Kozarek et al., 2010; Harrison et al. 2011). Originally developed for application to 2-D hydraulic model outputs by Crowder and Diplas (2000a, 2006), quantifications of velocity gradients ($VG1$, $VG2$) and circulation (AWV) have been applied in ADCP studies (Shields et al., 2003; Shields and Rigby, 2005). Other flow heterogeneity representations related to river mixing, including lateral (DCY) and longitudinal (DCX) dispersion coefficients, have been the subject of empirical calibration efforts making them potential characterizers of hydrodynamics (Rutherford, 1994; Seo and Chong, 1998; Kashefipour and Falconer, 2002; Shen et al., 2010; Kim and Muste, 2012).

3.3 Methods

3.3.1 Site Location

A 21 km reach of the Rainy River bound at the upstream end by the International Falls Dam (IFD) at Fort Frances, ON / International Falls, MN and at the downstream end by the confluence with the Littlefork River was selected as the study reach (Figure 3.1). Rainy Lake, the reservoir formed above the IFD, has an effective catchment area of 38,500 km^2 which is typified by Canadian Shield terrain with frequent rocky outcrops, mixed deciduous and coniferous forests, bogs and marshlands (Eibler and Anderson, 2004; O'Shea, 2005). The reach is predominantly a bedrock controlled U-shaped channel comprised of a heterogeneous substrate ranging between clay to boulder size fractions; over-consolidated clay deposits dominate the adjacent terraces originating from historical lake bed deposits (O'Shea, 2005). The channel averages 300 m in width, 3 – 4 m in depth (depending on seasonal stage and local hydraulic interactions), and flows at an average water surface elevation (WSE) gradient of 0.5%. At low flow conditions, there were no discernable bedform features, however, a series of bedrock outcrops are exposed within the first 6 km of the study reach (submerged in high flow regimes).

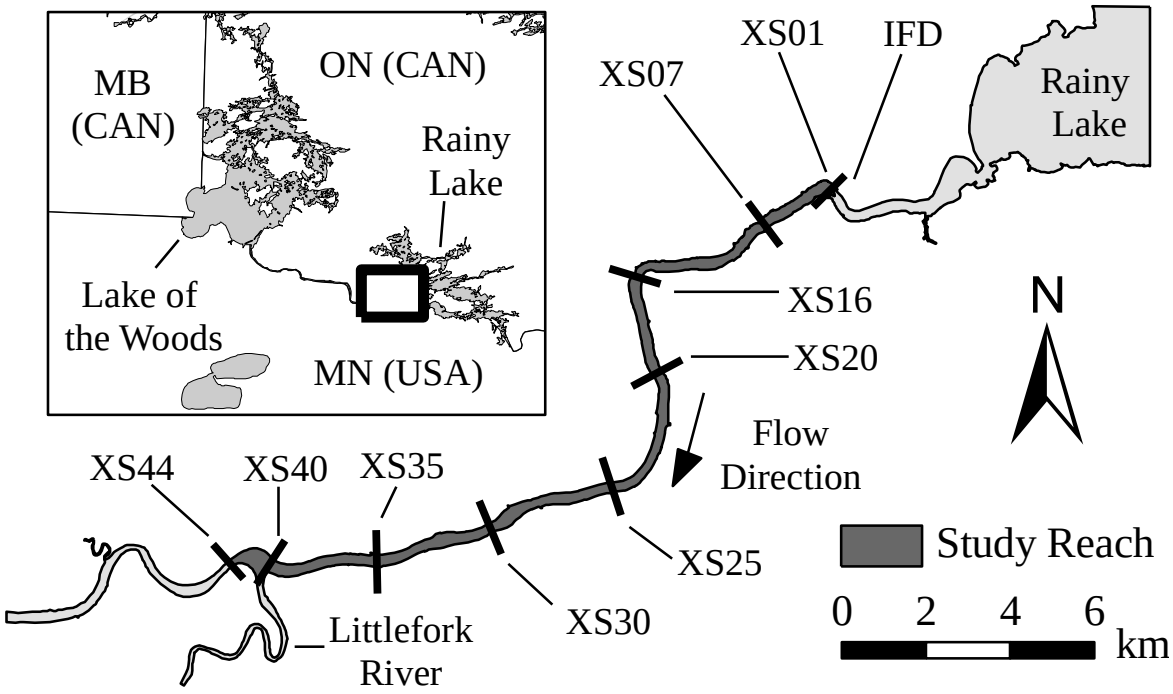

Figure 3.1: Study reach of Rainy River, Northern Ontario, Canada

Flow rates of the study reach are largely governed by IFD discharges (Q_{IFD}). No significant tributary confluences or additional flow contributions occur along the study reach until the downstream boundary condition with the Littlefork River. Mean annual discharge is 290 m^3/s, with seasonal flows typically ranging between 100 and 1000 m^3/s resulting in WSE fluctuations of approximately 4 m (327 – 331 masl observed in this study).

3.3.2 Field Data Collection

Survey control benchmarks were installed along the study reach and their positions obtained using a globally accurate Sokkia® GRX1 Real-Time Kinematic (RTK) Differential GPS (DGPS) system (Topcon, 2010). A total of 47 cross-sections were established at approximate 500 m intervals. Cross-section resolution was increased as necessary where morphological irregularities were observed.

Substrate inventories were conducted at each cross section and exposed feature during the low flow period of October 2012. Each inventory consisted of scaled quadrat photographic inventories pebble counts and grain size analysis consistent with the methods of Wolman (1954), Leopold (1970) and

Bundte and Abt, (2001). Grain size classes were of the pavement material were delineated consistent with the methods of Wentworth (1922) as listed in Table 3.1.

Table 3.1: Pavement layer substrate classes (after Wentworth, 1922; Bundt and Abt, 2001)

Substrate Class	Code	Predominant Size Range
Fines/Sand	FS	< 2 mm
Predominantly Fines/Sand, with Gravel	FS-G	< 2, some 2 – 64 mm
Predominantly Fines/Sand, with Cobbles/Boulders	FS-CB	< 2 mm, some 90 – 4000 mm
Predominantly Gravel, with Fines/Sand	G-FS	2 – 64 mm, some < 2 mm
Gravel	G	2 – 64 mm
Predominantly Gravel, with Cobbles/Boulders	G-CB	2 – 64 mm, some 90 – 4000 mm
Cobbles/Boulders	CB	90 – 4000 mm
Bedrock with Cobbles/Boulders	B-CB	Some 90 – 4000 mm
Bedrock	B	N/A

Cross-sections were categorized into one of three geomorphic complexity classifications (low, moderate, and high) according to a field-identified bathymetric- and substrate-complexity protocol (Figure 3.2). U-shaped cross-sections demonstrating homogeneous gravel/sand substrates in straight, featureless sections were considered low complexity (n = 29). Moderate complexity cross-sections (n = 15) exhibited more than one substrate type (i.e. sands and cobbles or cobbles and gravels) and included channel features such as islands, bedrock shoals, deep pools, and sandbars. High complexity cross sections (n = 3) were located at dam tailraces and areas of hydraulic control, and possessed significant bathymetric and substrate variation (e.g., cobble/boulder clusters, protruding bedrock formations) and visible turbulent flow patterns on the water surface. Morphological classifications as defined above have been frequently defined on smaller gravel-bed channels observing large roughness elements (LRE's) which introduce macroturbulent flow structure (Tritico and Hotchkiss, 2005). Although the current study is of significantly larger scale, macroturbulent structures observed here in the forms of boils and eddies are consistent with the findings of previous hydraulic investigations surrounding LREs (Buffin-Belanger and Roy, 1998; Smith et al., 2006; Lacey and Roy, 2007; Lacey and Roy, 2008). The inventory methods applied here were also considered readily definable to experienced river practitioners and researchers.

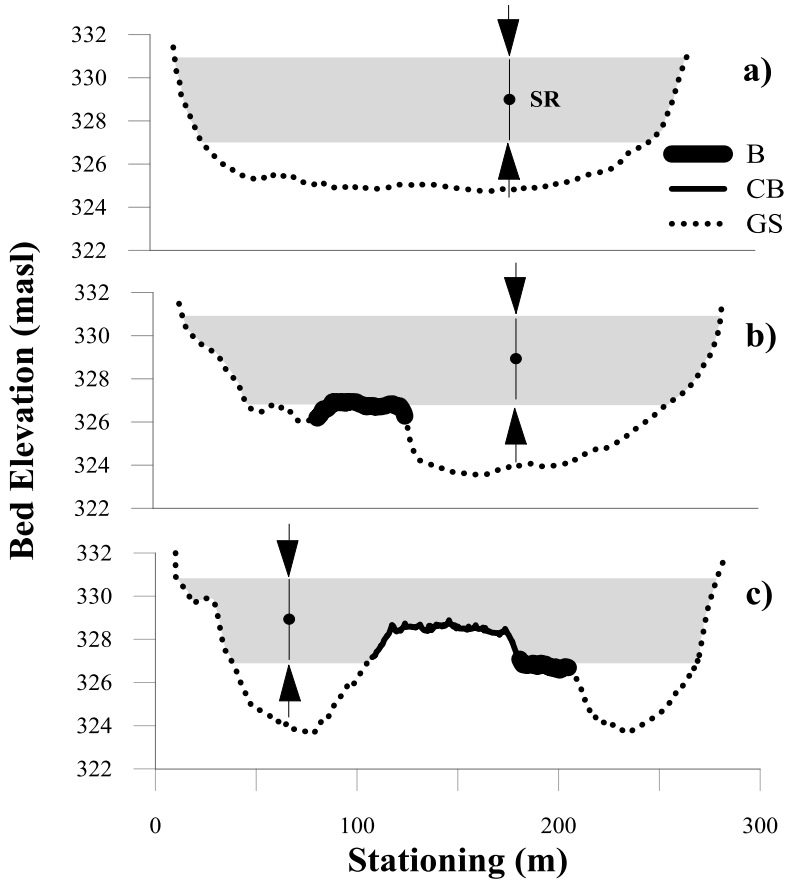

Figure 3.2: Typical substrate and bathymetry characteristics of a) low, b) moderate, and c) high complexity cross-sections (substrate classifications after Wentworth, 1922) with observed seasonal range (SR) in WSE (327 – 331 masl) indicated in grey

Transects comprised of vertical depth and velocity profiles were surveyed at each cross-section using a SonTek® M9 ADCP; a nine-beam system comprised of two sets (1 MHz, 3 MHz) of four velocity profiling beams and one vertical beam (0.5 MHz) for depth measurements (SonTek, 2011). Spatial coordinates of the ADCP measurements were referenced by use of a SonTek® RTK base station established on shore which communicated with the SonTek® M9 ADCP Power and Communications Module (PCM) via a spread spectrum radio connection (maximum range of 2 km). Global vertical accuracy of the SonTek® ADCP WSEs were ensured using the Sokkia® GRX1 DGPS system, resulting in a vertical accuracy of ± 0.03 m (Muirhead and Annable, 2014). When required, the SonTek® base station was moved throughout the study reach to ensure communication with the PCM unit.

Transects were obtained at 7 – 10 discrete Q_{IFD} levels over the seasonal range in flows (100 – 900 m^3/s) at each of the 47 cross-sections over a two year period (2012 – 2013), for a total of 427 transects. Similar to

methods of generating a stage-discharge relationship (Chow, 1959; Sauer, 2002), measurements were not surveyed in a linear progression of discharges. As illustrated in Figure 3.3 for transects obtained at XS02, variable WSE were observed for similar Q_{IFD}; these hysteresis and backwater effects are common on low-gradient, meandering rivers where confluences of tributaries possessing different hydrographic responses exist (Herschy, 1999, 2009; Hidayat, 2011).

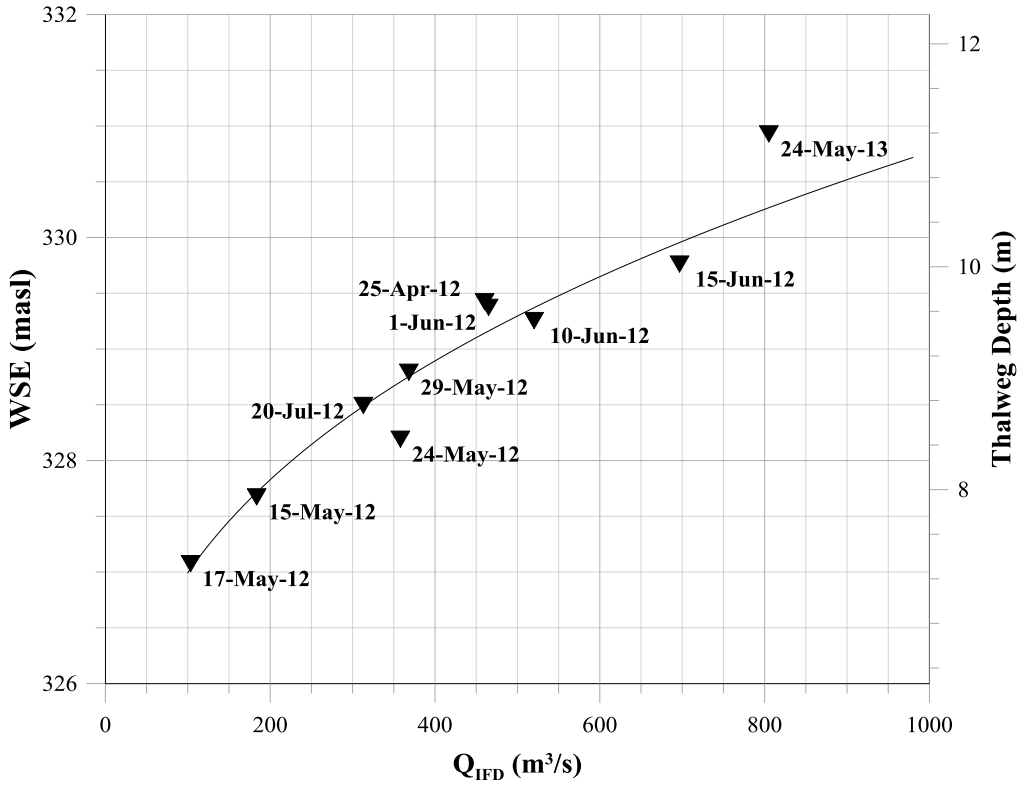

Figure 3.3: IFD discharges (Q_{IFD}) and water surface elevations (WSEs) for ADCP transects obtained at XS02, illustrating hysteresis and backwater effects in the study reach

Transects were obtained by traversing the river perpendicular to the mean flow direction at each cross-section using the moving-vessel method (Muste et al., 2004) (Figure 3.4). During collection, vessel path relative to cross-section location was monitored using the integrated SonTek® M9 real-time GPS. Each transect was composed of velocity profiles (*j*) obtained at a ping frequency of 1 Hz. Every profile was composed of vertically stacked rectangular cells (*k*) each with four velocity components (*x*, *y*, *z*, and a resultant, *mag*) (Figure 3.5). All transects were measured within a 15 minute duration with assumed constant discharge, resulting in an upper limit of 900 vertical profiles within a given transect. Following data collection, each profile in each transect was analytically projected onto the straight line path between

cross-sectional benchmarks to account for the slight deviations (typically ± 5 m) that commonly occur in a vessel's path when traversing a cross-section (Figure 3.4) consistent with Kim and Muste (2012).

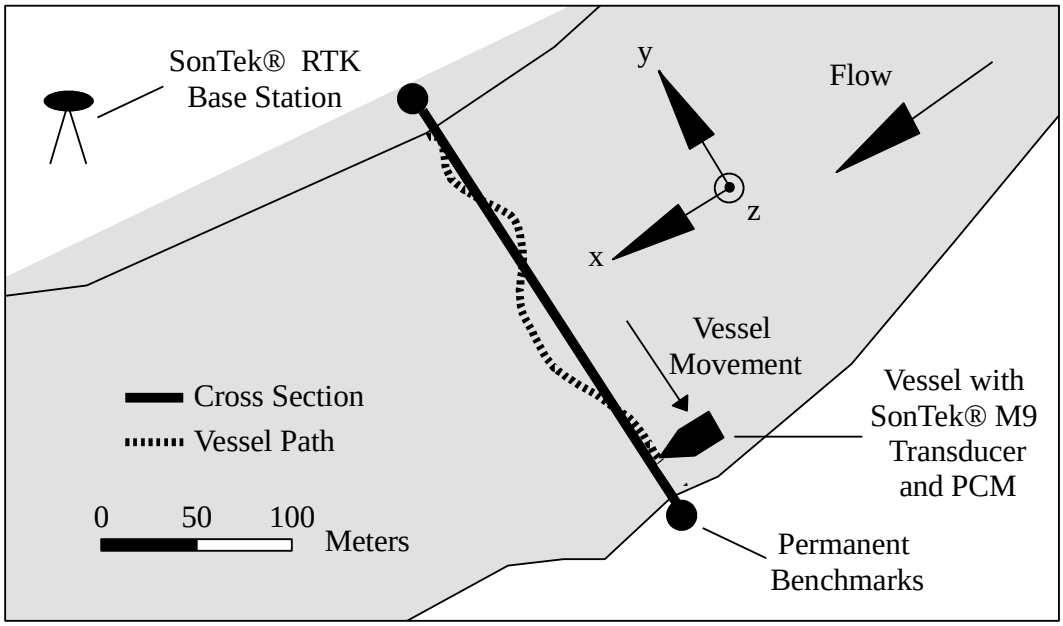

Figure 3.4: Planform schematic of moving-vessel ADCP transect collection

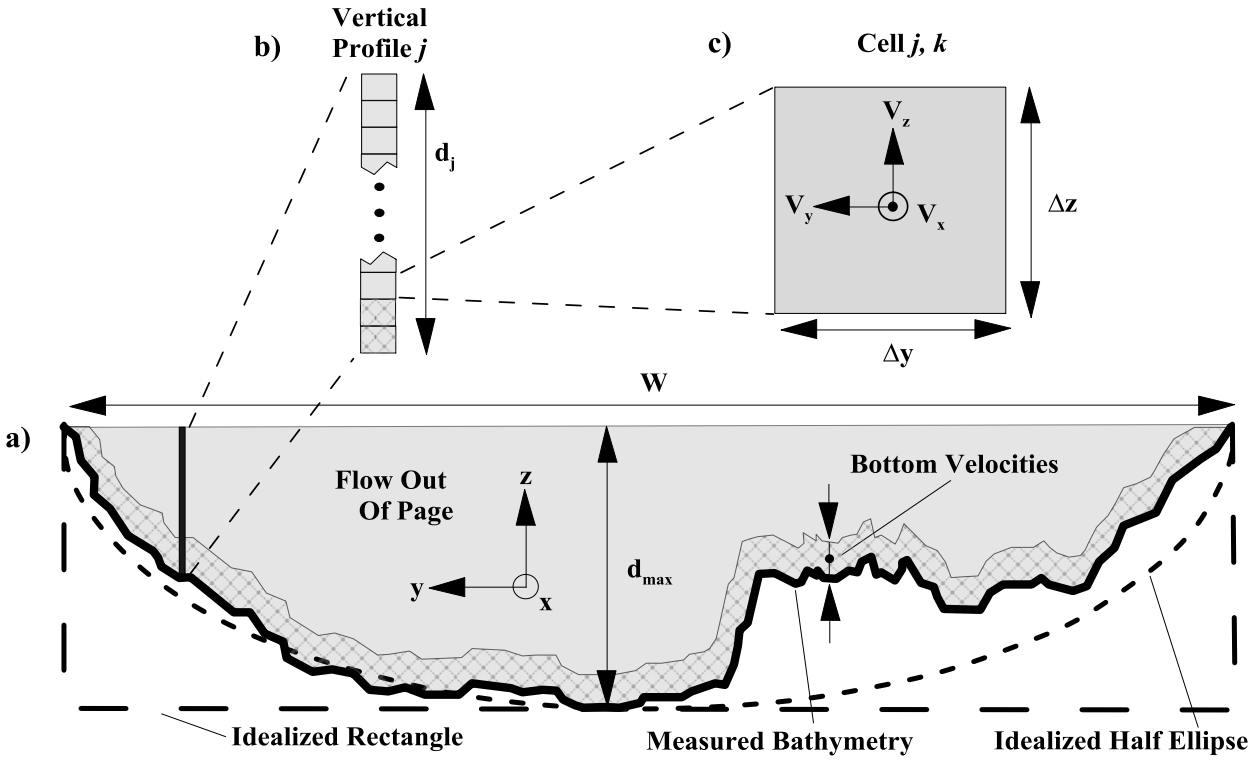

Figure 3.5: Cross-sectional schematic of a) ADCP transect, b) vertical velocity profile, and c) cell

3.3.3 Data Analysis

A multi-step post-processing procedure was applied using a MATLAB® script to ensure quality of velocity profile data within each transect (steps described sequentially below). Cell velocities were translated from East-North-Up to x-y-z as illustrated in Figure 3.4 and Figure 3.5. Profiles not demonstrating GPS reception of differential (±1 m) or RTK- (± 0.03 m) level precision (SonTek, 2011) or within 0.1 m of the previous profile were discarded. Profiles with pitch and/or roll angles greater than 5^{o} were removed (Ben Macone, SonTek®, personal communication, 8 April 2013) as the assumption of flow homogeneity across all beams was compromised (Simpson 2001; Muste et al. 2004; Mueller et al. 2007). Profiles demonstrating boat speed (BS) to water speed (WS) ratios greater than 2 were removed to reduce random error in recorded signals (Norris, 2001; Simpson, 2001), except where WS was less than 0.1 m/s (slack water observations were considered accurate in these regions). All velocity cells with a signal to noise ratio (SNR) of less than 1 were removed to reduce random error in Doppler shift (Ben Macone, personal communication, 8 April 2013; Simpson 2001; R.D. Instruments 1989). Cells demonstrating error velocity (EV) values outside of the acceptable scatter for the transect were removed via Chauvenet's criterion (Holman and Gajda, 1989) to ensure flow homogeneity and accuracy of vector resolution within the water volume bounded by the sampling beams (Mueller et al. 2007; Muste et al. 2004; Simpson 2001).

Equal spatial representation of velocity characteristics was required for computation of certain hydrodynamic parameters and for statistical representation of aggregate transects hydraulics. In previous ADCP studies, cell heights have been held constant, and profile width variations have been accounted for by removing profiles within a calculated minimum spacing (Sheilds and Rigby, 2005; Shields et al., 2003), or spatially averaging cells within a pre-determined horizontal distance (Kim and Muste, 2012). Here, cell heights and profile widths varied due to changing beam frequencies (1 MHz or 3 MHz) and variable boat speeds (SonTek, 2011). Velocity profile and cell properties were reproduced by the MATLAB® script according to unit heights and widths of 0.1 m and 0.05 m, respectively, as illustrated in Figure 3.6, producing matrices of equal spatial representation.

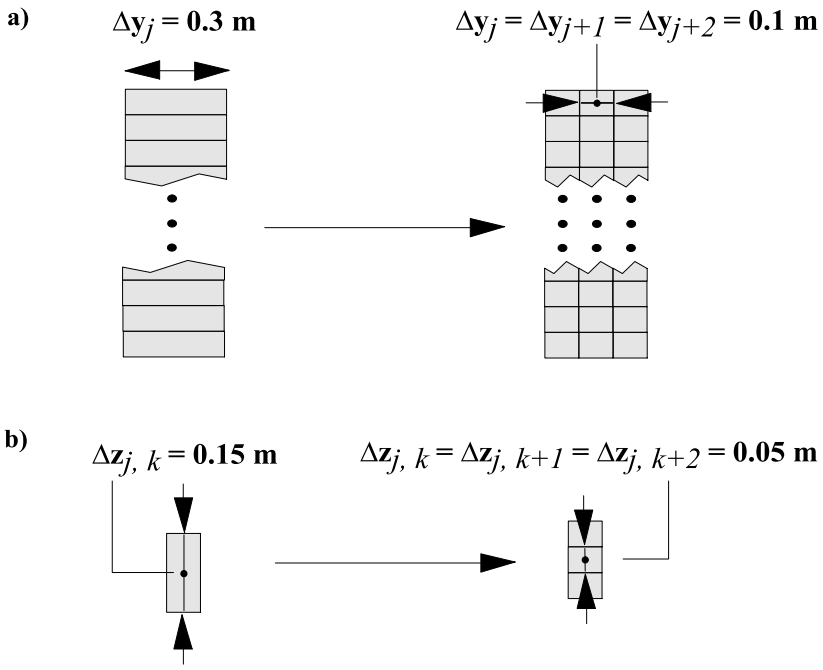

Figure 3.6: Scaling methodologies for a) profile width and b) cell height

3.3.4 Hydraulic Parameters

A contemporary collection of 23 commonly computed hydraulic parameters were selected for study here, as summarized in Table 3.2. Table 3.2 indicates applicable equations and whether the parameter was directly extracted from ADCP velocity profiles ("direct" – e.g., streamwise velocity), or required secondary calculation steps using the surveyed velocity/bathymetry data ("indirect" – e.g., Reynolds number). Parameter definitions can be found in the List of Symbols. Depending on calculation methodologies, each parameter could be obtained considering the entire transect, each profile within a transect, or each cell within a transect (Figure 3.5) – indicated by "T", "P", and "C" (respectively) in Table 3.2.

Table 3.2: Summary of computed hydraulic parameters

Metric Class	Parameter	Units	Equation	r	Direct/ Indirect	Metric Values	References
Bathymetry	Depth	m	-	-	Direct	P	-
	Hydraulic Radius	m	$R_h = A_{XS}/P_w$	-	Indirect	T	-
	Depth Ratio	-	$DR = d_{max}/d_{avg}$	-	Direct	T	Fahnestock, 1963
	Width-Depth Ratio	-	$WDR = W/d_{max}$	-	Direct	T	-
	Aspect Ratio	-	$AR = d_{max}/R_h$	-	Indirect	T	Mosley, 2006
	Rectangular Shape Factor	-	$RSF = A_{XS}/(Wd_{max})$	-	Indirect	T	-
	Elliptical Shape Factor	-	$ESF = 4A_{XS}/(\pi W d_{max})$	-	Indirect	T	-
	Depth Gradient	-	$DG_r = \left\lvert \frac{d_j - d_{j+1}}{\Delta s_j} \right\rvert$	median, IQ	Indirect	P	Wang et. al., 2013
Velocity	Cell Velocity	ms^{-1}	V_r	xmedian, xIQ; ymedian, yIQ; zmedian, zIQ; magmedian, magIQ; bxmedian, bxIQ; bymedian, byIQ; bzmedian, bzIQ; bmagmedian, bmagIQ	Direct	C	-
	Shear Velocity	ms^{-1}	$\frac{V_r}{u_{*r}} = \frac{1}{\kappa} ln\left(\frac{d_j}{e\, z_0}\right)$ $\frac{V_r}{u_{*r}} = \frac{1}{\kappa} ln\left(\frac{0.1 d_j}{z_0}\right)$	xmedian, xIQ; bxmedian, bxIQ	Indirect	P	Sime et. al., 2007; Wilcock, 1996
Flow Complexity	Kinetic Energy	Nm^{-1}	$KE_r = \gamma A_{j,k} \frac{V_r^3}{2g}$	magmedian, magIQ; bmagmedian, bmagIQ	Indirect	C	Chow, 1959
	Reynolds Number	-	$RE_r = \frac{\rho V_r R_h}{\mu}$	xmedian, xIQ; bxmedian, bxIQ	Indirect	P	Chow, 1959
	Froude Number	-	$FR_r = \frac{V_r}{\sqrt{g h_d}}$	xmedian, xIQ; bxmedian, bxIQ	Indirect	P	Chow, 1959
Velocity Variability	Velocity Gradient 1	ms^{-2}	$VG1_r \triangleq \left(\frac{V_{r,j+1} + V_{r,j}}{2}\right)\left\lvert \frac{V_{r,j+1} - V_{r,j}}{\Delta s_j} \right\rvert$	xmedian, xIQ; ymedian, yIQ; zmedian, zIQ; magmedian, magIQ; bxmedian, bxIQ; bymedian, byIQ; bzmedian, bzIQ; bmagmedian, bmagIQ	Indirect	P	Shields and Rigby, 2005; Crowder and Diplas, 2005; Crowder and Diplas, 2002; Crowder and Diplas, 2000a
	Velocity Gradient 2	s^{-1}	$VG2_r = \frac{\left(V_{r,j+1} + V_{r,j}\right)\left\lvert \frac{V_{r,j+1} - V_{r,j}}{\Delta s_j} \right\rvert}{V_{r,min}^2}$		Indirect	P	
	Area Weighted Vorticity	s^{-1}	$AWV = \frac{\sum \left\lvert \frac{V_{y,j,k+1} - V_{y,j,k}}{\Delta s_k} - \frac{V_{z,j+1,k} - V_{z,j,k}}{\Delta s_j} \right\rvert \Delta s_j \Delta s_k}{\sum \Delta s_j \Delta s_k}$	y & z; by & bz	Indirect	T	
	Lateral Dispersion Coefficient	-	$DCY = 0.6 u_{*r} d_j$	xmedian, xIQ; bxmedian, bxIQ	Indirect	P	Kim and Muste, 2012; Rutherford, 1994
Velocity	Longitudinal Dispersion Coefficient	-	$DCX = \left[7.428 + 1.775\left(\frac{W}{d_{max}}\right)^{0.620}\left(\frac{u_{*r}}{\overline{V_r}}\right)^{0.572}\right] d_{max} \overline{V_r}\left(\frac{\overline{V_r}}{u_{*r}}\right)$	x, bx	Indirect	T	Kashefipour and Falconer, 2002
Velocity Variability	Velocity Head Coefficient	-	$\alpha_r = \frac{\sum \gamma V_{j,k}^3 \frac{A_{j,k}}{2g}}{\gamma \overline{V_r}^3 \frac{A_{CS}}{2g}}$	mag, bmag	Indirect	T	Hulsing, 1966; Chow, 1959

The 23 parameters collectively addressed characteristics of bathymetry, velocity, flow condition, and velocity variability. Bathymetry parameters characterized riverbed topography and included depth of each profile (D), six transect shape factors (hydraulic radius – R_h, depth ratio – DR, width-depth ratio – WDR, aspect ratio – AR, rectangular shape factor – RSF, elliptical shape factor – ESF), and the depth gradient (DG) for each profile. Velocity parameters included component vectors (V_x, V_y, V_z) and current speed (V_{mag}) of each cell, along with shear velocity (u_*) of each profile. Two versions of shear velocity –one (u_*) employing depth-averaged velocity and another (u_{*b}) considering bottom velocity. Flow condition parameters consisted of kinetic energy (KE) calculated for each cell in addition to Reynolds number (RE) and Froude number (FR) obtained for each profile. Velocity variability parameters included velocity gradient 1 ($VG1$) and velocity gradient 2 ($VG2$) obtained for each profile, area-weighted vorticity (AWV) for the entire transect, lateral dispersion coefficient (DCY) for each profile, longitudinal dispersion coefficient (DCX) for the transect, and velocity head coefficient (α) for the transect.

The high-resolution velocity arrays obtained in this study sometimes permitted the computation of various forms of each parameter, as illustrated in Figure 3.7. Where applicable, calculations were performed using the full assemblage of transect velocities as well as those exclusively occurring within 1 m of the riverbed (Figure 3.7a)). The 1 m threshold was considered appropriate given that past eco-hydraulic studies have considered bottom velocities at a distance 0.5 m above the bed (Kieffer and Kynard, 1996; Kynard et al., 2000) and was consistent with the boundary layer grain roughness represented by $3D_{84}$ of the observed bed material (Julien, 2002). Also where applicable, parameters were calculated using respective component velocities for each of the abovementioned velocity subsets, as illustrated in Figure 3.7b).

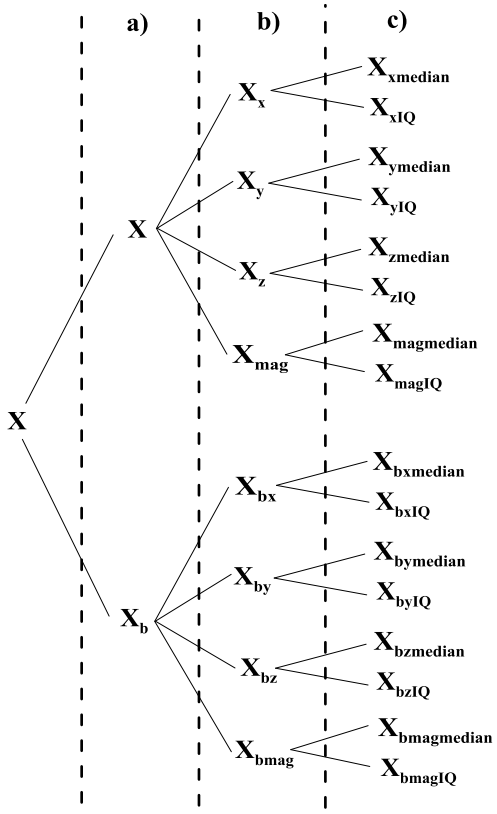

Figure 3.7: Schematic of metric expressions for a given parameter, X, where a pool of values of parameter X is obtained for a given transect, divided sequentially by considering a) all velocities and bottom velocities, b) streamwise (x), lateral (y), vertical (z), and resultant current speed (mag), and c) median and interquartile (IQ) expressions (note: not every parameter will produce all of the 16 metric expressions illustrated; refer to Table 3.2 for applicable expressions, *r*, of each parameter)

3.3.5 Hydraulic Metrics

As is typical in ADCP projects, selection of methods which numerically and effectively summarize the voluminous amount of hydrodynamic data in hydraulically and ecologically meaningful ways is challenging and unique to the objectives of each individual study (Shields et al., 2003; Shields et al., 2005). Given the source data provided by the ADCP surveys, parameters from Table 3.2 could be calculated in numerous ways as illustrated in Figure 3.7.

In this study, the meaning of the terms "parameter" and "metric" differ. Parameters were described in Section 3.3.4 (23 in total). Metrics, however, were transect-scale quantifications which summarize the multiple values of a given parameter produced within a given transect and were either a measure of spatial average of the parameter values, or an expression of heterogeneity of the parameter values. Such quantifications were possible where value of a given parameter was calculated for each profile or cell (indicated by "P" or "C" in Table 3.2). In these cases, median and

interquartile range (IQ) summarizations of the collection of the given transect's parameter values were calculated as illustrated in Figure 3.7c), applying Equations 3.1a) and 3.1b) (Walpole et. al., 2007).

$$X_{1/m} = \begin{cases} X_{(n+1)(1/m)} & if\ n\ is\ not\ a\ multiple\ of\ m \\ 1/m\left(X_{n(1/m)} + X_{[n(1/m)]+1}\right) & if\ n\ is\ a\ multiple\ of\ m \end{cases} \quad 3.1a)$$

$$X_{IQ} = X_{0.75} - X_{0.25} \quad 3.1b)$$

where X represents the parameter of interest, n is the number of parameter values obtained within the transect, $X_{median} = X_{0.5}$ is the median value, X_{IQ} is the IQ value, and $1/m$ is the percentile (e.g., $1/m = 0.25$ for 25th percentile). Median metrics were considered to characterize the spatial average of a given hydraulic parameter within a transect, while IQ metrics quantified the spatial heterogeneity of a given hydraulic parameter within a transect. Median and IQ statistics were utilized rather than mean and standard deviation to minimize bias of outlier values otherwise not removed by post-processing procedures (Walpole et al., 2007).

Other parameters considered the entire transect in calculation (indicated by "T" in Table 3.2), and therefore were inherently quantifications of the overall cross section characteristics (e.g., R_h). These parameters were considered representative of spatial averages and were termed "single value", or SV, metrics. In total, 83 different metrics (11 SV, 36 median, and 36 IQ) were computed for each of the 427 transects in this study (Table 3.2, Figure 3.7). The specific summarization method (all/bottom velocities, velocity component, median/IQ) of a given metric are indicated by its subscript, r, as specified in Table 3.2.

3.3.6 Statistical Analysis

Correlations between the 83 metrics were evaluated considering Spearman correlation coefficients (R_{Sp}). Metrics were considered to be correlated where R_{Sp} between any two metrics was greater than 0.7 (Dormann et al., 2013). A single, "representative", metric from within correlated groups was then selected based on directness of metric measurement and computation (e.g., V_{mag} selected over FR). The metrics within the correlated group which were not selected as representative are henceforth referred to as "correlated" metrics. In the culling of metrics, SV and median values were never considered representative of IQ values (and vice versa) regardless of R_{Sp}, owing to the fact that their objectives differ; the former characterized spatial average while the latter represented spatial heterogeneity.

Metric values could vary as a function of Q_{IFD} in two ways: 1) positive or negative trend or 2) variability – heretofore simply referred to as discharge-related trend and inter-discharge variance, respectively. The dynamics of

these evaluations are best visualized using a "metric-discharge" plot, exemplified in Figure 3.8a) for *DR* and Figure 3.8b) for α_b. Each metric-discharge plot contains 47 data series (i.e., lines) of metric values corresponding to the 47 cross-sections in the study reach; each data series consists of the 7-10 metric values (corresponding to the 7 – 10 transects) obtained over the range of surveyed Q_{IFD} at the given cross-section.

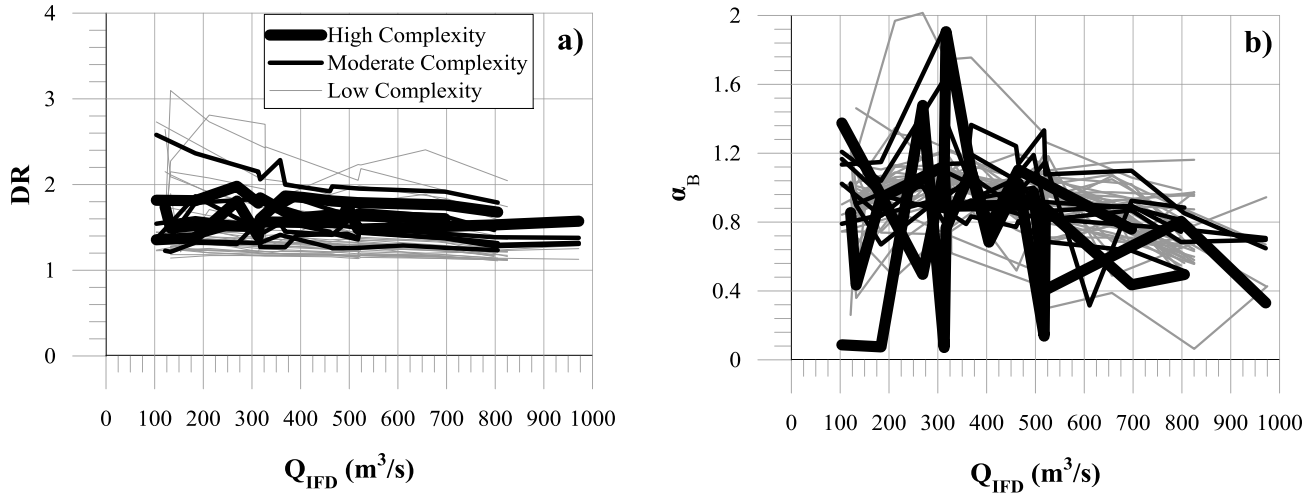

Figure 3.8: Metric discharge plots for a) bottom velocities velocity head coefficient (α_b) demonstrating statistical homogeneity in ${\sigma^2}_{norm}$ between high, moderate, and low complexity locations and b) depth ratio (DR) demonstrating statistical heterogeneity in ${\sigma^2}_{norm}$ between high, moderate, and low complexity locations

Discharge-related trend and inter-discharge variability were evaluated for cross-section location, for each metric. Trend was assessed considering linear regressions of the 7 – 10 metric values for each cross-section; the significance levels of the regression slope coefficients (a) determined whether discharge-related trending was present. Inter-discharge variability in metric values at each cross section location was evaluated considering the variance (σ^2) within each data series in each metric-discharge plot, as in Equation 3.2 (Walpole et al., 2007):

$$\sigma^2 = \frac{\sum_{i=1}^{n}(X_i - \bar{X})^2}{n-1} \qquad 3.2$$

where X = metric of interest, $\bar{X}$ = mean metric value within the given cross-section data series, i = a discrete metric measurement at the cross-section location, and n = the number of metric values at the cross-section location of analysis. Given that magnitudes of σ^2 vary between metrics by orders of magnitude, between metrics, inter-metric comparisons necessitated computation of normalized variance (${\sigma^2}_{norm}$), as in Equation 3.3, producing $0 < {\sigma^2}_{norm} < 1$:

$${\sigma^2}_{norm} = \frac{\sigma^2}{{\sigma^2}_{max}} \qquad 3.3$$

where ${\sigma^2}_{max}$ = maximum σ^2 for a given metric calculated amongst cross-section locations. Significant differences in mean ${\sigma^2}_{norm}$ for high, moderate, and low complexity cross-sections (Figure 3.2) were tested for employing standard ANOVA with post-hoc Tukey tests (Walpole et al., 2007). Parametric statistics were assumed applicable based on visual comparison of ${\sigma^2}_{norm}$ value quantile distributions in comparison to those of a Gaussian distribution. In most circumstances normality prevailed, however to guard against the implications of minor departures from the Gaussian distribution, non-parametric Kruskal-Wallis tests were run in parallel to parametric standard ANOVAs. This analysis produced identical results in the vast majority (79%) of cases, validating the initial assumption parametric statistics.

Statistical analysis above compared ${\sigma^2}_{norm}$ for cross-sections considering groupings based on complexity level. For a more explicit investigation of cross-section-specific inter-discharge variability, the arithmetic average of all ${\sigma^2}_{norm}$ observed at a given cross section ($\overline{{\sigma^2}_{norm,XS}}$), as in Equation 3.4, was computed. $\overline{{\sigma^2}_{norm,XS}}$ represented the average degree of variability observed across all hydrodynamic metrics at a given cross-section location.

$$\overline{{\sigma^2}_{norm,XS}} = \frac{1}{n}\sum_{i=1}^{n} {\sigma^2}_{norm} \qquad 3.4$$

where n = the number of metrics (and therefore number of ${\sigma^2}_{norm}$ values) being considered at a given cross-section XS, and i = a discrete instance of ${\sigma^2}_{norm}$ for the cross-section.

3.4 Results

3.4.1 Data Reduction

Table 3.3 and Table 3.4 summarize results of the Spearman correlation analysis for median/SV and IQ metrics, respectively. A set of 22 representative metrics from the original set of 83 were identified and are listed vertically in the left-most column of each table. These 7 SV, 8 median, and 7 IQ representative metrics statistically embody the various characterizations of hydrodynamics in the study reach; the remaining 61 metrics (i.e., correlated metrics) were considered to be correlated with the representative metrics and are listed horizontally in the top-most row of respective tables. Separate Partial Correlation Analysis (PCA), not shown, confirmed the correlated groupings of metrics obtained from the Spearman correlation matrix. Figure 3.9 illustrates the range in values of the 22 representative metrics (on a logarithmic scale for illustrative purposes) observed over the range in surveyed Q_{IFD}.

Table 3.3: Summary of representative and correlated SV and median metrics considering Spearman correlation coefficients (direct metrics in bold)

Represent-ative Metrics	Correlated Metrics																																
	R_h	$\mathbf{V_{bymedian}}$	$VG1_{ymedian}$	$VG1_{bymedian}$	$VG2_{ymedian}$	$VG2_{bymedian}$	$\mathbf{V_{bzmedian}}$	$VG1_{zmedian}$	$VG1_{bzmedian}$	$\mathbf{V_{xmedian}}$	$\mathbf{V_{bxmedian}}$	$\mathbf{V_{bmagmedian}}$	$u_{*median}$	$u_{b*median}$	KE_{median}	$KE_{bmedian}$	RE_{median}	$RE_{bmedian}$	FR_{median}	$FR_{bmedian}$	$VG1_{xmedian}$	$VG1_{magmedian}$	$VG1_{bxmedian}$	$VG1_{bmagmedian}$	DCY_{median}	$DCY_{bmedian}$	DCX	$VG2_{bzmedian}$	$VG2_{xmedian}$	$VG2_{bxmedian}$	AR	ESF
DR																																	
RSF																																	
WDR																																	
AWV																																	
AWV_b																																	
α																																	
α_b																																	
$\mathbf{D_{median}}$																																	
DG_{median}																																	
$\mathbf{V_{ymedian}}$																																	
$\mathbf{V_{zmedian}}$																																	
$\mathbf{V_{magmedian}}$																																	
$VG2_{zmedian}$																																	
$VG2_{magmedian}$																																	
$VG2_{bmagmedian}$																																	

$0.7 \leq R_{Sp} < 0.8$ $0.8 \leq R_{Sp} < 0.9$ $R_{Sp} \geq 0.9$

Table 3.4: Summary of representative and correlated IQ metrics considering Spearman correlation coefficients (direct metrics in bold)

Representative Metrics	Correlated Metrics																													
	DG_{iq}	$\mathbf{V_{bziq}}$	$VG1_{ziq}$	$VG1_{magiq}$	$VG1_{bxiq}$	$VG1_{bziq}$	$\mathbf{V_{xiq}}$	$\mathbf{V_{yiq}}$	$\mathbf{V_{bxiq}}$	$\mathbf{V_{byiq}}$	$\mathbf{V_{bmagiq}}$	u_{*iq}	u_{b*iq}	KE_{iq}	KE_{biq}	RE_{iq}	RE_{biq}	FR_{iq}	FR_{biq}	$VG1_{xiq}$	$VG1_{bmagiq}$	DCY_{iq}	DCY_{biq}	$VG1_{byiq}$	$VG2_{byiq}$	$VG2_{bziq}$	$VG2_{xiq}$	$VG2_{bxiq}$	$VG2_{bmagiq}$
$\mathbf{D_{iq}}$	■																													
$\mathbf{V_{ziq}}$		■	■	■	■	■	■	■		■										■	■								
$\mathbf{V_{magiq}}$							■	■	■	■	■	■	■	■	■	■	■	■	■	■	■	■	■							
$VG1_{yiq}$								■		■														■						
$VG2_{yiq}$																									■					
$VG2_{ziq}$																										■				
$VG2_{magiq}$																											■	■	■	

■ $0.7 \leq R_{Sp} < 0.8$ ■ $0.8 \leq R_{Sp} < 0.9$ ■ $R_{Sp} \geq 0.9$

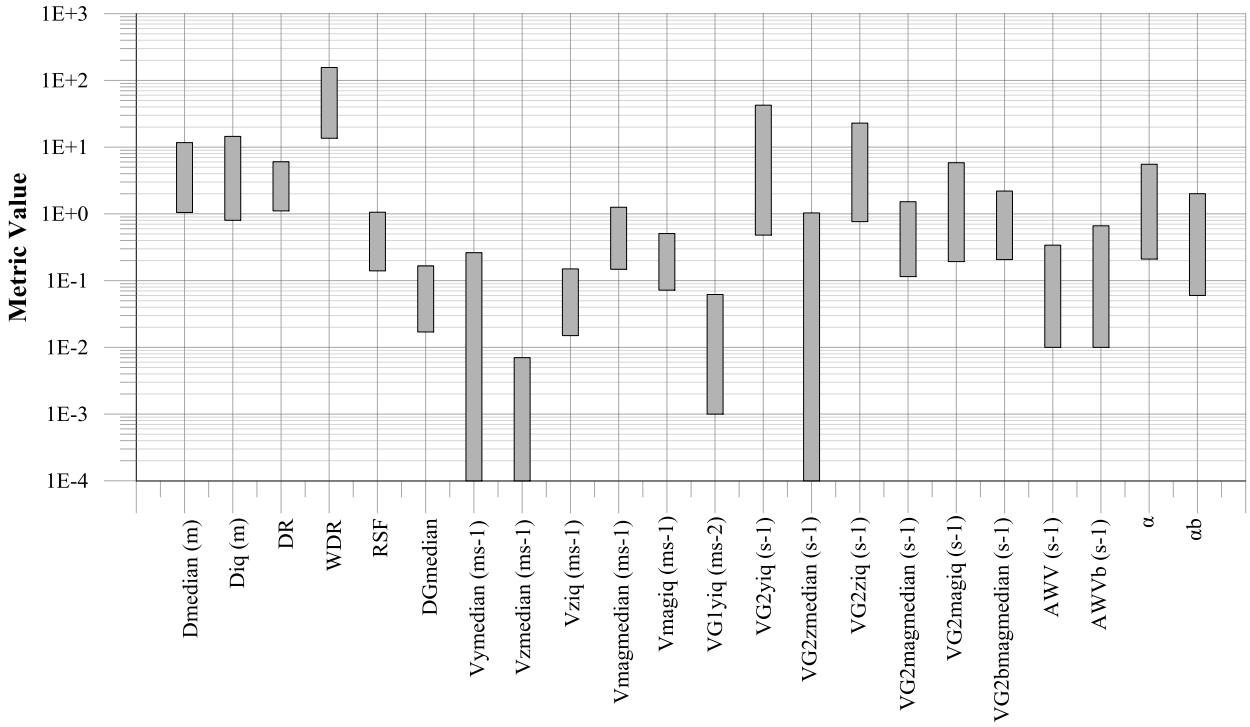

Figure 3.9: Range in representative metric values over the range in surveyed IFD discharges (note: minimum values of $V_{ymedian}$ = -0.372 ms^{-1}, $V_{zmedian}$ = -0.089 ms^{-1}, and $VG2_{zmedian}$ = -1.835 s^{-1} not shown due to logarithmic scaling of ordinate axis)

The following observations are in reference to Table 3.3 and Table 3.4. The majority of computed SV metrics (7/11 = 64%) demonstrated statistical independence and were classified as representative. Conversely, median and IQ metrics both demonstrated large degrees of statistical redundancy in their respective datasets as of the 36 median and 36 IQ metrics, only 8 (22%) and 7 (19%), respectively, were representative. Direct characterizations of current speed ($V_{magmedian}$and (V_{magIQ}), often the most readily obtained velocity component in field surveys, was representative of the vast majority of median and IQ datasets [18/36 (50%) and 17/36 (47%), respectively]. All metrics considering bottom velocities (with the exception of $VG2_{bmagmedian}$, AWV_b, and α_b) were correlated with their parallel equivalents considering all velocities.

Of the 22 representative metrics, the 9 which are directly extractable (as specified in Table 3.2) collectively represent 51 of the 61 (84%) correlated metrics. Further, of those 51 which are correlated, 40 (78%) are indirect metrics, indicating that indirect metrics can often be represented by direct metrics. Indirect metrics commonly computed in hydraulically-related studies (e.g., Lamouroux et al., 1999; Kemp et al., 2000; Marchildon et al., 2011) that were never classified as representative in this study were expressions of u_*, KE, RE, FR, DCY, and DCX. These were all correlated with respective median and IQ characterizations of V_{mag}. Only 1 of the 16 expressions of $VG1$ was representative ($VG1_{yIQ}$); the others were often represented by corresponding component velocity metrics

(e.g., $VG1_{zmedian}$ represented by $V_{zmedian}$). The only indirect metrics which demonstrated statistical independence on a consistent basis were characterizations of $VG2$, RSF, AWV, and α.

3.4.2 Hydrodynamic Sensitivity

Analysis of hydrodynamic sensitivity below exclusively considers the 22 identified representative metrics, as they demonstrated the ability to statistically characterize the full suite of 83 metrics.

No significant positive or negative trend with respect to Q_{IFD} was present in metric-discharge regressions of representative parameters, as only 5/22 representative metrics produced *a* significantly different from zero for the majority (75%) of the 47 data series. Regression fits were generally poor, with only 4/22 representative metrics demonstrating the majority (75%) of coefficient of determination (R^2) values greater than 0.5 signifying considerable variation in metric values as a function of Q_{IFD}.

Table 3.5 summarizes Tukey test results for ${\sigma^2}_{norm}$ in terms of homogeneous/heterogeneous pairings ($p < 0.05$) considering complexity classification (high, moderate, low) as the fixed factor. A total of 7/22 (32%) representative metrics exhibited homogeneous subgroups of ${\sigma^2}_{norm}$ across high, moderate, and low complexity cross-sections, indicating no statistical difference in temporal variability of those 7 metrics between spatial locations of different complexity. As a visual example, Figure 3.8a) illustrates the metric-discharge plot for depth ratio (DR), which demonstrated homogeneity between high, moderate, and low complexity cross-sections (Table 3.5). The remaining 15/22 (68%) representative metrics demonstrated statistical heterogeneity between at least two complexity classifications, with 13/22 (59%) demonstrating statistical heterogeneity between high-low complexity cross-sections. 9 of those 13 (9/22 = 41%) simultaneously demonstrated heterogeneity between high-moderate complexity locations. As a visual example, Figure 3.8b) illustrates the metric-discharge plot for velocity head coefficent considering bottom velocities (α_b), which demonstrated heterogeneous subgroups between all of high, moderate, and low complexity locations (Table 3.5).

Table 3.5: Heterogeneous (significantly different) and homogeneous pairs from Tukey test analysis of $\sigma^2{}_{norm}$ ($p < 0.05$) considering complexity level as a fixed factor (Hom = homogeneous, Het = heterogeneous pair)

High-Low	Het	Het	Het	Hom	Hom	Hom	Het
High-Moderate	Het	Het	Hom	Hom	Hom	Het	Het
Moderate-Low	Het	Hom	Hom	Hom	Het	Het	Het
Metrics	α_b	D_{iq} DG_{median} $V_{zmedian}$ V_{ziq} $VG1_{yiq}$ $VG2_{magiq}$ $VG2_{bmagmedian}$ α	D_{median} V_{magiq} $VG2_{magmedian}$ AWV	DR WDR $V_{ymedian}$ $V_{magmedian}$ $VG2_{zmedian}$ $VG2_{ziq}$ AWV_b	RSF $VG2_{yiq}$		
Count Percentage	1 5%	8 36%	4 18%	7 32%	2 9%	0 0%	0 0%

Figure 3.10 illustrates $\overline{\sigma^2}_{norm,XS}$ considering the 15 metrics with statistically significant differences in $\sigma^2{}_{norm}$ between high, moderate, and/or low complexity locations (identified above). Complexity classification of each cross-section is indicated. Aggregate mean values of $\overline{\sigma^2}_{norm,XS}$ for high, medium, and low complexity cross-sections were 0.42, 0.17, and 0.14, respectively. Therefore, significant differences of Table 3.5 take the following forms: high complexity cross-sections exhibit higher $\sigma^2{}_{norm}$ than moderate and low complexity locations, with moderate complexity cross-sections not usually demonstrating higher $\sigma^2{}_{norm}$ than low complexity locations.

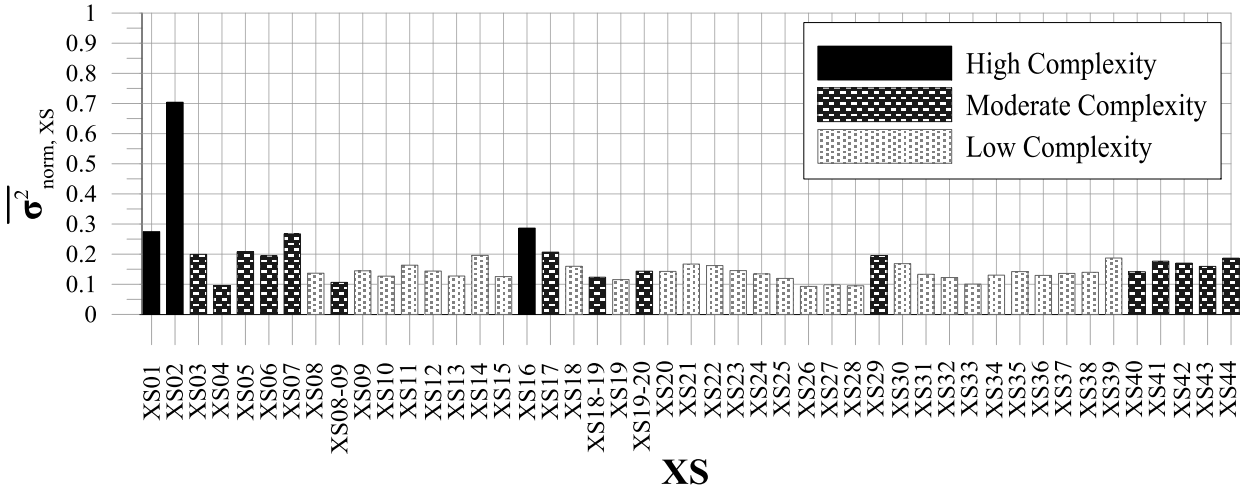

Figure 3.10: Average cross-section normalized variance ($\overline{\sigma^2}_{norm,XS}$) for the 15 representative metrics demonstrating significantly different variances between geomorphic sub-unit complexity levels, with respect to cross-section

3.5 Discussion

Previous hydrodynamic and hydraulic habitat studies have examined hydrodynamics i) on smaller rivers, and ii) considering only a few metrics. Examination of the large dataset of hydraulic metrics for the low relief Rainy River via data reduction analysis indicated that the majority (61/83 = 74%) of the full suite of hydraulic metrics were highly correlated with, and can be represented by, a smaller rudimentary subset of 22 representative metrics. Many of these statistical correlations (Table 3.3, Table 3.4) were confirmations of intuitive relationships (e.g., V_{bmag} is represented by V_{mag}), while others could be predicted based on the equations in Table 3.2 (e.g., KE is calculated from, and can therefore be represented by, V_{mag}). However, the finding that direct metrics can represent large percentages of not only the entire metric suite, but specifically the collection of indirect metrics, is of great importance for streamlining efforts for hydrodynamic characterizations on large, low-relief rivers. Several indirect parameters (u_*, KE, RE, FR, DCY, and DCX) which have frequently been emphasized in aquatic habitat and hydraulic investigations (Jowett 1993; Lamouroux et al., 1999; Kemp et al., 2000; Marchildon et al., 2011) were all shown to be correlated with simpler characterizations of hydrodynamic conditions. Current speed (V_{mag}), perhaps the most easily obtained hydraulic parameter, represented over half of the total correlated metrics (35/61 = 57%) between its two metric quantifications ($V_{magmedian}$ and V_{magIQ}). In contrast, the 13 representative metrics which were indirect collectively represented only 10 metrics in total. Therefore, in large, low-relief rivers, simple and directly extractable hydraulic parameters and their appropriate metric quantifications are equally effective as more complex, indirectly calculated metrics in hydrodynamic characterizations. Focusing field and analysis efforts on the acquisition of these simple hydraulic expressions will often yield equally representative hydraulic characterization results.

Statistical analysis indicates hydrodynamics do not trend positively or negatively as a function of Q_{IFD}, indicating the relative insensitivity of hydraulic metrics to discharge within the range of metric values measured. Further, Figure 3.10 clearly depicts relatively low degrees of discharge-related metric variability at low complexity cross-sections. The demonstrated temporal stability in hydrodynamic characteristics at areas of low complexity would likely stem from the non-existence of macroturbulent flow structures in these regions; homogenous and unobstructed morphologies demonstrate lower bed roughness, limiting turbulent structures to primarily the micro scale. Although low complexity areas will experience discharge-related variations in velocities, approximate spatial uniformity in velocity fluxes mean the aggregate transect assemblage of velocities is more or less temporally constant and is adequately characterized through high frequency sampling in the moving-vessel method. Therefore, river reaches with predominantly U-shaped cross sections and uniform substrate can be considered relatively constant in terms of their hydrodynamic characteristics. At these sections, adequate hydraulic characterization may be achieved by a reduced spatial resolution of cross sections and a lower frequency of transect measurements.

In contrast, Figure 3.10 illustrates larger temporal variability in metric values at high complexity cross-sections. Statistically significant differences in $\overline{\sigma^2}_{norm,XS}$ (Table 3.5) were observed between high and low complexity cross-sections in 59% of representative metric cases, and between high and moderate complexity cross-sections in 41% of metric cases. The increased temporal variability in hydrodynamics at these areas of geomorphological complexity may be driven by the instantaneous nature of ADCP-surveyed velocity profiles and associated limitations, as identified by Muste et al. (2004). Velocities collected with ADCP's represent instantaneous velocities acquired using 4 profiling beams at a specific point in time. Micro-scale turbulent structures occur on spatial and temporal time scales too detailed to be of interest in macro-scale studies and are negligible considering the calculation methodologies of the technique. However, macroturbulent flow structures resulting from the large-river equivalents of LREs in high complexity locations occur over appreciable spatial and temporal scales (Lacey and Roy, 2008; Roy et al., 2004). Such flow structures were visually apparent during field surveys as boils, vortices, and eddies reaching the surface. In taking instantaneous measurements, ADCP's obtained a "snapshot" of the velocity profile within these macroturbulent flow structures at a given location, at a specific point in time. Even where sampling frequency is high (1 Hz in this study), obtaining a single snapshot of portions of turbulent features means variability in cross-section velocities are likely independent of Q_{IFD} and instead driven by the space-time fractions of the turbulent structure captured by instantaneous ADCP measurements for a given transect. The fluctuations in these turbulent structures on spatial and temporal scales means velocity profile assemblages obtained using the moving-vessel method will likely differ from transect to transect even if discharge is held constant, and as observed, definitely if it is altered. Given the observed temporal variability and proposed mechanism above, adequate hydraulic characterization of high complexity regions requires cross-sections established at a high spatial resolution for sufficient planform coverage, paired with a large number of intra- and inter-discharge transects to adequately capture patterns of cross-section specific temporal variability. This is in agreement with recommendations by Muste et al. (2004), who suggest at least 10 transect repeats be performed at each cross-section location to characterize velocity profiles using the moving-vessel method.

3.6 Conclusions

Aquatic habitat studies have frequently linked spatial and temporal variability/heterogeneity in physical habitat characteristics with increased biodiversity and ecological function (Shields and Rigby, 2005; Booker et al., 2004; Crowder and Diplas, 2000a). The behaviour of hydraulic habitat features and how they relate to geomorphological elements observable on large rivers by experienced field practitioners (namely bathymetry and substrate) has been more challenging. The findings of this study provide insights into discharge-related hydrodynamic metric behaviours at locations of different geomorphological complexities on a large, regulated, low-relief river, providing tools for improving the effectiveness of future hydrodynamic and physical aquatic habitat characterizations employing moving-vessel ADCP surveys. More specifically, this study has provided evidence for the occurrence

and absence of macroturbulent flow structures at locations of high and low geomorphological complexity (respectively) in large, low relief rivers, while also highlighting the susceptibility of moving vessel ADCP surveys to such large-scale velocity fluctuations. Further, while the presence of interdependencies between hydrodynamic parameters is not a novel concept, the degree to which simple, directly extractable velocity metrics represent the suite of computed hydrodynamic parameters in this large, low relief river is of consequence for eco-hydraulic researchers. Therefore, the implementation of field collection and data analysis protocols employing increased temporal and spatial resolution of relatively simple hydraulic metrics at locations of high bathymetric and substrate complexity are necessary to adequately characterize hydrodynamics and related aquatic habitat. The increased field effort requirements are offset by the likely sufficiency of reduced spatial and temporal resolution of transects at locations of low bathymetric and substrate complexity. Relating large river, cross-section specific, single-discharge hydraulic variability to geomorphological sub-unit complexity levels by employing repeat transects should be an aim of future studies.

4.0 The role of spatial habitat heterogeneity in walleye (*Sander vitreus*) and lake sturgeon (*Acipenser fulvescens*) critical spawning habitat in a large, northwestern Ontario river

4.1 Introduction

Aquatic ecosystem structure and function is a result of biotic and abiotic factors (Gilliam and Fraser, 2001; Peres-Neto, 2004). Biotic factors include predator-prey interactions, competition for food, and issues involving invasive species, while abiotic factors consist of physical variables such as substrate, water temperature, water quality, flow depth, and current velocity. Of these abiotic components, current velocity and associated hydraulic conditions have often been cited as the most influential on aquatic organism behaviour (Hynes, 1970; Jowett and Duncan, 1990). The spatial and temporal variation of hydraulic conditions within a watercourse are largely related to the flow regime, and the geomorphological structures present, both of which have been subject to widespread anthropogenic alteration.

Dams, in particular, are responsible for a significant proportion of anthropogenic impacts on flow regimes and have had significant impacts on lotic ecosystems (Dynesius and Nilsson, 1994; Ward and Stanford, 1995; Bunn and Arthington, 2002; Murchie et. al., 2008; Sabater, 2008; Poff and Zimmerman, 2010). Some of the specific impacts of dams, i.e., fish passage, stranding, and egg exposure, have been well studied (e.g. Coutant, 2000; Berland et al., 2004; Fisk et al., 2012) and led to the pervasive adoption of minimum low flow requirements for spawning and recruitment of fishes in regulated rivers (Stalnaker et al., 1995; Humphries and Lake, 2000). More recent recognition of natural flow regime variability as an overarching determinant of ecological health and biotic composition has further redefined "environmental flows" to include a naturally diverse set of discharges (Junk et al., 1989; Poff, 1997; Bunn and Arthington, 2002; Poff et al., 2009). However, the natural flow regime of each river is unique (Poff, 1997), and although river-specific environmental flow techniques have improved in recent years (Brown and Joubert, 2003; Annear et al., 2004; Arthington et al., 2004), time requirements for the completion of ecologically meaningful river-specific studies typically exceed those afforded by development and political timeframes (Poff et al., 2009). Moreover, river regulation projects are often subject to multiple management objectives (e.g., flood mitigation, hydropower generation, water supply) which may restrict flexibility to vary flows in accordance with pre-regulation conditions. Even if complete re-introduction of a natural flow regime is possible, anthropogenic development has often caused alteration of river geomorphologies (channelization, floodplain encroachment, levee construction), introducing a new set of boundary conditions and resulting in altered hydraulic habitat conditions throughout the watercourse. With complete reversion to pre-development conditions unlikely, the logical alternative is creation of physical habitat niche conditions required by aquatic organisms under the new flow regime and river configurations.

Accordingly, habitat rehabilitation and ecological flow projects have commonly employed physical models such as PHABSIM (PHysical HABitat SIMulation) and one-dimensional (1-D) or two-dimensional (2-D) hydraulic simulations (HEC-RAS, River2-D) to predict aquatic habitat quality under alternative river regulation and restoration schemes (Bovee, 1982; Stalnaker et al., 1995; Acreman and Dunbar, 2004; O'Shea 2005; Gillenwater et al., 2006, Kelder and Farrell, 2009). These techniques assess habitat quality by comparing simulated hydraulic conditions to pre-determined ranges of physical habitat parameters, such as those provided by Habitat Suitability Index (HSI) curves for substrate, depth, and velocity (Aadland and Kuitunen, 2006; Gillenwater et al., 2006). However, the approach has been criticized as it depends on the validity of the eco-hydraulic HSI relationships being applied (Gore and Nestler, 1988; Freeman et al., 1997; Lowie et al., 2001), and inaccuracies are potentially the root cause of long-term habitat rehabilitation failures (Thompson, 2002; Champoux et al., 2003; Cockerill and Anderson, 2014).

In the past, these eco-hydraulic relationships have been developed under wadable and relatively static flow conditions that consider only point assessments of substrate, depth, and velocity (typically at 60% depth or nose velocity) obtained at observed fish locations and/or regularly spaced cross-sections (Aadland and Kuitunen, 2006; Kelder and Farrell, 2009). The approach neglects both spatial (e.g. macro- and meso-scale hydraulics) and temporal (flood events above channel forming flows) hydraulic and hydrologic influences on spatial habitat heterogeneity (SHH) and habitat quality, which fish and other aquatic organisms are known to utilize (Fausch and White, 1981; Rempel et al., 1999; Crowder and Diplas, 2000b, 2006). Indeed, the idea that increased SHH results in greater biodiversity is one of the most cited concepts in ecological restoration (Power et al., 1995; Ward, 1998; Ward and Tochner, 2001; Fausch et. al., 2002; Thorp et al., 2006; Palmer et al., 2010), and numerous studies have highlighted the value of different habitat niches over large spatial scales used by organisms to fulfill their life cycle (Schlosser, 1991; Schlosser and Angermeier, 1995; Dingle, 1996).

Recognizing the value of SHH, a commonly applied restoration strategy has been to simply increase the structural heterogeneity of the channel, theoretically increasing the resulting hydraulic variability and subsequently elevating biodiversity (Ward, 1998; Baxter and Hauer, 2000; Fausch et al., 2002; Thoms and Parsons, 2002; Thorp et al., 2006). However a recent review by Palmer et al. (2010) found no evidence that solely increasing the structural heterogeneity of the channel (i.e., meanders, boulders, wood, etc.) was the primary factor in controlling stream invertebrate diversity. Therefore, a deeper understanding of the meso-scale hydraulics resulting from geomorphological complexities and their implications for behaviour of aquatic organisms is warranted if restoration concepts such as SHH are to be properly applied (Shamloo et al., 2001; Thompson, 2002; Tritico and Hotchkiss, 2005; Carre et al., 2007; Biron et al., 2009).

Recent technological advances have allowed for efficient field survey of velocities at increased spatial and temporal resolutions [e.g., acoustic Doppler current profilers (ADCPs)] (Simpson, 2001; Oberg et al., 2005). However, the resulting hydraulic characterizations have thus far been related solely to geomorphological channel features (e.g., natural, channelized, and abandoned channels; downstream of weirs or bends) and not to observations from simultaneous biological surveys (Shields et al., 2003; Shields and Rigby, 2005; Chapter 3). Indeed, as both biological and hydraulic research has progressed, it has become widely recognized that inter-disciplinary efforts employing simultaneous surveys of river biology and flow heterogeneity are required to understand the eco-hydraulic relationships needed for effective river management and rehabilitation, including SHH (Power et al., 1995; Maddock, 1999; Shields and Rigby, 2005; Kelder and Farrell, 2009; Cockerill and Anderson, 2014).

This study employed simultaneous fish spawning and hydraulic surveys on a large, low-gradient, regulated river to evaluate the specific physical habitat characteristics influencing spawning behaviour. The specific objectives were i) to determine if discharge-related patterns in physical habitat (as measured by hydrodynamic metrics) could differentiate between walleye (*Sander vitreus*) and lake sturgeon (*Acipenser fulvescens*) spawning and non-significant spawning habitats, and ii) if so, what were the particular types of hydrodynamic metrics (specifically, quantifications of spatial average vs. habitat heterogeneity) that could perform this differentiation. Thus, a comprehensive suite of hydrodynamic metrics at cross-sectional locations throughout the study reach were examined as a means of determining which habitat types were used most heavily for spawning and which habitat types were not used by the species of interest.

4.2 Background

As part of a larger study on the impacts of discharge regime on the Rainy River in northwestern Ontario/northern Minnesota, walleye and lake sturgeon were identified as key species of concern (Kallemeyn et al., 2009). A limiting factor in walleye and lake sturgeon populations is the amount of available spawning habitat, and the success of spawning efforts at said locations (Johnson, 1961; Newburg, 1975; Martin, 2008; Roseman et al., 2011).

Both walleye and lake sturgeon are broadcast spawners, where eggs and sperm are released simultaneously into the water column and fertilized eggs settle to the bottom and into crevices in the substrate (Kerr et al. 1997). Spawning cues are believed to be temperature related for both species (5 – 10^{o}C for walleye, 9 – 18^{o}C for lake sturgeon) (Kerr et al., 1997; Scott and Crossman, 1998; Fortin et al., 2002). Walleye can spawn in lakes or rivers over a variety of substrates, from silt/detritus to boulders/bedrock – however clean gravels and cobbles are believed to be best for egg incubation (Kerr et al., 1997). Flow depths at spawning sites typically range from 0.3 – 1.0 m (Colby et al., 1979; Kerr et al., 1997). Spawning usually occurs in flow velocities of 0.05 – 1.5 m/s and is unlikely in current speeds over 2 m/s (Minor, 1984; Cholmondeley, 1985; Eckersley, 1986). Lake sturgeon typically spawn in fast

flowing rivers below waterfalls, rapids, or dams over a wide variety of hard substrates including hardpan clay, sand, gravels, cobbles, boulders, flat shelving rock, or rip rap (LaHaye et al., 1992; Lane et al., 1996), however clean, rocky substrates with interstitial spaces are widely considered as optimal (Bruch and Binkowski, 2002; Manny and Kennedy, 2002). Spawning can occur over a range of depths (1 – 12 m) but typically occurs in 1 – 6 m of water (LaHaye et al., 1992; Lane et al., 1996; Scott and Crossman, 1998; Manny and Kennedy, 2002; COSEWIC, 2006; Randall, 2008). Flow velocities at spawning sites have been found to range from 0.5 – 2 m/s (LaHaye et al., 2004; Randall, 2008). Where spawning occurs in rivers, the substrate and hydraulic conditions of spawning habitat outlined above for the two species may overlap.

The published physical habitat conditions of walleye and lake sturgeon spawning habitat summarized above are limited to simple variables (depth, velocity, substrate) in traditional point value frameworks which consider the explicit locations of observed fish spawning. Restoration efforts have proceeded accordingly, typically consisting of the introduction of boulder, cobble, and gravel substrates (Johnson, 1961; Pitlo, 1989, Lowie et al., 2001; Katt et al., 2011) and in some cases, targeting optimal depths and velocities (Geiling et al., 1996). However, these frameworks do not account for variation of flow direction or representation of proximal spatial variations in velocity fields (vortices, eddies, velocity gradients, etc.) which offer organisms opportunities to rest, forage, reproduce, take refuge, and of particular interest for this study, spawn (Fausch and White, 1981; Hayes and Jowett, 1994; Jones et al., 2003; Booker et al., 2004). Obtaining velocities at resolutions suitable for heterogenic investigation has been the objective of numerous computer simulation and laboratory studies, however, these often employ simplified river features and produce generalized micro- and meso-scale hydraulic conditions which fail to represent the local and proximal flow patterns exploited by fish and other organisms (Ghanem et al., 1996; Crowder and Diplas, 2000a, 2000b, 2002; Booker, 2003; Gillenwater et al., 2006; Hilldale and Mooney, 2007; Biron et al., 2009; Harrison et al., 2011). Logistical and technological challenges of velocity surveys in large rivers have limited the number of field-based studies acquiring detailed velocity data sufficient for heterogenic characterization (e.g., Shields and Rigby, 2005; Carre et al., 2007). Accordingly, eco-hydraulic linkages considering SHH on a reach scale have historically proved difficult to establish as requisite data quality and resolution is difficult to calculate, and even more difficult to survey (Shields et al. 2003).

Recent advances in acoustic Doppler current profiler (ADCP) technology allow for the efficient field survey of river transects composed of high resolution three-dimensional (3-D) velocity vectors. Originally deployed for the exclusive measurement of river discharge (Gordon 1989; Simpson, 2001; Oberg et al., 2005; Rennie and Rainville, 2006, Oberg and Mueller, 2007), ADCP technology and the 3-D velocity arrays obtained via the moving-vessel method (Muste et al., 2004) have been applied by practitioners in the analyses of hydraulic characteristics, bathymetry, and sediment transport(e.g. Sheilds et. al. 2003; Conaway and Moran 2004; Czuba and Barton 2011; Jamieson et. al. 2011; Guerrerro et. al. 2013).

ADCP velocity assemblages may be further used to investigate the heterogeneity of hydraulic characteristics and subsequent relationships to aquatic habitat (Shields and Rigby, 2005). In addition to spatial variability of basic component velocities, the high-resolution datasets have allowed researchers to compute a wide variety of complex hydraulic metrics for quantifying spatial variations in hydrodynamics, some of which may prove influential in an aquatic habitat context. Examples include expressions of kinetic energy gradients, vorticity, and circulation (Shields et. al., 2003; Shields and Rigby, 2005). Hydraulic variables considered in other eco-hydraulic investigations, such as shear velocity, Reynolds number, Froude number, and dispersion coefficients (Kemp et al., 2000; Shen, 2010; Marchildon 2011) may also be computed from ADCP data. The strength of eco-hydraulic linkages between the above metrics and ecological processes have proven to be variable. For example, Marchildon (2011) showed that some complex variables, e.g., Reynolds number, did not correlate with brown (*Salmo trutta*) and rainbow (*Onchorhynchus mykiss*) trout redd placement while others, such as turbulent kinetic energy, did. Regardless, the increasing evidence that complex hydrodynamic conditions influence habitat quality (e.g., in the distribution of macroinvertebrates – Statzner et al. 1988) has supported the investigation of SHH and its role in ecosystem management.

4.3 Methods

4.3.1 Site Location

The Rainy River is a border river separating northwestern Ontario from northern Minnesota and is the largest tributary to Lake of the Woods (LotW), accounting for 70% of the lake's annual inflow (Eibler and Anderson, 2004). From the outfall of Rainy Lake at the International Falls Dam (IFD) in Fort Frances, ON/International Falls, MN, the river flows westward over an approximate 145 km length before discharging to LotW. The watershed upstream of the IFD is approximately 38 590 km^2 in size, underlain by the Canadian Shield and typified by thin soils with frequently exposed bedrock in forest, bog, and marsh dominated landscapes (Eibler and Anderson, 2004). Below the IFD, the river flows through an ancient lake bed dominated by lacustrine clays and occasional rock outcrops (Eibler and Anderson, 2004; O'Shea, 2005). The river is a recreationally navigable waterway and is predominantly straight and wide (typically 200 – 300 m) with a low water surface elevation (WSE) gradient (< 0.5%). Cross-sectional geometry is typically U-shaped, with visually definable bedforms largely absent except for occasionally interspersed bedrock outcrops.

A 21 km reach bounded at the upstream by the IFD and at the downstream by the Rainy River confluence with the Littlefork River (Figure 4.1) was identified for study by the International Joint Commission (IJC) as a portion of the river for which discharges and resulting hydrodynamics are heavily influenced by dam discharges. The study reach is known to support the spawning and rearing of ecologically significant fish species, including walleye and lake sturgeon (Kallemeyn et al., 2009). Flow rates in the study reach are largely governed by IFD discharges (Q_{IFD}) with

mean and seasonal ranges in flows of 290 m^3/s and 100 – 1000 m^3/s (respectively), resulting in seasonal WSE fluctuations of up to 4 m.

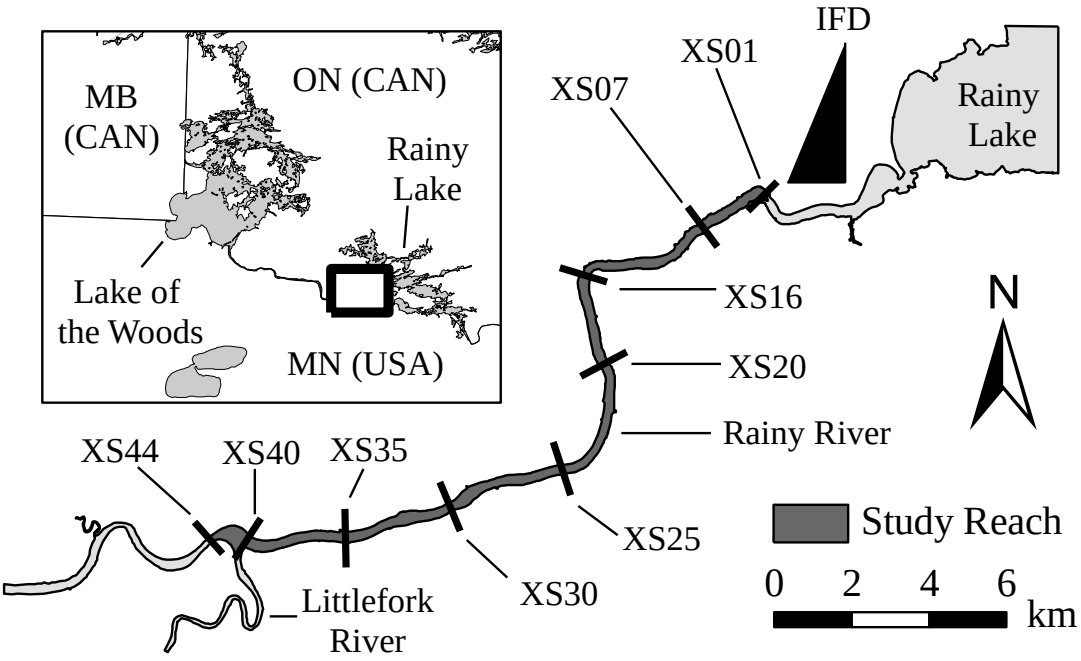

Figure 4.1: Site location (insert) and study reach of the Rainy River bounded at the upstream by the International Falls Dam (IFD and at the downstream by the confluence with the Littlefork River. Significant sampling locations are located at XS01, XS02 and XS16.

4.3.2 Field Data Collection

Parallel biological and hydraulic surveys were performed during April – July 2012 and April – June 2013. Biological sampling consisted of both fish surveys and spawning surveys, each completed in conjunction with Fisheries and Oceans Canada (DFO) for both walleye and lake sturgeon. All sampling was completed during the peak spawning windows for the respective target species in 2012 and 2013; April – early May for walleye, and early May – early June for lake sturgeon. Fish surveys consisted of nighttime boat electrofishing for walleye and lake sturgeon, and overnight setting of 25.4 and 30.5 cm mesh gill nets for lake sturgeon. Boat electrofishing transects were completed moving upstream and total shock time was recorded. Gill nets were set following protocols described in Dubreuil and Cuerrier (1950) (i.e., parallel or at an angle to river flow in currents and back eddies).

At locations where ripe individuals were captured in fish surveys, spawning survey methods were employed to verify successful spawning had occurred. Egg mats were deployed immediately following fish capture, and larval

drift nets were set at downstream locations 5 – 14 days following spawning events (Nichols et al., 2003; Wei et al., 2009).

Hydraulic surveys consisted of ADCP transects obtained at 47 cross-section locations established at approximate 500 m intervals throughout the study reach (spatial resolution increased in areas of morphological heterogeneity). ADCP transects were obtained at 7 – 10 discrete discharges over the range of experienced seasonal flows (100 – 900 m^3/s) at each of the 47 cross-section locations using the moving-vessel method (Muste et. al., 2004), for 427 transects in total. The planform and cross-sectional anatomies of a typical transect are illustrated in Figure 4.2 and Figure 4.3.

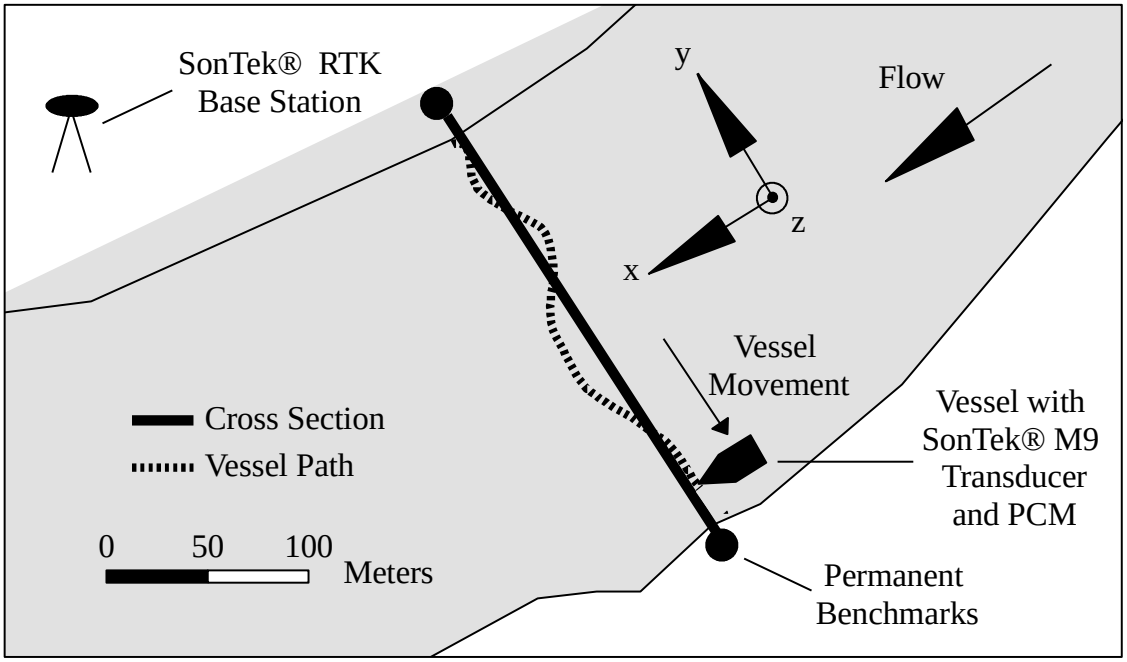

Figure 4.2: Planform schematic of ADCP transect illustrating cross-section straight line from installed permanent benchmarks and ADCP moving vessel path

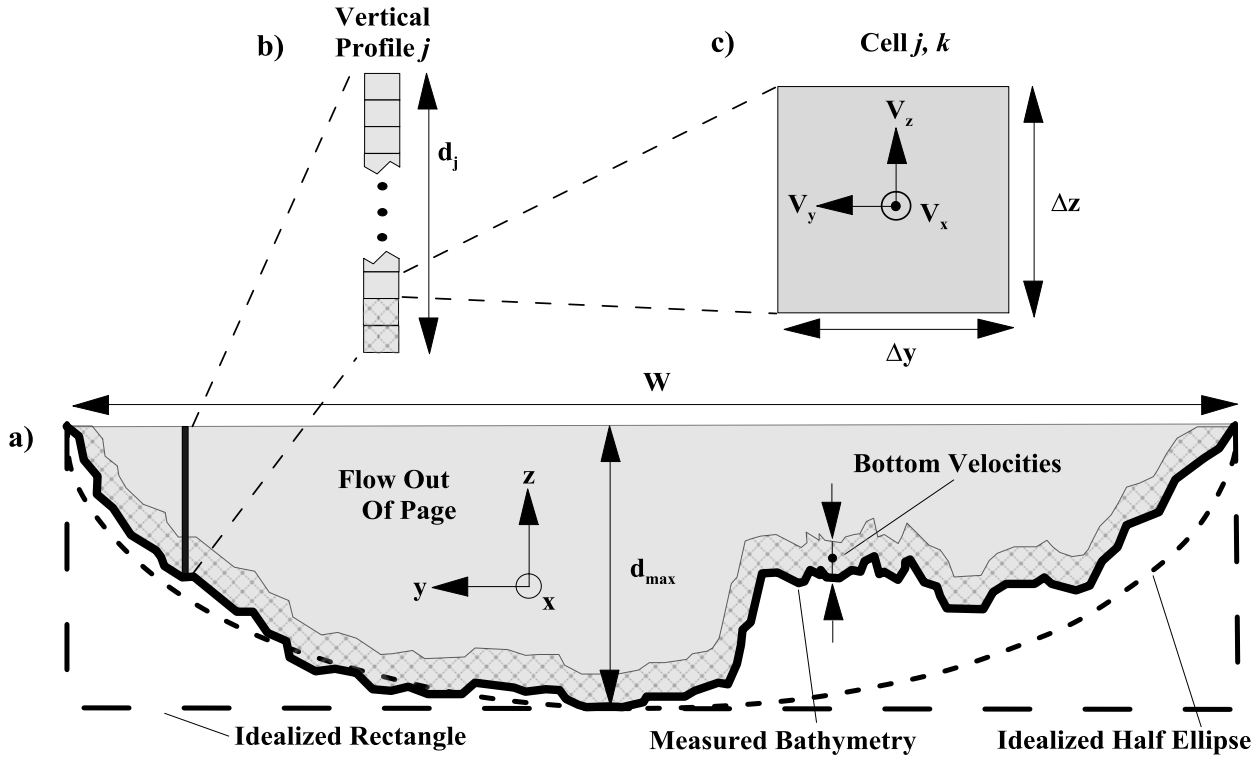

Figure 4.3: Cross-sectional schematic of a) ADCP transect illustrating bathymetry, idealized geometries, bottom velocities, and vertical velocity profile, b) vertical velocity profile illustrating profile depth and velocity cells, and c) velocity cell illustrating component velocities and cell height and width

4.3.3 Data Analysis

At each of the 47 cross-section locations, parallel spawning utilization and hydrodynamic characterizations were completed. Results of egg mat, electrofishing, and gillnet efforts were assigned to the cross-section location of closest proximity. Positive egg mat (EM) % was calculated for each species at each cross-section location according to Equation 4.1, considering results from the entire 2-year sampling program.

$$Positive\ EM\ \% = 100 * (EM_P/EM_T) \quad 4.1$$

where EM_P is the number of EMs found with eggs and EM_T is the total number of EMs deployed over the total number of EMs set. Normalized catch per unit effort ($CPUE_{norm}$) was calculated for each cross-section location as defined in Equation 4.2 considering electrofishing and gillnet captures over the entire 2-year sampling program.

$$CPUE_{norm} = CPUE_{XS}/CPUE_{MAX} \quad 4.2$$

where $CPUE_{XS}$ is the catch per unit effort at cross-section location XS, and $CPUE_{MAX}$ is the maximum $CPUE$ for the species, across all cross-section locations. Cross-sections with $CPUE_{norm}$ in the upper ($CPUE_{norm} \geq 0.75$) quartile were categorized as spawning (S) locations. Non-significant spawning (NS) cross-sections had no positive egg mat results and no catches from electrofishing and gillnet surveys. Cross-sections with $0.25 < CPUE_{norm} < 0.75$ were considered to observe spawning occasionally, however were not included in analysis given the primary objective of this study was identifying the physical habitat characteristics which differentiate between S and NS habitat.

The simultaneous hydraulic characterization consisted of computation of 23 hydraulic "parameters", sourced from past studies in hydraulics, geomorphology, and ecology (e.g., Chow, 1959; Rutherford, 1994; Shields and Rigby, 2005; Sime et al., 2007; Marchildon et al., 2011; Wang et al., 2013). Parameters were considered to represent at least one of the following categories of hydraulic habitat: bathymetry, velocity, flow condition, or velocity variability. Background and potential ecological relevance of each of the 23 parameters are briefly discussed below with calculation methodologies summarized in Table 4.1.

Table 4.1: Summary of computed hydraulic parameters

Metric Class	Parameter	Units	Equation	r	Direct/ Indirect	Metric Values	References
Bathymetry	Depth	m	-	-	Direct	P	-
	Hydraulic Radius	m	$R_h = A_{XS}/P_w$	-	Indirect	T	-
	Depth Ratio	-	$DR = d_{max}/d_{avg}$	-	Direct	T	Fahnestock, 1963
	Width-Depth Ratio	-	$WDR = W/d_{max}$	-	Direct	T	-
	Aspect Ratio	-	$AR = d_{max}/R_h$	-	Indirect	T	Mosley, 2006
	Rectangular Shape Factor	-	$RSF = A_{XS}/(Wd_{max})$	-	Indirect	T	-
	Elliptical Shape Factor	-	$ESF = 4A_{XS}/(\pi W d_{max})$	-	Indirect	T	-
	Depth Gradient	-	$DG_r = \left\lvert \frac{d_j - d_{j+1}}{\Delta s_j} \right\rvert$	median, IQ	Indirect	P	Wang et. al., 2013
Velocity	Cell Velocity	ms^{-1}	V_r	xmedian, xIQ; ymedian, yIQ; zmedian, zIQ; magmedian, magIQ; bxmedian, bxIQ; bymedian, byIQ; bzmedian, bzIQ; bmagmedian, bmagIQ	Direct	C	-
	Shear Velocity	ms^{-1}	$\frac{V_r}{u_{*r}} = \frac{1}{\kappa} ln\left(\frac{d_j}{e\, z_0}\right)$ $\frac{V_r}{u_{*r}} = \frac{1}{\kappa} ln\left(\frac{0.1 d_j}{z_0}\right)$	xmedian, xIQ; bxmedian, bxIQ	Indirect	P	Sime et. al., 2007; Wilcock, 1996
Flow Complexity	Kinetic Energy	Nm^{-1}	$KE_r = \gamma A_{j,k} \frac{V_r^3}{2g}$	magmedian, magIQ; bmagmedian, bmagIQ	Indirect	C	Chow, 1959
	Reynolds Number	-	$RE_r = \frac{\rho V_r R_h}{\mu}$	xmedian, xIQ; bxmedian, bxIQ	Indirect	P	Chow, 1959
	Froude Number	-	$FR_r = \frac{V_r}{\sqrt{g h_d}}$	xmedian, xIQ; bxmedian, bxIQ	Indirect	P	Chow, 1959
Velocity Variability	Velocity Gradient 1	ms^{-2}	$VG1_r \triangleq \left(\frac{V_{r,j+1} + V_{r,j}}{2}\right)\left\lvert \frac{V_{r,j+1} - V_{r,j}}{\Delta s_j} \right\rvert$	xmedian, xIQ; ymedian, yIQ; zmedian, zIQ; magmedian, magIQ; bxmedian, bxIQ; bymedian, byIQ; bzmedian, bzIQ; bmagmedian, bmagIQ	Indirect	P	Shields and Rigby, 2005; Crowder and Diplas, 2005; Crowder and Diplas, 2002; Crowder and Diplas, 2000a
	Velocity Gradient 2	s^{-1}	$VG2_r = \frac{\left(V_{r,j+1} + V_{r,j}\right)\left\lvert \frac{V_{r,j+1} - V_{r,j}}{\Delta s_j} \right\rvert}{V_{r,min}^2}$		Indirect	P	
	Area Weighted Vorticity	s^{-1}	$AWV = \frac{\sum \left\lvert \frac{V_{y,j,k+1} - V_{y,j,k}}{\Delta s_k} - \frac{V_{z,j+1,k} - V_{z,j,k}}{\Delta s_j} \right\rvert \Delta s_j \Delta s_k}{\sum \Delta s_j \Delta s_k}$	y & z; by & bz	Indirect	T	
	Lateral Dispersion Coefficient	-	$DCY = 0.6 u_{*r} d_j$	xmedian, xIQ; bxmedian, bxIQ	Indirect	P	Kim and Muste, 2012; Rutherford, 1994
Velocity	Longitudinal Dispersion Coefficient	-	$DCX = \left[7.428 + 1.775\left(\frac{W}{d_{max}}\right)^{0.620}\left(\frac{u_{*r}}{\bar{V}_r}\right)^{0.572}\right] d_{max} \bar{V}_r \left(\frac{\bar{V}_r}{u_{*r}}\right)$	x, bx	Indirect	T	Kashefipour and Falconer, 2002
Velocity Variability	Velocity Head Coefficient	-	$\alpha_r = \frac{\sum \gamma {V_{j,k}}^3 \frac{A_{j,k}}{2g}}{\gamma \bar{V}_r^3 \frac{A_{CS}}{2g}}$	mag, bmag	Indirect	T	Hulsing, 1966; Chow, 1959

Bathymetry parameters characterized riverbed topography and included depth (D) and hydraulic radius (R_h), five shape factors [depth ratio – DR (Fahnestock, 1963), width-depth ratio – WDR, aspect ratio – AR (Mosley, 2006), rectangular shape factor – RSF, and elliptical shape factor – ESF], and depth gradient – DG. D and R_h were obtained to represent the efficiency of the channel (less flow resistance from riverbed grains/forms). DR (Fahnestock, 1963), WDR, AR (Mosley, 2006), RSF, and ESF were calculated to quantify bathymetric variation for a given cross-section (Fahnestock, 1963; Mosley, 2006). RSF compared transect cross-sectional area to that of an idealized rectangle considering D_{max}; ESF is analogous to RSF however it makes the comparison to an idealized half-ellipse considering D_{max} (both illustrated in Figure 4.3). Irregularity of riverbed bathymetry was characterized by DG, which expresses the slope in riverbed elevation between two adjacent vertical profiles (Wang et. al., 2013).

Velocity parameters included component velocities (V_x, V_y, V_z), current speed (V_{mag}), and shear velocity. V_x, V_y, V_z, and V_{mag} and provided information on flow direction while two versions of shear velocity – considering depth-averaged velocity (u_*) and bottom velocity (u_{*b}) in calculation – characterized near-bed hydraulic conditions (Wilcock 1996; Biron et. al. 2004; Sime et. al. 2007).

Flow condition parameters consisted of kinetic energy (KE), Reynolds number (RE), and Froude number (FR) (Chow, 1959; Gordon et. al., 2006).

Velocity variability parameters included velocity gradient 1 ($VG1$), velocity gradient 2 ($VG2$), area-weighted vorticity (AWV), lateral dispersion coefficient (DCY), longitudinal dispersion coefficient (DCX), and velocity head coefficient (α). $VG1$, $VG2$, and AWV have been specifically applied in past eco-hydraulic investigations using ADCP data (Shields and Rigby, 2005), and were calculated to quantify the energy gradients within the flow field (Crowder and Diplas, 2000a). $VG1$ quantified the drag force acting on a specific object or organism at a given location, distinguishing between non-uniform/uniform flow locations (Crowder and Diplas, 2000a). $VG2$ indicated the energy required for an organism to move from a lower velocity location to a higher velocity location (Crowder and Diplas, 2000a). AWV quantified circulation and vorticity within a cross-sectional plane and portrayed hydraulic behaviour not captured by $VG1$ or $VG2$ (Shields and Rigby, 2005). DCY (Fischer et. al. 1979; Rutherford, 1994) and DCX (Seo and Cheong, 1998; Kashefipour and Falconer, 2002; Shen, 2010) were computed to quantify dispersive capacity – commonly considered in contaminant transport (Seo and Cheong, 1998; Kim and Muste, 2012) and potentially relevant for broadcast spawners such as walleye and lake sturgeon. α, also known as the

kinetic energy or Coriolis coefficient, quantified nonuniformity of cross-sectional flow (Chow, 1959; Hulsing, 1966).

The high-resolution velocity arrays obtained in this study sometimes permitted the computation of various forms of each parameter, as illustrated in Figure 4.4. Where applicable, calculations were performed using the full assemblage of transect velocities as well as those exclusively occurring within 1 m of the riverbed (Figure 4.4a)). The 1 m threshold was considered appropriate given that past eco-hydraulic studies have considered bottom velocities at a distance 0.5 m above the bed (Kieffer and Kynard, 1996; Kynard et. al., 2000) and was consistent with the boundary layer grain roughness represented by $3D_{84}$ of the observed bed material (Julien, 2002). Also where applicable, parameters were calculated using respective component velocities for each of the abovementioned velocity subsets, as illustrated in Figure 4.4b).

4.3.4 Hydraulic Representation

Regarding the physical habitat characteristics computed in this study, the meaning of the terms "parameter" and "metric" differ. Parameters were described in Section 4.3.3 (23 in total), and given the source data provided by the ADCP surveys, could be calculated in numerous ways as illustrated in Figure 4.4a) and Figure 4.4b). Metrics, however, were transect-scale quantifications which summarize the multiple values of a given parameter produced within a given transect and were either a measure of spatial average of the parameter values, or an expression of heterogeneity of the parameter values. Such quantifications were possible where value of a given parameter was calculated for each profile or cell (indicated by "P" or "C" in Table 4.1). In these cases, median and interquartile range (IQ) summarizations of the collection of the given transect's parameter values were calculated as illustrated in Figure 4.4c), applying Equations 4.3a) and 4.3b) (Walpole et. al., 2007).

$$X_{1/m} = \begin{cases} X_{(n+1)(1/m)} & if\ n\ is\ not\ a\ multiple\ of\ m \\ 1/m\left(X_{n(1/m)} + X_{[n(1/m)]+1}\right) & if\ n\ is\ a\ multiple\ of\ m \end{cases} \quad 4.3a)$$

$$X_{IQ} = X_{0.75} - X_{0.25} \quad 4.3b)$$

where X represents the parameter of interest, n is the number of parameter values obtained within the transect, $X_{median} = X_{0.5}$ is the median value, X_{IQ} is the IQ value, and $1/m$ is the percentile (e.g., $1/m =$

0.25 for 25th percentile). Median metrics were considered to characterize the spatial average of a given hydraulic parameter within a transect, while IQ metrics quantified the spatial heterogeneity of a given hydraulic parameter within a transect. Median and IQ statistics were utilized rather than mean and standard deviation to minimize bias of outlier values otherwise not removed by post-processing procedures (Walpole et al., 2007).

Other parameters considered the entire transect in calculation (indicated by "T" in Table 4.1), and therefore were inherently quantifications of the overall cross section characteristics (e.g., R_h). These parameters were considered representative of spatial averages and were termed "single value", or SV, metrics. In total, 83 different metrics (11 SV, 36 median, and 36 IQ) were computed for each of the 427 transects in this study (Table 4.1, Figure 4.4). The specific summarization method (all/bottom velocities, velocity component, median/IQ) of a given metric are indicated by its subscript, *r*, as specified in Table 4.1.

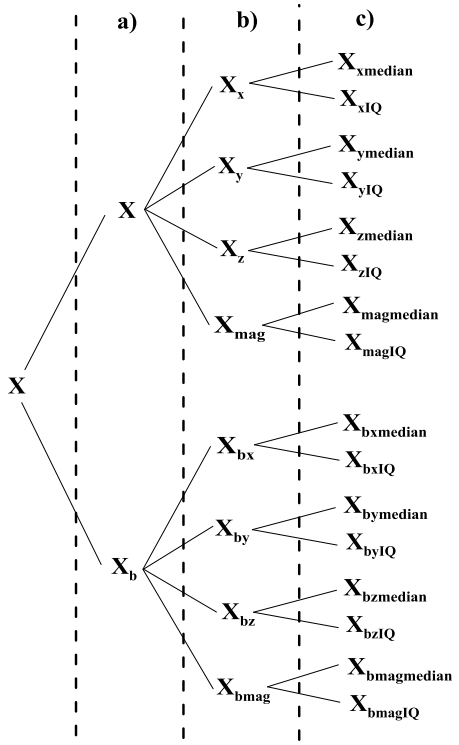

Figure 4.4: Schematic of metric expressions for a given parameter, X, where a pool of values of parameter X is obtained for a given transect, divided sequentially by considering a) all velocities and bottom velocities, b) streamwise (x), lateral (y), vertical (z), and resultant current speed (mag), and c) median and interquartile (IQ) expressions (note: not every parameter will produce all of the 16 metric expressions illustrated; refer to Table 4.1 for applicable expressions, *r*, of each parameter)

Analysis in Chapter 3 demonstrated no significant positive or negative trend in SV, median, and IQ metric values with respect to Q_{IFD}. Therefore, the location and shape of hydrodynamic metrics were adequately quantified by mean (μ) and variance (σ^2) of the 7 – 10 metric values obtained over the range in surveyed discharges. Therefore in total, 47 values of μ and σ^2 were obtained (corresponding to the 47 cross-section locations) for each of the 83 metrics. Therefore hydrodynamic characterization examined the i) average magnitude and ii) inter-discharge variability of metric values at each spatial location, as quantified by (respectively) the mean (μ) and variance (σ^2) of metric values observed over the surveyed range of Q_{IFD} at each cross-section.

Chapter 3 identified a set of 22 metrics which statistically represented the remaining 61 metrics. For the purposes of Chapter 4 here, all 83 of the hydraulic metrics were considered to ensure no eco-hydraulic correlations were overlooked.

4.3.5 Statistical Analysis

In the interest of consistency in methods, significant differences in values of mean μ and σ^2 between S and NS cross-sections were both tested for employing standard ANOVA with post-hoc Tukey tests (Walpole et al., 2007). Parametric statistics were assumed applicable based on visual comparison of σ^2 value quantile distributions in comparison to those of a Gaussian distribution. In most circumstances normality prevailed, however to guard against the implications of minor departures from the Gaussian distribution, non-parametric Kruskal-Wallis tests were run in parallel to parametric standard ANOVAs. This analysis produced identical results in the vast majority (79%) of cases, validating the initial assumption parametric statistics. This analysis was performed individually for each of the 83 hydrodynamic metrics.

Statistical analysis above produced four distinct scenarios representing how strongly the given metric differentiated between S and NS cross-sections. These are best conceptualized in Figure 4.5 depicting metric values (ordinate axis) as a function of Q_{IFD} (abscissa) in a "metric-discharge" plot. Here, each data series (i.e., line) is formed by the metric values for a given cross-section. The two line types in Figure 4.5 distinguish between the patterns of S and NS cross-sections; the magnitude (μ) and inter-discharge variability (σ^2) are indicated by the height on the y-axis and straight/jagged nature of the lines, respectively. Scenario 1 (Figure 4.5a)) occurred where S and NS cross-sections significantly differed in

both their magnitude and inter-discharge variability ($p < 0.05$ for both μ and σ^2), representing the strongest indicators of spawning habitat usage. Scenario 2 (Figure 4.5b), Figure 4.5c)) occurred where the metric magnitudes, but not inter-discharge variability, differed between S and NS cross-sections ($p < 0.05$ for μ, $p > 0.05$ for σ^2). Scenario 3 (Figure 4.5d)) occurred where the inter-discharge variability of metric values, but not magnitude, differed between S and NS cross-sections ($p < 0.05$ for σ^2, $p > 0.05$ for μ). Scenario 2 and Scenario 3 metrics were considered to indicate weaker relationships – their variable nature obscuring any potential conclusions for inclusive metrics. Scenario 4 (Figure 4.5e), Figure 4.5f)) occurred where S and NS cross-sections did not significantly differ in their magnitude or inter-discharge variability ($p > 0.05$ for both μ and σ^2), therefore not providing useful indicators of spawning habitat utilization in any manner.

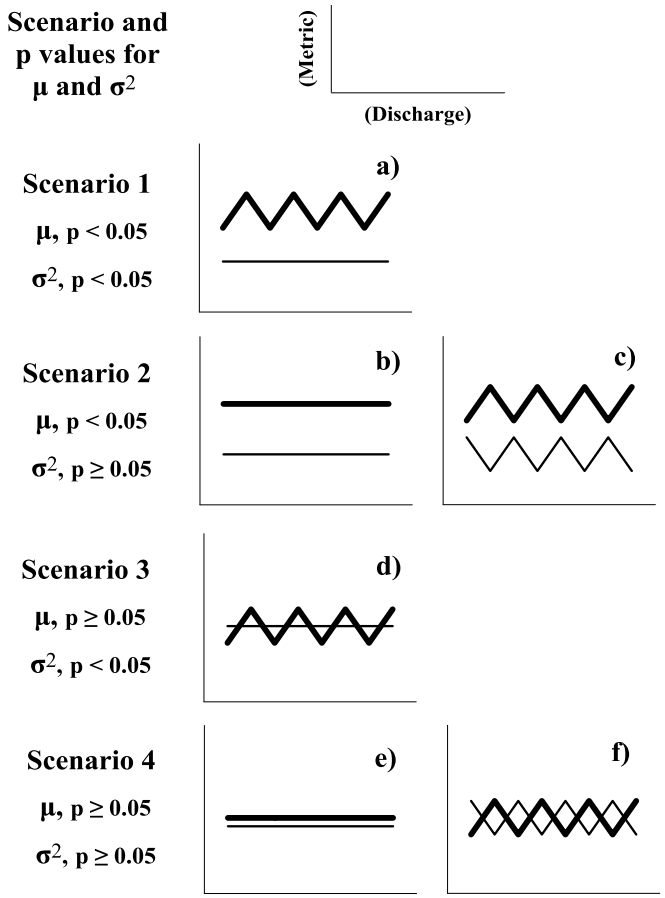

Figure 4.5: Potential scenario classifications according to significant difference ($p < 0.05$) or no significant difference ($p \geq 0.05$) between spawning (S) and no spawning (NS) cross-sections with respect to metric magnitude (μ) and/or inter-discharge variability (σ^2) as illustrated in on conceptual metric-discharge plots (metric values on the ordinate axis, Q_{IFD} on the abscissa)

Spatial averaging metrics (SV and median) total 47 of the 83 metrics, or 56.5% of the metric dataset. Spatial heterogeneity metrics (IQ) total 36 of the 83 metrics, representing 43.5% of the dataset. Deviations from these natural percentage splits within each scenario and/or within each metric class (bathymetry, velocity, flow condition, or velocity variability) in results indicated biasing towards the corresponding types of characterizations.

4.4 Results

Figure 4.6a) and 4.6b) respectively illustrate walleye and lake sturgeon Positive EM% and $CPUE_{norm}$ values for cross sections with positive egg mat results and/or electrofishing and gillnet captures. As indicated on Figure 4.6, 3 cross-sections were significant spawning (S) locations (Positive EM % accompanied by $CPUE_{norm}$ > 0.75), and 4 cross-sections were considered occasional spawning locations. While Positive EM % and $CPUE_{norm}$ for XS03 and XS04 appear to potentially indicate successful spawning, sample sizes were considered too small to classify them as S. The majority (40/47) of the cross-sections did not demonstrate any positive egg or fish capture results, and were considered non-significant spawning (NS) locations and not included in Figure 4.6.

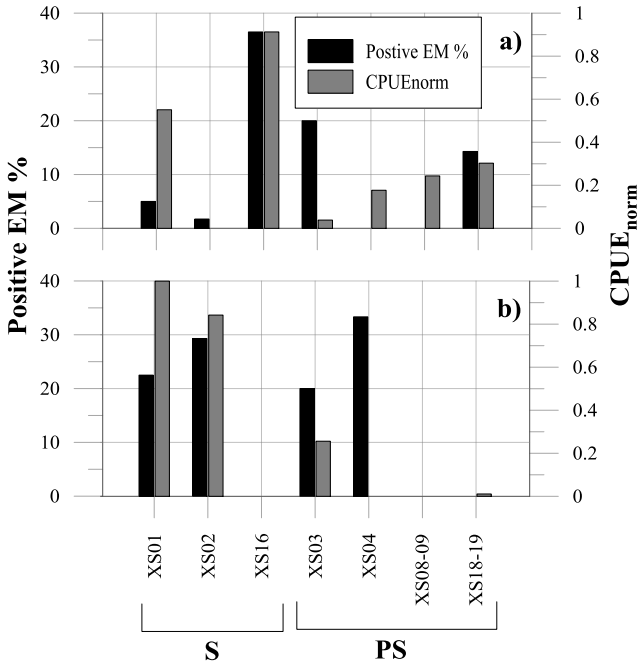

Figure 4.6: Positive egg mat percentages (Positive EM %) and normalized catch per unit effort ($CPUE_{norm}$) for a) walleye and b) lake sturgeon on the Rainy River. 40 non-significant spawning locations (NS) were observed and are not included

Within the set of 83 metrics, 44 (53%) demonstrated significant differences in S and NS for μ and 32 (39%) demonstrated significant differences for σ^2. Table 4.2 summarizes the results of the post-hoc Tukey tests comparing S and NS cross-sections for both μ and σ^2. Scenario classifications according to Figure 4.5 are indicated by shaded black boxes; Scenario 1 metrics are strong statistical differentiators between S and NS habitats, and Scenario 4 metrics do not statistically differentiate between S and NS habitats. A total of 24 (29%) metrics observed significant differences in both μ and σ^2 (Scenario 1). Conversely, there was no significant difference in μ or σ^2 (Scenario 4) in 31 (37%) of cases. A total of 20 (24%) metrics demonstrated Scenario 2, and 8 (10%) demonstrated Scenario 3. Table 4.3 summarizes the number of metrics under each scenario classification by metric class (bathymetry, velocity, flow condition, and velocity variability), and further separates results by metric class (SV, median, or IQ). Findings of these tables are highlighted in the following Sections 4.4.1 and 4.4.2.

4.4.1 Scenario and SV/Median/IQ Totals

The percentage splits between SV, median, and IQ metrics support the importance of SHH in differentiating between spawning habitat utilization for walleye and lake sturgeon, as metrics expressing spatial heterogeneity (IQ) accounted for 20/24 (84%) of the Scenario 1 metrics – almost double the 43.5% natural composition. In contrast, SV and median metrics (representing spatial average) collectively accounted for only 4/20 (16%) of Scenario 1 metrics (much lower than their combined 56.5% natural contribution), and in fact were all indirect quantifications of within-transect spatial heterogeneity (DG_{med}, $VG1_{bzmedian}$, $VG2_{bmagmedian}$, and α). DG characterized the irregularity of the bottom contours (Wang et. al., 2013), $VG1$ distinguished between areas of uniform and non-uniform flow (Crowder and Diplas, 2000a), $VG2$ quantified the energy required for an organism to move from a location of lower velocity to one of higher velocity (Crowder and Diplas, 2000a), and α characterized nonuniformity of cross sectional flow (Hulsing, 1966).

Scenario 2 and Scenario 4 respectively demonstrated 75% and 74% combined SV and median metrics, which are each almost 20% higher than the natural percentage split. As Scenario 2 represents differentiation between S and NS and Scenario 4 does not, this suggests it is difficult to ascertain spawning vs. non-significant spawning habitat using SV and median metrics. The equivalent corollary holds that indicators of spatial heterogeneity (IQ) are observed much more frequently in cases where

differentiation exists between S and NS (28/36 = 78% of IQ metrics present in Scenario 1, Scenario 2, and Scenario 3 as compared to 24/47 = 51% of SV and median metrics).

4.4.2 Scenarios and Hydraulic Metric Classes

Separate analysis (not shown) did not indicate definitive patterns in the scenario presentations with respect to whether the metric was computed considering velocities from the full depth or exclusively the bottom 1 m. This is consistent with results from Chapter 3, where the bottom velocity metrics were consistently correlated with their equivalents applying the full depth of velocities.

The bathymetry metrics calculated in this study were not overly indicative of spawning habitat usage, as 5/10 = 50% were classified as Scenario 4. Non-relationships were especially true for spatial average expressions, as only 1 of the 6 SV bathymetry metrics was not Scenario 4. The few metrics which did present as Scenario 1 provided evidence for the crucial role of SHH in bottom topography in spawning habitat utilization; the only 2 IQ metrics in the bathymetry class (D_{IQ}, DG_{IQ}) both were Scenario 1 and the only other Scenario 1 bathymetry metric (DG_{median}), although a median metric, inherently quantifies the changes, or diversity, in riverbed bathymetry as discussed previously.

The velocity class of metrics also provided support for the importance of SHH in spawning habitat utilization. All of the 7 Scenario 1 velocity metrics were IQ expressions, with no IQ metrics presenting as Scenario 4 (2 IQ metrics were Scenario 2, 1 was Scenario 3). More specifically, spatial heterogeneity (IQ) expressions of streamwise velocities, vertical velocities, and shear velocities (both along the bottom and over the full depth) proved to consistently be indicative of spawning habitat usage. The majority (5/7) of velocity Scenario 2 metrics were SV or median expressions, indicating that spatial average expressions generally would differ in spawning usage with respect to metric magnitude, but not inter-discharge variability. However, this trend may not be reliable as the only 4 Scenario 4 metrics in the velocity class were also median expressions.

Flow condition metrics (KE, RE, FR) have often been the target of past hydraulic investigations of aquatic habitat (e.g., Kemp et. al., 2000; Marchildon et. al., 2011). However, results here do not indicate they are good indicators of spawning habitat usage. Half (6/12) of these metrics presented as Scenario 4 (3 median, 3 IQ), while only 2 (RE_{bIQ},FR_{bIQ}) presented as Scenario 1.

Velocity variability metrics accounted for almost half (40/83) of the full collection of metrics, with most (32/40) being variations of VG1 and VG2 presented by Crowder and Diplas (2000a, 2006). Velocity variability metrics likely predominantly presented as either strong indicators or non-indicators of spawning habitat usage, as the majority were split into either Scenario 1 (12) or Scenario 4 (16) (as compared to 12 for Scenario 2 and 3 combined). Of the Scenario 1 metrics, 9/12 (75%) were IQ quantifications. In contrast, 11/16 (69%) of the Scenario 4 metrics were SV or median quantifications. Therefore for this class of metric, it is the spatial diversity in the variation of velocities which is more indicative of spawning habitat usage, further supporting the importance of spatial heterogeneity over spatial average in habitat considerations.

$VG1$ and $VG2$ have specifically been applied in several eco-hydraulic investigations (Crowder and Diplas, 2000a, Shields and Rigby, 2005; Crowder and Diplas, 2006; Harrison et al., 2011), and theoretically hold excellent promise as indicators of aquatic habitat. Table 4.4 summarizes results for $VG1$ and $VG2$ specifically (analogous to Table 4.3). Patterns are consistent with findings for each of the metric categories: no consistent distinction exists between all velocity and bottom velocity metrics, IQ metrics are typically more prevalent in Scenario 1, and median metrics are more common in Scenario 4 classifications. These findings indicate that these two metrics in particular do not offer any greater relationships with spawning habitat usage than would be found using other parameters.

It is recognized that $VG1$ and $VG2$ may more commonly be calculated using either streamwise velocities or resultant current speeds (e.g., Shields and Rigby, 2005). From Table 4.4, 6 of the 8 VG1 variants employing streamwise or resultant velocities in calculation presented as Scenario 4, and none presented as Scenario 1. In contrast, 5 of the 8 $VG2$ variants using streamwise or resultant velocities were classified as Scenario 1, and only 1 was categorized as Scenario 4. This suggests that $VG2$ provides better indications than $VG1$ if calculated using traditionally applied velocity components.

Table 4.2: Results of standard ANOVA and post-hoc Tukey test analysis, indicating the p values between spawning (S) and no spawning (NS) cross-sections for both metric magnitude (μ) and inter-discharge variability (σ^2). Scenario classifications of each metric are indicated by black boxes.

Metric Class	Code	p for μ	p for σ^2	Scenario				Metric Class	Code	p for μ	p for σ^2	Scenario			
				1	2	3	4					1	2	3	4
Bathymetry	D_{median}	0	0.442		■			Velocity Variability	$VG1_{xmedian}$	0.001	0.804		■		
	D_{iq}	0	0.005	■					$VG1_{xiq}$	0.209	0.997				■
	R_h	0	0.512		■				$VG1_{ymedian}$	0.301	0.438				■
	DR	0.991	0.12				■		$VG1_{yiq}$	0.053	0.002			■	
	WDR	0.597	0.077				■		$VG1_{zmedian}$	0.063	0.001			■	
	AR	0.863	0.123				■		$VG1_{ziq}$	0	0	■			
	RSF	0.738	0.566				■		$VG1_{magmedian}$	0.153	0.475				■
	ESF	0.738	0.566				■		$VG1_{magiq}$	0.688	0			■	
	DG_{median}	0	0	■					$VG1_{bxmedian}$	0.063	0.979				■
	DG_{iq}	0	0.005	■					$VG1_{bxiq}$	0.866	0.788				■
Velocity	$V_{xmedian}$	0	0.567		■				$VG1_{bymedian}$	0.662	0.347				■
	V_{xiq}	0.001	0	■					$VG1_{byiq}$	0.001	0	■			
	$V_{ymedian}$	0.238	0.796				■		$VG1_{bzmedian}$	0.01	0	■			
	V_{yiq}	0.01	0.363		■				$VG1_{bziq}$	0	0	■			
	$V_{zmedian}$	0.205	0.001			■			$VG1_{bmagmedian}$	0.809	0.604				■
	V_{ziq}	0	0.036	■					$VG1_{bmagiq}$	0.542	0.083				■
	$V_{magmedian}$	0.004	0.499		■				$VG2_{xmedian}$	0.345	0.535				■
	V_{magiq}	0.122	0.029			■			$VG2_{xiq}$	0	0	■			
	$V_{bxmedian}$	0	0.774		■				$VG2_{ymedian}$	0.34	0.935				■
	V_{bxiq}	0.011	0	■					$VG2_{yiq}$	0.646	0.971				■
	$V_{bymedian}$	0.71	0.904				■		$VG2_{zmedian}$	0	0.907		■		
	V_{byiq}	0.02	0.051		■				$VG2_{ziq}$	0	0.637		■		
	$V_{bzmedian}$	0.999	0			■			$VG2_{magmedian}$	0	0.729		■		
	V_{bziq}	0.007	0	■					$VG2_{magiq}$	0	0	■			
	$V_{bmagmedian}$	0.013	0.924		■				$VG2_{bxmedian}$	0.345	0			■	
	V_{bmagiq}	0.019	0	■					$VG2_{bxiq}$	0	0.001	■			
	$U_{*median}$	0.063	0.425				■		$VG2_{bymedian}$	0.762	0.994				■
	U_{*iq}	0	0	■					$VG2_{byiq}$	0.852	0.958				■
	$U_{b*median}$	0.539	0.221				■		$VG2_{bzmedian}$	0.035	0.661		■		
	U_{*biq}	0	0	■					$VG2_{bziq}$	0.045	0.527		■		
	DCX	0.015	0.61		■				$VG2_{bmagmedian}$	0	0.004	■			
Flow Condition	KE_{median}	0.299	0.966				■		$VG2_{bmagiq}$	0	0.001	■			
	KE_{iq}	0.862	0.989				■		AWV	0	0.64		■		
	$KE_{bmedian}$	0.306	0.94				■		AWV_b	0.1	0.989				■
	KE_{biq}	0.995	0.789				■		DCY_{median}	0.625	0.806				■
	RE_{median}	0.06	0.712				■		DCY_{iq}	0	0	■			
	RE_{iq}	0.001	0.086		■				$DCY_{bmedian}$	0.994	0.379				■
	$RE_{bmedian}$	0	0.879		■				DCY_{biq}	0	0	■			
	RE_{biq}	0.003	0	■					α	0	0	■			
	FR_{median}	0	0.706		■				$α_b$	0.732	0			■	
	FR_{iq}	0.299	0.911				■								
	$FR_{bmedian}$	0	0.821		■										
	FR_{biq}	0.002	0	■											

Table 4.3: Summary of total number of metrics demonstrating Scenario 1, Scenario 2, Scenario 3, and Scenario 4 for bathymetry, velocity, flow condition, and velocity variability metric classes, further discretized into SV, median, or IQ metric types

	Scenario 1	Scenario 2	Scenario 3	Scenario 4	Total
Bathymetry	3	2	0	5	10
SV	0	1	0	5	6
Median	1	1	0	0	2
IQ	2	0	0	0	2
Velocity	7	7	3	4	21
SV	0	1	0	0	1
Median	0	4	2	4	10
IQ	7	2	1	0	10
Flow Condition	2	4	0	6	12
SV	0	0	0	0	0
Median	0	3	0	3	6
IQ	2	1	0	3	6
Velocity Variability	12	7	5	16	40
SV	1	1	1	1	4
Median	2	4	2	10	18
IQ	9	2	2	5	18
Total	24	20	8	31	83
SV	1	3	1	6	11
Median	3	12	4	17	36
IQ	20	5	3	8	36

Table 4.4: Summary of scenario classifications for $VG1$ and $VG2$ with respect to SV/median/IQ quantifications and computation applying all velocities/bottom velocities

	Scenario 1	Scenario 2	Scenario 3	Scenario 4	Total
VG1	4	1	3	8	16
Median	1	1	1	5	8
IQ	3	0	2	3	8
VG2	5	5	1	5	16
Median	1	3	1	3	8
IQ	4	2	0	2	8
Total	9	6	4	13	32
Median	2	4	2	8	16
IQ	7	2	2	5	16

4.5 Discussion

From the comprehensive suite of hydraulic metrics at the cross-sectional locations examined throughout the study reach it was possible to clearly differentiate between spawning and non-significant spawning locations for both walleye and lake sturgeon. Metrics expressing spatial habitat heterogeneity proved most useful for purposes of differentiating between habitat types; specific examples and potential explanations are discussed in the following sections.

4.5.1 Non-Indicative Metrics

The specific metrics presenting as Scenario 4 are of interest, as many of them have been the subject of past eco-hydraulic investigations. For example, 5 of the 6 SV shape factors (DR, WDR, AR,RSF, and ESF) were all classified as Scenario 4, however these and other expressions of cross-sectional geometry are often the logical target of morphological and habitat investigations owing to their relative ease of calculation (Annable, 1995; Rosgen, 1996; Mosley, 2006). Shear velocity (or the related shear stress) is a commonly computed parameter characterizing hydraulic conditions near the riverbed in sediment transport and hydraulic studies and, more recently, has been investigated in studies investigating aquatic habitat structures relating to their long-term stability (Carre et al., 2007; Biron et al., 2009). Here, the median expressions of u_* and u_{*b} both presented as Scenario 4, however their IQ equivalents both demonstrated Scenario 1 – offering an especially illustrative example of the importance of SHH over

spatial averaging. Various forms of kinetic energy have been the subject of numerous aquatic habitat studies (e.g., Smith and Brannon, 2007; Kozarek et al., 2010; Marchildon et al., 2011; Wang et al., 2013), however in this study, all KE quantifications demonstrated Scenario 4. $VG1$, quantifying the drag force on an organism, was developed specifically for aquatic habitat characterization by Crowder and Diplas (2000a) and has been subsequently applied in eco-hydraulic ADCP studies (Shields and Rigby, 2005), however did not differentiate between S and NS habitats in half (8/16) its variations, in being directly compared to spawning habitat here.

4.5.2 Spatial Habitat Heterogeneity and Large Roughness Elements

The results presented in this study provide a consistent argument for the significance of SHH in walleye and lake sturgeon spawning habitat usage. The prevalence of IQ metrics in Scenario 1, along with the higher percentages of spatial average metrics (SV, median) in Scenario 4 emphasize the importance of maintaining a diversity of hydraulic niches for spawning walleyes and lake sturgeon. The concept of SHH is not entirely new to the biological community, and has been cited previously in literature. Zimmer and Power (2006) recognized that a low tolerance existed for variation at the macrohabitat level, however increased diversity of microhabitats at the mesohabitat scale (as is quantified in this study with IQ metrics) facilitated reduced spawning site competition in brown trout, leading to more successful population-wide spawning. While the majority of walleye and lake sturgeon restoration studies target the satisfaction of site-scale hydraulic spawning characteristics (Geiling et al., 1996; Lowie et al., 2001; Johnson et al., 2006; Roseman et al., 2011; Katt et al., 2011), several more recent projects have considered the role of multiple habitat niches and the value of SHH in overall reproductive success for organisms and ecosystems as a whole (Newbury and Gaboury, 1993; Jones et al., 2003; Palmer et al., 2007; Daugherty et al., 2008).

Many of the results supporting SHH here can be explained by the presence of hydraulic conditions induced by large roughness elements (LREs) such as large boulder clusters, bedrock protrusions, and variation in bathymetry and substrate grain roughness. These features have been correlated with higher fish densities in past works, albeit often in smaller systems (Van Zyll de Jong et. al., 1997; Smith et. al., 2005; Smith and Brannon, 2007). As was discussed in Chapter 3, LREs cause the formation of macroturbulent flow structures such as vortices, boils, and eddies which have been recognized as important hydraulic habitat features (Enders et. al., 2003; Tritico and Hotchkiss, 2005); in some cases, fish have even shown the ability to capture kinetic energy in vortices to economize energy expenditures

(Videler et. al., 1999; Liao et. al., 2003). The macroturbulent flow structures would vary both spatially at a point in time (SHH, increased IQ expressions) and at-a-station between sampling instances (increased σ^2). In observing both increased IQ expressions and, to a lesser degree, inter-discharge variabilities at locations of high spawning habitat utilization, this study has supported the linkages observed between LREs, macroturbulent flow structures, and ecological function observed in smaller watercourses and for other species.

It is interesting to note, however, that in the majority of cases where inter-discharge variability differed between S and NS, so too did inter-discharge metric magnitudes (only 8 Scenario 3 metrics compared to 24 Scenario 1 metrics). This may suggest that walleye and lake sturgeon select locations where higher inter-discharge metric magnitudes would prevent the inter-discharge variations from introducing hydraulic conditions below a given threshold, whether it be spatial average or heterogeneity based.

4.5.3 Comparison to Past Spawning Habitat Studies

Spawning habitat investigations for both walleye and lake sturgeon has typically emphasized substrate type, perhaps rightly so as studies have shown consistent agreement between observed walleye and lake sturgeon spawning habitat and published HSIs with respect to substrate, but less so with depth and velocity (Lowie et al., 2001; Manny and Kennedy, 2002). Corresponding restoration efforts have demonstrated mixed success for walleyes (variable adult abundance increases, but regular increases in live egg densities - Newbury and Gaboury, 1993; Geiling et al., 1996) and good success for lake sturgeon, provided substrate remains clean (Johnson et al., 2006; Roseman et al., 2011). Uncertainties in effectiveness of restoration initiatives are partially due to the variability in methods used to evaluate success (electrofishing, gillnetting, egg surveys, etc.) and duration of post-restoration monitoring, which when combined with region-specific differences in year-to-year hydrological and biological behaviour patterns make definitive conclusions challenging (Geiling et al., 1996; Katt et al., 2011).

Regarding substrate, literature typically has considered clean boulders, cobbles, and gravels with observable interstitial spaces for egg settling as optimal for both walleye and lake sturgeon spawning (Geiling et al., 1996; Lowie et al., 2001; Bruch and Binkowski, 2002; Manny and Kennedy, 2002; Chiotti et al., 2008). While this study did not explicitly specify substrate types of spawning cross-sections, results here do agree with these historical substrate preferences in other ways. The interquartile range of depths in a transect (D_{IQ}) presented as Scenario 1, as did both median and interquartile expressions of

depth gradient (DG_{median} and DG_{IQ}). In each of these three cases, a diversity of larger particle sizes (boulders, cobbles) with void interstitial spaces – considered important for spawning habitat (Chiotti et al., 2008) – would result in larger magnitudes and inter-discharge variabilities which logically correlates to their classification as Scenario 1.

The presence of void interstitial spaces within appropriate substrate has been emphasized repeatedly as a crucial component for both walleye and lake sturgeon spawning habitat (Geiling et al., 1996; Johnson et al., 2006; Roseman et al., 2011). Maintenance of these interstitial spaces would be accomplished by higher flow velocities (which lake sturgeon preferred on a man-made spawning shoal on the Detroit River – Roseman et al., 2011) and/or increased near-bed turbulence (as would occur from barchans/shelves along the bottom at lake sturgeon spawning locations on the Big Manistee River – Chiotti et al., 2008). While not directly quantified in this study, the importance of void interstitial spaces was supported, as metrics representing increased near-bed turbulence and subsequent ability to maintain clean substrate often presented as Scenario 1. LREs associated with increased D_{IQ}, DG_{median}, and DG_{IQ} (all Scenario 1) would work to flush fines away from the spawning location. Other metrics including RE_{bIQ} and FR_{bIQ} (both indicators of the heterogeneity of bottom velocity turbulence) and interquartile ranges of bottom velocity streamwise velocity (V_{bxIQ}), bottom velocity resultant current speed (V_{bmagIQ}), and shear velocity (u_{*IQ}, u_{b*IQ}) (all representations of near-bed hydraulic variability) would also maintain interstitial spaces between particles.

It is conceivable that these substrate-related, site-level restoration measures are actually having a hydraulic impact which is the driving influence behind observed spawning usage preferences. By installing boulder and cobble substrates, LREs and macroturbulent flow structures are induced, working to a) maintain clean substrate and b) introduce SHH at a macro-scale, both of which have heretofore been identified as important components of spawning habitat. Indeed, increased production of larvae (i.e., spawning success) was observed at locations where pool-riffle sequences were introduced, as compared to the existing channelized sections (Newbury and Gaboury, 1993). Therefore, although it hasn't been explicitly been identified in literature thus far, the findings of this and other studies supporting SHH may be one in the same with historical walleye and lake sturgeon restoration approaches, whether the mechanism for spawning usage be purely substrate-related or driven by resulting hydraulics. Therefore, if SHH is the fundamental, overarching component driving spawning habitat usage and success, future restoration efforts should potentially target strategically placed boulder and cobble substrates in order to promote reach-scale diversity in habitat niches. This diversity would allow for spawning, rearing,

juvenile, and adult life stages to all be successful (Jones et al., 2003; Daugherty et al., 2009), and may explain why increased production of walleye larvae was found at introduced pool-riffle sequences in a formerly channelized river reach (Newbury and Gaboury, 1993).

4.6 Conclusions

The importance of relating ecological function with hydraulic classifications and/or quantifications (e.g., Newbury and Gaboury, 1993; Annable, 1995; Rosgen, 1996) will become progressively more important for fisheries management in lieu of increasing development pressures (Zimmer and Power, 2006). Effective ecological management of watercourses depends on the validity of the eco-hydraulic relationships available to decision makers, along with the application of these habitat quantifications in ecologically meaningful frameworks. In this study, the frequent correlation of SHH hydraulic metrics with increased spawning habitat usage provides evidence that proximal diversity in habitat types (SHH) plays a role in walleye and lake sturgeon spawning habitat site selection. The traditional micro- and meso-scale evaluation approach may therefore be overlooking key components influencing walleye and lake sturgeon spawning site selection. This is not to say that past restoration approaches focused on substrate are not valid – SHH through formation of macroturbulent flow structures is produced by the presence of LREs in large rivers, and this corresponds well to historical methods of walleye and lake sturgeon spawning site evaluation/rehabilitation which promote coarse substrate sizes (cobbles, boulders). However, the findings of this study suggest that spawning site selection is potentially influenced not just by larger substrate but also driven by the diversity of hydraulics they introduce, and as such single point measurements are not sufficient when evaluating eco-hydraulics.

5.0 Conclusions and Recommendations

During the open-water seasons of 2012 and 2013, a total of 7 – 10 ADCP transects were obtained over the range in seasonal flows (100 – 900 m^3/s) at 47 cross-section locations on a 21 km reach of the Rainy River in northwestern Ontario, totalling 427 transects in all. For each of the 427 transects, 83 hydrodynamic metric expressions of 23 commonly computed hydraulic parameters were computed. Statistical analysis investigated i) correlations between metrics, ii) discharge-related patterns in spatial average and spatial heterogeneity between locations of different morphological complexities, and iii) correlations with walleye and lake sturgeon spawning habitat use. Eco-hydraulic relationships in iii) employed findings from parallel walleye and lake sturgeon spawning surveys.

As an ancillary byproduct of the field program, an investigation into the global accuracy of nongeorectified RTK-GPS ADCP systems was performed. Global accuracy of a parallel georeferenced RTK-DGPS system was confirmed, and served as the comparator for the nongeorectified GPS system. The nongeorectified system proved to be globally accurate in only 7% of base station setups, however when the setup-specific vertical datum was corrected using the georeferenced RTK-DGPS, 80% of the base station setups demonstrated sufficient global accuracy. Therefore, nongeorectified RTK-GPS ADCP readings should be augmented by georeferenced RTK-GPS survey data if global accuracy is desired.

Chapter 3.0 identified large degrees of correlations in the set of 83 hydrodynamic metrics, identifying a more rudimentary set of 21 "representative" metrics which statistically represented the remaining 61 "correlated" metrics. Only 7 of the 22 representative metrics were considered directly extractable (i.e., simple expressions of depth or velocity components) yet collectively represented 51 of the 61 correlated metrics. Of those 51 metrics, 40 were "indirect" metrics (i.e., requiring computation based on simple measurements of depth and velocity). Therefore, when sufficient spatial coverage is obtained, simple, directly extractable metrics such as those based on current speed (V_{mag}) are statistically representative of the majority of more complex, indirect hydraulic quantifications commonly computed in literature for purposes of sediment transport, contaminant dispersion, and aquatic habitat evaluation.

Statistical analysis indicates hydrodynamics do not trend positively or negatively as a function of discharge; only 5 of 22 representative metrics demonstrated regression slope coefficients significantly different from zero. Rather, sensitivity to discharge was observed in terms of discharge-related variability in metric values at specific cross-section locations. High complexity cross-sections demonstrated higher inter-discharge variation than low complexity cross-sections for 13 of the 22 representative metrics. The

demonstrated stability and lack of trend in metric values at low complexity locations indicates overall insensitive hydraulics at these locations, suggesting lower spatial and temporal frequency of ADCP transects is likely sufficient for hydraulic characterization at these locations. In contrast, large fluctuations in metric values were observed at high complexity cross-sections, likely due to increased presence of LREs and the resulting macroturbulent flow structures (e.g., boils and vortices). This macroturbulence would change based on watercourse discharge, but also temporally at a constant discharge, highlighting the need for increased spatial and temporal frequency of ADCP transects at areas of high geomorphological complexity in order to adequately characterize hydraulics – especially given the instantaneous profiling of ADCPs.

Chapter 4.0 provided evidence supporting the role of spatial habitat heterogeneity in spawning site selection through comparison of the above hydraulic metrics to confirmed locations of walleye and lake sturgeon spawning. For metrics which differentiated between spawning and non-significant spawning locations (Scenario 1), 84% were IQ metrics. Even where SV and median metrics differentiated between S and NS locations, often these were indirect quantifications of SHH, such as for DG_{IQ}. Further, the three high complexity cross-sections from Chapter 3.0 are the same three cross-sections classified as spawning (S) locations in Chapter 4.0. Thus, areas of geomorphological complexity and the presence of LREs causing macroturbulent flow structures (and increased SHH) were more highly used by spawning walleye and lake sturgeon. The above two observations suggest a preference by walleye and lake sturgeon for hydraulic habitat diversity in spawning sites and proximal areas. Therefore, traditionally obtained single point measurements are likely not sufficient when evaluating velocities and hydraulics related to ecological function. However, results here do lend credibility to past walleye and lake sturgeon spawning habitat rehabilitation approaches emphasizing large substrate sizes (cobbles and boulders), which would represent LREs and induce the macroturbulence and SHH correlated with spawning site selection in this study.

Given the above findings, this study recommends that, in large, low-relief rivers, resources be directed towards the collection of easily obtained, directly extractable hydrodynamic metrics at increased spatial and temporal scales at locations of high geomorphological complexity. This may be offset by the reduced spatial and temporal sampling at locations of low geomorphological complexity. Lastly, when evaluating spawning habitat for walleye and lake sturgeon, single point hydraulic measurements are likely insufficient, and increased spatial coverage is necessary to characterize critical components of SHH.

References

Aadland, L.P. and Kuitunen, A. 2006. Habitat suitability criteria for stream fishes and mussels of Minnesota. *Ecological Services Division, Minnesota Department of Natural Resources*, Fergus Falls, MN, 169 pp.

Acreman, M. and Dunbar, M.J. 2004. Defining environmental river flow requirements – a review. *Hydrology and Earth System Sciences* **8**(5), 861 – 876.

Annable, W.K. 1995. Morphological relationships of rural water courses in southwestern Ontario for use in natural channel designs. *M.ASc. Thesis, Faculty of Graduate Studies, University of Guelph,* Guelph, ON, 400 pp.

Annear, T., Chisholm, I., and Beecher, H. 2004. *Instream Flows for Riverine Resource Stewardship, revised ed.*. Instream Flow Council, Cheyenne, WY.

Arthington, A.H., Tharme, R., Brizga, S.O., Puseh, B.J., and Kennard, M.J. 2004. Environmental flow assessment with emphasis on holistic methodologies. In: *Proceedings of the Second International Symposium on the Management of Large Rivers for Fisheries, Vol. II*. (Eds. Welcomme, R. and Petr, T.), 37 – 65.

Babaeyan-Koopaei, K., Ervine, D.A., Carling, P.A., and Cao, Z. 2002. Velocity and turbulence measurements for two overbank flow events in River Severn. *Journal of Hydraulic Engineering* **128**(10), 891 – 900.

Baxter, C.V. and Hauer, F.R. 2000. Geomorphology, hyporheic exchange, and selection of spawning habitat by bull trout (*Salvelinus Confluentus*). *Canadian Journal of Fisheries and Aquatic Sciences* **57**, 1470 – 1481.

Berland, G., Nickelsen, T., Heggenes, J., Okland, F., Thorstad, E.B., and Halleraker, J. 2004. Movements of wild atlantic salmon parr in relation to peaking flows below a hydropower station. *River Research and Applications* **20**, 957 – 966.

Biron, P.M., Carre, D.M., and Gaskin, S.J. 2009. Hydraulics of stream deflectors used in fish-habitat restoration schemes. *WIT Transactions on Ecology and the Environment* **124**, 305 – 314.

Biron, P.M., Robson, C., LaPointe, M.F., and Gaskin, S.J. 2004. Comparing different methods of bed shear stress estimates in simple and complex flow fields. *Earth Surface Processes and Landforms* **29**: 1403 – 1415.

Booker, D.J. 2003. Hydraulic modelling of fish habitat in urban rivers during high flows. *Hydrological Processes* **17**, 577 – 599.

Booker, D.J., Dunbar, M.J., and Ibbotson, A. 2004. Predicting juvenile salmonid drift-feeding habitat quality using a three-dimensional hydraulic-bioenergetic model. *Ecological Modelling* **177**, 157 – 177.

Bovee, K.D. 1982. A guide to stream habitat analysis using the Instream Flow Incremental Methodology. *Instream Flow Information Paper 12, U.S. Fish and Wildlife Service*, Fort Collins, CO, 273 pp.

Bowen, Z.H., Bovee, K.D., and Waddle, T.J. 2003. Effects of flow regulation on shallow-water habitat dynamics and floodplain Connectivity. *Transactions of the American Fisheries Society* **132**, 809 – 823.

Bowlby, J.N. and Roff, J.N. 1986. Trout biomass and habitat relationships in southern Ontario streams. *Transactions of the American Fisheries Society* **115**, 503 – 514.

Brandt, S.A. 2000. Classification of geomorphological effects downstream of dams. *Catena* **40**, 375 – 401.

Brierley, G.J. and Fryirs, K. 2000. River styles, a geomorphic approach to catchment characterization: Implications for river rehabilitation in Bega catchment, New South Wales, Australia. *Environmental Management* **25**(6): 661 – 679.

Brown, C.A. and Joubert, A. 2003. Using multicriteria analysis to develop environmental flow scenarios for rivers targeted for water resource development. *Water SA* **29**, 365 – 374.

Bruch, R. and Binkowski, F. 2002. Spawning behaviour of lake sturgeon (*Acipenser fulvescens*). *Journal of Applied Ichthyology* **18**(4-6), 570 – 579.

Buffin-Belanger, T. and Roy, A.G. 1998. Effects of a pebble cluster on the turbulent structure of a depth-limited flow in a gravel-bed river. *Geomorphology* **23**(3 – 4), 249 – 267.

Bunn, S.E. and Arthington, A.H. 2002. Basic principles and ecological consequences of altered flow regimes for aquatic biodiversity. *Environmental Management* **30**(4), 492 – 507.

Cardinale, B.J., Srivastava, D.S., Duffy, J.E., Wright, J.P., Downing, A.L., Sankaran, M., and Jouseau, C. 2006. Effects of biodiversity on the functioning of trophic groups and ecosystems. *Nature* **443**, 989 – 992.

Carre, D.M., Biron, P.M., and Gaskin, S.J. 2007. Flow dynamics and bedload sediment transport around paired deflectors for fish habitat enhancement: A field study in the Nicolet River. *Canadian Journal of Civil Engineering* **34**(6), 761 – 769.

Ciborowski, J.J.H. 1991. Head tube: a simple device for estimating velocity in running water." *Hydrobiologia* **22**, 109 – 114.

Champoux, O., Biron, P.M., and Roy, A.G. 2003. The long-term effectiveness of fish habitat restoration practices: Lawrence Creek, Wisconsin. *Annals of the Association of American Geographers* **93**(1): 42 – 54.

Chezy, A. 1775. Thesis on the velocity of the flow in a given ditch. *des Ponts et Chaussees, Library in France* **847**, 1915.

Chiotti, J.A., Holtgren, M.J., Auer, N.A., and Ogren, S.A. 2008. Lake sturgeon spawning habitat in the Big Manistee River, Michigan. *North American Journal of Fisheries Management* **28**, 1009 – 1019.

Cholmondeley, R. 1985. Assessment of walleye spawning grounds in the Raising River and Hoople Creek. *File Report, Ontario Ministry of Natural Resources*, Cornwall, ON, 30 pp.

Chow, V.T. 1959. *Open Channel Hydraulics*. McGraw Hill Book Company, Inc., New York, NY.

Christilaw, S. 1996. Bathymetric Automated Survey System Data Collection User Manual. *South Central Science and Technology Unit*, North Bay, ON.

Cockerill, K. and Anderson, W.P. Jr. 2014. Creating false images: Stream restoration in an urban setting. *Journal of the American Water Resources Association* **50**(2), 468 – 482.

Colby, P.J., McNicol, R.E., and Ryder, R.A. 1979. Synopsis of biological data on the walleye. *Fisheries Synopsis No. 119, Food and Agriculture Organization*, Rome, Italy, 139 pp.

Conaway, J.S. and Moran, E.H. 2004. Development and calibration of a two-dimensional hydrodynamic model of the Tanana River near Tok, Alaska." *USGS Open File Report 2004-1225*, Reston, VA, 13 pp.

COSEWIC 2006. COSEWIC assessment and update status report on the lake sturgeon *Acipenser fulvescens* in Canada. *Committee on the Status of Endangered Wildlife in Canada*. Ottawa, ON, 118 pp.

Coutant, C.C. 2000. Fish behaviour in relation to passage through hydropower turbines: A review. *Transactions of the American Fisheries Society* **129**, 351 – 380.

Crowder, D.W. and Diplas, P. 2000a. Evaluating spatially explicit metrics of stream energy gradients using hydrodynamic model simulations. *Canadian Journal of Fisheries and Aquatic Sciences* **57**, 1497 – 1507.

Crowder, D.W. and Diplas, P. 2000b. Using two-dimensional hydrodynamic models at scales of ecological importance. *Journal of Hydrology* **230**, 172 – 191.

Crowder, D.W. and Diplas, P. 2002. Vorticity and circulation: spatial metrics for evaluating flow complexity in stream habitats. *Canadian Journal of Fisheries and Aquatic Sciences* **59**, 633 – 645.

Crowder, D.W. and Diplas, P. 2006. Applying spatial hydraulic principles to quantify stream habitat. *River Resources and Applications* **22**, 79 – 89.

Cunge, J.A., Holly, F.M., and Verwey, A. 1980. *Practical aspects of computational river hydraulics*. Pitman Publishing, Boston, MA.

Czuba, C.R. and Barton, G.J. 2011. Updated one-dimensional hydraulic model of the Kootenai River, Idaho – a supplement to scientific investigations report 2005–5110." *USGS Scientific Investigations Report 2011–5128*, Reston, VA, 36 pp.

Daugherty, D.J., Sutton, R.M., and Elliot, R.F. 2008. Potential for reintroduction of lake sturgeon in five northern Lake Michigan tributaries: A habitat suitability perspective. *Aquatic Conservations: Marine and Freshwater Ecosystems* **18**, 692 – 702.

Daugherty, D.J., Sutton, T.M., and Elliott, R.F. 2009. Suitability modeling of lake sturgeon habitat in five northern Lake Michigan tributaries: Implications for population rehabilitation. *Restoration Ecology* **17**(2), 245 – 257.

Davies, N.M., Norris, R.H., and Thoms, M.C. 2000. Prediction and assessment of local stream habitat features using large-scale catchment characteristics. *Freshwater Biology* **45**, 343 – 369.

Dinehart, R.L. and Burau, J.R. 2005. Repeated surveys by acoustic Doppler current profiler for flow and sediment dynamics in a tidal river." *Journal of Hydrology* **314** (1), 1 – 21.

Dingle, H. 1996. *Migration: The biology of life on the move*. Oxford University Press, Oxford, UK.

Dormann, C.F., Elith, J., Bacher, S., Buchmann, C., Carl, G., Carre, G., Marquez, J.R.G., Gruber, B., Lafourcade, B., Leitao, P.J., Munkemller, T., McClean, C., Osborne, P.E., Reineking, B., Schroeder, B., Skidmore, A.K., Zurell, D., and Lautenbach, S. 2013. Collinearity: A review of methods to deal with it and a simulation study evaluating their performance. *Ecography* **36**, 27 – 46 doi: 10.1111/j.1600-0587.2012.07348.

DuBoys, D. 1879. Le Rhone et les rivieres a lit affoullable. *Annales des Ponts et Chaussees* **5**(18), 141 – 195.

Dubreuil R., and Cuerrier J.P. 1950. Cycle du maturation des glands génitales chez l'esturgeon de lac (*Acipenser fulvescens*, Raf.). *Institut de Biologie géneral et de Zoologie*, Université de Montréal, Montreal, QC.

Dyhouse, G., Hatchett, J., and Benn, J. 2003. Floodplain modeling using HEC-RAS, 1st Edition. *Haestad Methods*, Haestad Press, Waterbury, CT, 696 pp.

Dynesius, M. and Nilsson, C. 1994. Fragmentation and flow regulation of river systems in the northern third of the world. *Science* **266**(5186), 753 – 762.

Dyer, F.J. and Thoms, M.C. 2006. Managing river flows for hydraulic diversity: an example of an uplandregulated gravel-bed river." *River Research and Applications* **22**, 257 – 267.

Eckersley, M. 1986. Assessment of walleye spawning grounds in Hoople Creek. *In 1986 Report of the St. Lawrence Subcommittee to the Lake Ontario Committee, Great Lakes Fishery Commission*, Ann Arbour, MI, 48 pp.

Eibler, J. and Anderson, A. 2004. Upper Rainy River 2002-03. *Division of Fisheries, Minnesota Department of Natural Resources*, International Falls, MN, 89 pp.

Enders, E.C., Boisclair, D., and Roy, A.G. 2003. The effect of turbulence on the cost of swimming for juvenile Atlantic salmon (*Salmo salar*). *Canadian Journal of Fisheries and Aquatic Science* **60**(9), 1149 – 1160.

Fahnestock, R.K. 1963. Morphology and hydrology of a glacial stream – White River, Mount Ranier, Washington. *Geological Survey Professional Paper 422-A*, Washington, D.C., 70 pp.

Fausch, K.D. and White, R.J. 1981. Competition between brook trout (*Salvelinus fontalis*) and brown trout (*Salmo Trutta*) for positions in a Michigan stream. *Canadian Journal of Fisheries and Aquatic Science* **38**, 1220 – 1227.

Fischer, H.B., List, E.J., Koh, R.C., Imberger, J., and Brooks, N.H. 1979. *Mixing in Inland and Coastal Waters*. Academic Press, New York, NY.

Fisk, J.M., Kwak, T.J., Heise, R.J., and Sessions, F.W. 2012. Redd dewatering effects on hatching and larval survival of the robust redhorse. *River Research and Applications* **29**(5), 574 – 581.

Flagg, C.N., and Smith, S.L. 1989. On the use of the acoustic Doppler current profiler to measure zooplankton abundance. *Deep Sea Research Part A: Oceanographic Research Papers* **36** (3), 455 – 474.

Fortin, R., D'Amours, J.D., and Thibodeau, S. 2002. Éffets de l'aménagement d'un nouveau secteur de frayère sur l'utilisation du milieu en période de fraie et sur le succèss de reproduction de l'esturgeon jaune (*Acipenser fulvescens*) à la frayère de la rivière des Prairies. *Rapport synthèse 1995-1999. Pour l'Unité Hydraulique et Environment, Hydro-Québec et la Société de la faune du Québec, Direction de l'aménagment de la faune de Montréal, de Laval et de la Montérégie. Département des Sciences biologiques, Université du Québec à Montréal*. Montreal, QC.

Freeman, M.C., Bowen, Z.H., and Crance, J.H. 1997. Transferability of habitat suitability criteria for fishes in warmwater streams. *North American Journal of Fisheries Management* **17**, 20 – 31.

Geiling, W.D., Kelso, J.R.M., and Iwachewski, E. 1996. Benefits from incremental additions to walleye spawning habitat in the Current River, with reference to habitat modification as a walleye management tool in Ontario. *Canadian Journal of Fisheries and Aquatic Sciences* **53**, 79 – 87.

Gillenwater, D., Granata, T., and Zika, U. 2006. GIS-based modeling of spawning habitat suitability for walleye in the Sandusky River, Ohio, and implications for dam removal and river restoration. *Ecological Engineering* **28**(3), 311 – 323.

Gilliam, J.F. and Fraser, D.F. 2001. Movement in corridors: Enhancement by predation threat, disturbance, and habitat structure. *Ecology* **82**(1), 258 – 273.

Ghanem, A., Steffler, P., Hicks, F., and Katopodis, C. 1996. Two-dimensional hydraulic simulation of physical habitat conditions in flowing streams. *Regulated Rivers: Research & Management* **12**, 185 – 200.

Guegan, J-F., Lek, S., and Oberdorff, T. 1998. Energy availability and habitat heterogeneity predict global riverine fish diversity. *Nature* **391**, 382 – 384.

Guerrerro, M., Di Frederico, V., and Lamberti, A. 2013. Calibration of a 2-D morphodynamic model using water-sediment flux maps derived from an ADCP recording. *Journal of Hydroinformatics* **15**(3), 813 – 828.

Gilbert, G.K. 1914. Transportation of debris by running water. *US Geological Survey Professional paper, 294-B.*

Gordon, N.D., McMahon, T.A., Finlayson, T.A., Gippel, B.L., and Nathan, R.J. 2006. *Stream Hydrology: An Introduction for Ecologists, 2nd Ed.*. John Wiley and Sons, Inc., Chichester, UK.

Gordon, R.L. 1989. Acoustic measurement of river discharge. *Journal of Hydraulic Engineering* **115**(7), 925 – 936.

Gore, J.A. and Nestler, J.M. 1988. Instream flow studies in perspective. *Regulated Rivers: Research and Management* **2**, 93 – 101.

Graf, W.H. 1984. *Hydraulics of sediment transport*. Water Resources Publications, Fort Collins, CO.

Graf, W.L. 2006. Downstream hydrologic and geomorphic effects of large dams on American rivers. *Geomorphology* **79**, 336 – 360.

Guerrero, M., Di Frederico, V., and Lamberti, A. 2013. Calibration of a 2-D morphodynamic model using water-sediment flux maps derived from an ADCP recording." *Journal of Hydroinformatics* **15.3**, 813 – 828.

Harrison, L.R., Legleiter, C.J., Wydzga, M.A., and Dunne, T. 2011. Channel dynamics and habitat development in a meandering, gravel bed river." *Water Resources Research* **47**; W04513, doi:10.1029/2009WR008926.

Herschy, R.W. 1999. *Hydrometry: Principles and Practices, 2nd Ed.* John Wiley and Sons, Chichester, UK.

Herschy, R.W. 2009. *Streamflow Measurement, 3rd Ed.* Taylor & Francis, London, UK and New York, NY.

Hidayat, H., Vermeulen, B., Sassi, M.G., Torfs, P.J.J.F., and Hoitink, A.J.F. 2011. Discharge in a backwater affected river reach. *Hydrology and Earth System Sciences* **15**, 2717 – 2728.

Hilldale, R.C. and Mooney, D.M. 2007. Identifying stream habitat features with a two-dimensional hydraulic model. *Bureau of Reclamation, US Department of the Interior*, Denver, CO, 39 pp.

Hobbs, D.F. 1937. Natural reproduction of quinnat salmon, brown and rainbow trout in certain New Zealand waters. *New Zealand Marine Department of Fisheries Bulleting No. 6*.

Holman, J.P. and Gajda Jr, W.J. 1989. *Experimental Methods for Engineers, 5th Ed.* McGraw-Hill, Blacklick, OH.

Hooper, D.U., Chapin, F.S. III, Ewel, J.J., Hector, A., Inchausti, P., Lavoral, S., Lawton, J.H., Lodge, D.M., Loreau, M., Naeem, S., Schmid, B., Setala, H., Symstad, A.J., Vandermeer, J., and Wardle, D.A. 2005. Effects of biodiversity on ecosystem functioning: A consensus of current knowledge. *Ecolgical Monographs* **75**, 3 – 35.

Hulsing, H., Smith, W., and Cobb, E.D. 1966. Velocity-head coefficients in open channels. *Geological Survey Water-Supply Paper 1869-C*, United States Government Printing Office, Washington, DC. 56 pp.

Humphries, P. and Lake, P.S. 2000. Fish larvae and the management of regulated rivers. *Regulated Rivers Research and Management* **16**, 421 – 432.

Hynes, H.B.N. 1970. *The Ecology of Running Waters.* The Blackburn Press, Caldwell, NJ.

Jamieson, E.C., Rennie, C.D., Jacobson, R.B. and Townsend, R.D. 2011. 3-D flow and scour near a submerged wing dike: ADCP measurements on the Missouri River." *Water Resources Research* **47**, doi: 10.1029/2010WR010043.

Julien, P.Y. 2002. *River Mechanics*. Cambridge University Press, New York, NY.

Junk, W.J., Bayley, P.B., and Sparks, R.E. 1989. The flood pulse concept in river-floodplain systems. *Canadian Special Publication of Fisheries and Qquatic Science* **106**, 110 – 127.

Johnson, J.H., LaPan, S.R., Klindt, R.M., and Schiavone, A. 2006. Lake sturgeon spawning on artificial habitat in the St. Lawrence River. *Journal of Applied Ichthyology* **22**, 465 – 470.

Johnson, F.H., 1961. Walleye egg survival during incubation on several types of bottom in Lake Winnibigoshish, Minnesota, and connecting waters. *Transactions of the American Fisheries Society* **90**, 312 – 322.

Jones, M.L., Netto, J.K., Stockwell, J.D., and Mion, J.B. 2003. Does the value of newly accessible spawning habitat for walleye (*Stizostedion vitreum*) depend on its location relative to nursery habitats? *Canadian Journal of Fisheries and Aquatic Sciences* **60**, 1527 – 1538.

Jowett, I.G. 1997. Instream flow methods: a comparison of approaches." *Regulated Rivers: Research & Management* **13**, 115 – 127.

Jowett, I.G. and Duncan, M.J. 1990. Flow variability in New Zealand rivers and its relationship to in-stream habitat and biota. *New Zealand Journal of Marine and Freshwater Research* **24**(3), 305 – 317.

Kallemeyn, L., Darby, W.R., Eaton, E., Peterson, K., Smokorowski, K., and Van den Broeck, 2009. Plan of study for the evaluation of the IJC 2000 Order for Rainy and Namakan lakes and Rainy River. *Unpublished report prepared for the International Joint Commission by the 2000 Rule Curve Assessment Workgroup*, 55 pp.

Kashefipour, S.M. and Falconer, R.A. 2002. Longitudinal dispersion coefficients in natural channels." *Water Research* **36**, 1596 – 1608.

Katt, J.D., Peterson, B.C., Koupal, K.D., Shoenebeck, C.W., and Hoback, W.W. 2011. Changes in relative abundance of adult walleye and egg density following the addition of walleye spawning habitat in a Midwest irrigation reservoir. *Journal of Freshwater Ecology* **26**(1), 51 – 58.

Kauffman, J.B., Beschta, R.L., Otting, N., and Lytjen, D. 1997. An ecological perspective of riparian and stream restoration in the western United States. *Fisheries, Watershed Restoration* **22**(5), 12 – 24.

Kelder, B.F. and Farrell, J.M. 2009. A spatially explicit model to predict walleye spawning in an eastern Lake Ontario tributary. *North American Journal of Fisheries Management* **29**, 1686 – 1697.

Keller, E.A. 1971. Areal sorting of bed-load material: the hypothesis of velocity reversal. Geological Society of America Bulletin **82**(3), 753 – 756.

Keller, E.A. 1982. Bed material sorting in pools and riffles. *Journal of Hydraulic Engineering* **109**(9), 1243 – 1245.

Kellerhals, R. 1972. *Hydraulic and geomorphic characteristics of rivers in Alberta*. Alberta Cooperative Research Program in Highway and River Engineering, Edmonton, AB.

Kellerhals, R. and Bray, D.I. 1971. Sampling procedures for coarse fluvial sediments. *Journal of Hydraulic Engineering* **103**(HYB), 2265 – 1180.

Kemp, J.L., Harper, D.M., and Crosa, G.A. 2000. The habitat-scale ecohydraulics of rivers. *Ecological Engineering* **16**, 17 – 29.

Kerr, S.J., Corbett, B.W., Hutchinson, J.J., Kinsman, D., Leach, J.H., Puddister, D., Stanfield, L., and Ward, N. 1997. Walleye habitat: A synthesis of current knowledge with guidelines for conservation. *Percid Community Synthesis, Walleye Habitat Working Group, Ontario Ministry of Natural Resources*, Peterborough, ON, 98 pp.

Keulegan, G.H. 1938. Laws of turbulent flow in open channels. *Journal of Research of the National Institute of Standards and Technology* **6**, 707 – 742.

Kieffer, M.C. and Kynard, B. 1996. Spawning of the Shortnose Sturgeon in the Merrimack River, Massachusetts." *Transactions of the American Fisheries Society* **125**: 179 – 186.

Kim, D. and Muste, M. 2012. Multi-dimensional representation of river hydrodynamics using ADCP data processing software. *Environmental Modelling & Software* **38**,158 – 166.

Knighton, A.D. and Nanson, G.C. 2002. Inbank and overbank velocity conditions in an arid zone anastomosing river. *Hydrological Processes* **16**, 1771 – 1791.

Kostaschuk, R., Best, J., Villard, P., Peakall, J., and Franklin, M. 2005. Measuring flow velocity and sediment transport with an acoustic Doppler current profiler. *Geomorphology* **68** (1-2), 25 – 37.

Kozarek, J.L., Hession, W.C., Dolloff, C.A., and Diplas, P. 2010. Hydraulic complexity metrics for evaluating in-stream Brook Trout habitat. *Journal of Hydraulic Engineering* **136** (12): 1067 – 1076.

Kynard, B., Horgan, M., Kieffer, M.C., and Seibel, D. 2000. Habitats used by Shortnose Sturgeon in two Massachusetts rivers, with notes on estuarine Atlantic Sturgeon: a hierarchical approach. *Transactions of the American Fisheries Society* **129**: 487 – 503.

Lacey, R.W.J. and Roy, A.G. 2007. A comparative study of the turbulent flow field with and without a pebble cluster in a gravel-bed river. *Water Resources Research* **43**, W05502, doi: 10.1029/2006WR005027.

Lacey, R.W.J. and Roy, A.G. 2008. The spatial characterization of turbulence around large roughness elements in a gravel-bed river. *Geomorphology* **102**, 542 – 553.

LaHaye, M., Branchaud, A., Gendron, M., Verdon, R., and Fortin, R. 1992. Reproduction, early life history, and characteristics of the spawning grounds of the lake sturgeon (*Acipenser fulvescens* in Des Praires and L'assomption rivers near Montreal, Quebec. *Canadian Journal of Zoology* **70**, 1681 – 1689.

LaHaye, M., Desloges, S., Cote, C., Rice, A., Phillips Jr., S., Deer, J., Giroux, B., de Clerk, K., and Dumont, P. 2004. Search for and characterization of lake sturgeon (*Acipenser fulvescens*) spawning grounds in the upstream portion of the Lachine Rapids, St. Lawrence River, in 2003. *Technical Report 16 – 20E, Ministere des Resources Naturelles, de la Faune et des Parcs, Direction de L'amenagement de la faune de Mondtreal, de Laval et de la Monteregie*, Longueuil, QC, 59 pp.

Lamouroux, N., Olivier, J.M., Persat, H., Pouilly, M., Souchon, Y., and Statzner, B. 1999. Predicting Community Characteristics from Habitat Conditions: Fluvial Fish and Hydraulics. *Freshwater Biology* **42**, 275 – 299.

Lane, J.A., Portt, C.B., and Minns, C.K. 1996. Spawning habitat requirements of Great Lakes fishes. *Canadian Manuscript Report of Fisheries and Aquatic Sciences No. 2368*, Guelph, ON, 55 pp.

Leopold, L. 1970. An improved method for size distribution of stream bed gravel. *Water Resources Research* **6**(5), 1357 – 1366.

Levec, F. 1996. B.A.S.S. Bathymetric Automated Survey System GIS technical guide. *South Central Science and Technology Unit*, North Bay, ON.

Levec, F. and Skinner, A. 2004. Manual of instructions: Bathymetric surveys. *Ontario Ministry of Natural Resources*, Peterborough, ON, 27 pp.

Liao, J.C., Beal, D.N., Lauder, G.V., and Triantafyllou, M.S. 2003. The karman gait: Novel body kinematics of rainbow trout swimming in a vortex street. *Journal of Wxperimental Biology* **206** 1059 – 1073.

Lisle, T.E. 1987. Using "residual depths" to monitor pool depths independently of discharge. *Forest Service, United States Department of Agriculture*, Berkeley, CA, 4 pp.

Lowie, C.E., Haynes, J.M., and Walter, R.P. 2001. Comparison of walleye habitat suitability index (HSI) information with habitat features of a walleye spawning stream. *Journal of Freshwater Ecology* **16**(4), 621 – 631.

Macone, B. 2013. "RE: RiverSurveyor Data Post Processing." bmacone@sontek.com. 8 April, 2013.

Maddock, I. 1999. The importance of physical habitat assessment for evaluating river health. *Freshwater Biology* **41**, 373 – 391.

Manny, B.A. and Kennedy, G.W. 2002. Known lake sturgeon (*Acipenser fulvescens*) spawning habitat in the channel between lakes Huron and Erie in the Laurential Great Lakes. *Journal of Applied Ichthyology* **18**, 486 – 490.

Marceau, G., Morse, B., and Bouchard, G. 1997. Bathymetry in the St. Lawrence. *Sea Technology* **38**(3), 40 – 45.

Marchildon, M.A., Annable, W.K., Power, M., and Imhof, J.G. (2011). A hydrodynamic investigation of Brown Trout (*Salmo trutta*) and Rainbow Trout (*Oncorhynchus mykiss*) redd selection at the riffle scale." *River Research and Applications* doi: 10.1002/rra.1478.

Marriott, F. H. C. 1990. *A Dictionary of Statistical Terms, 5th Edition*. Prepared for the International Statistical Institute, Wiley, New York.

Martin, D.R. 2008. *Habitat selection by spawning walleye and white bass in irrigation reservoirs of the Republican River basin, Nebraska, MS Thesis*. University of Nebraska at Lincoln, Lincoln, Nebraska.

Milan, D.J., Heritage, G.L., Large, A.R.G., and Charlton, M.E. 2001. Stage dependent variability in tractive force distribution through a riffle-pool sequence." *Catena* **44**, 85 – 109.

Minor, J.D. 1984. Seasonal movements and postulated spawning locations of walleyes, *Stizostedion vitreum vitreum*, in Lake Scugog, Ontario, as determined by radiotelemetry. *Ontario Ministry of Natural Resources and the Royal Ontario Museum*, Lindsay, ON.

Mueller, D.S., Abad, J.D., Garcia, C.M., Gartner, J.W., Garcia, M.H., and Oberg, K.A. 2007. Errors in acoustic Doppler profiler velocity measurements caused by flow disturbance. *Journal of Hydraulic Engineering* **133**(12), 1411 – 1420.

Mueller, D.S. 2002. Field asssessment of acoustic-Doppler based discharge measurements. *Hydraulic Measurements and Experimental Methods*, Estes Park, CO; 9 pp.

Murchie, K.J., Hair, K.P.E., Pullen, C.E., Redpath, T.D., Stephens, H.R., and Cooke, S.J. 2008. Fish response to modified flow regimes in regulated rivers: Research methods, effects and opportunities. *River Research and Applications* **24**, 197 – 217.

Muste, M., Yu, K., and Spasojevic, M. 2004. Practical aspects of ADCP data for quantification of mean river flow characteristics; part 1: moving-vessel measurements. *Flow Measurement and Instrumentation* **15**, 1 – 16.

Milhous, R.T., Updike, M.A., and Schneider, D.M. 1989. Physical Habitat Simulation System (PHABSIM) Reference Manual, Version II. *Instream Flow Information Paper No. 26, U.S. Fisheries and Wildlife Service Biological Report 89* (16), Washington, DC., 404 pp.

Montgomery, D.R. and Buffington, J.M. 1997. Chanel-reach morphology in mountain drainage basins. *Bulletin of the Geological Society of America* **109**, 596 – 611.

Monroe, B. and Betteridge, G. 2000. The Algonquin Fisheries Assessment Unit Real-time GPS lake bathymetry system. *Algonquin Fisheries Assessment Unit*, Algonquin Park, ON.

Mosley, P.M. 2006. Semi-determinate hydraulic geometry of river channels, South Island, New Zealand. *Earth Surface Processes and Landforms* **6**(2), 127 – 137.

Muirhead, J.W. and Annable, W.K. 2014. Limitations in extraction of survey data from Real-Time Kinematic GPS (RTK-GPS) ADCP systems. *Journal of Hydraulic Engineering* 10.1061/(ASCE)HY.1943-7900.0000893, 06014012.

Munson, B.R., Young, D.F., and Okiishi, T.H. 1990. *Fundamentals of Fluid Mechanics, 2nd Edition*. John Wiley & Sons, Inc., New York, NY.

Newburg, H.J. 1975. Evaluation of an improved walleye (*Stizostedion vitreum*) spawning shoal with criteria for design and placement. *Minnesota Department of Natural Resources Investigative Report No. 340*, St. Paul, MN.

Newbury, R. and Gaboury, M. 1993. Exploration and rehabilitation of hydraulic habitats in streams using principles of fluvial behaviour. *Freshwater Biology* **29**, 195 – 210.

Nichols, S.J., Kennedy, G., Crawford,E., Allen, J., French III, J., Black, G., Blouin, M., Hickey, J., Chernyák, S., Haas, R., & Thomas, M. 2003. Assessment of lake sturgeon (*Acipenser fulvescens*) spawning efforts in the Lower St. Clair River, Michigan. *Journal of Great Lakes Research* **29**(3): 383 – 391.

Norris, M.J. 2002. Policy and technical guidance on discharge measurements using acoustic Doppler current profilers. *US Geological Survey, Office of Surface Water Technical Memorandum 2002.02*. 4 pp.

O'Neill, M.P. and Abrahams, A.D. 1984. Objective identification of pools and riffles. *Water Resources Research* **20**(7), 921 – 926.

O'Shea, D. 2005. Water management recommendations for the Rainy River. *Stream Habitat Program, Final Advisory Report, Rainy River Peaking Group, Division of Ecological Services, Minnesota Department of Natural Resources*, Saint Paul, MN, 62 pp.

Oberg, K.A. and Mueller, D.S. 2007. Validation of streamflow measurements made with acoustic Doppler current profilers. *Journal of Hydraulic Engineering* **133** (12), 1421 – 1432.

Oberg, K.A., Morlock,. S.E., and Caldwell, W.S. 2005. Quality assurance plan for discharge measurements using acoustic Doppler current profilers. *USGS Scientific Investigations Report* 2005-5183.

Onset Computer Corporation. 2013. *HOBO U20 Water Level Data Logger – U20-001-01*. http://www.onsetcomp.com/products/data-loggers/u20-001-01. Accessed: 05/03/2014.

Ottaway, E.M., Carling, P.A., Clark, A., and Reaer, N.A. 1981. Observations on the structure of brown trout, *Salmo trutta* Linnaeus, redds. *Journal of Fish Biology* **19**, 593 – 607.

Pacific Crest Corporation 2005. *PDL documentation and software*. Pacific Crest Corporation, Santa Clara, CA.

Palmer, M.A., Allan, J.D., Meyer, J.L., and Bernhardt, E.S. 2007. River restoration in the twenty-first century: Data and experiential future efforts. *Restoration Ecology* **15**, 472 – 481.

Palmer, M.A., Menninger, H.L., and Bernhardt, E. 2010. River restoration, habitat heterogeneity and biodiversity: A failure of theory or practice? *Freshwater Biology* **55**, 205 – 222.

Peres-Neto, P.R. 2004. Patterns in the co-occurrence of fish species in streams: The role of site suitability, morphology, and phylogeny versus species interactions. *Oecologia* **140**, 352 – 360.

Pitlo, J. Jr. 1989. Walleye spawning habitat in Pool 13 of the upper Mississippi River. *North American Journal of Fisheries Management* **9**, 303 – 308.

Poff, N.L., Allan, J.D., Bain, M.B., Karr, J.R., Prestegaard, K.L., Richter, B.D., Sparks, R.E., and Stromberg, J.C. 1997. The natural flow regime. *Bioscience* **47**(11), 769 – 784.

Poff, N.L. and Zimmerman, J.K.H. 2010. Ecological responses to altered flow regimes: A literature review to inform the science and management of environmental flows. *Freshwater Biology* **55**, 194 – 205.

Poff, L.N., Richter, B.D., Arthington, A.H., Bunn, S.E., Naiman, R.J., Kendy, E., Acreman, M., Apse, C., Bledsoe, B.P., Freeman, M.C., Henriksen, J., Jacobson, R.B., Kennen, J.G., Merritt, D.M., O'Keeffe, J.H., Olden, J.D., Rogers, K., Tharme, R.E., and Warner, A. 2009. The ecological limits of hydrologic alteration (ELOHA): A new framework for developing regional environmental flow standards. *Freshwater Biology* **55**(1), 147 – 170.

Power, M.E. Dietrich, W.E., and Finlay, J.C. 1995. Dams and downstream aquatic biodiversity: Potential food web consequences of hydrologic and geomorphic change. *Environmental Management* **20**(6), 887 – 895.

Randall, R.G. 2008. Narrative description and quantification of the habitat requirements of Lake Sturgeon, *Acipenser fulvescens* in the Great Lakes and upper St. Lawrence River. *Canadian Science Advisory Secretariat Research Document 2008/015, Department of Fisheries and Oceans*, Burlington, ON, 16 pp.

Rempel, LL., Richardson, J.S., and Healey, M.C. 1999. Flow refugia for benthic macroinvertebrates during flooding of a large river. *Journal of the North American Benthological Society* **18**(1), 34 – 48.

Rennie, C.D. and Church, M. 2010. Mapping spatial distributions and uncertainty of water and sediment flux in a large gravel bed river reach using an acoustic Doppler current profiler. *Journal of Geophysical Research* **115**, F03035,doi:10.1029/2009JF001556.

Rennie, C.D. and Rainville, F. 2006. Case study of precision of GPS differential correction strategies: influence on ADCP velocity and discharge estimates." *Journal of Hydraulic Engineering* **132**(3), 225 – 234.

Rhoads, B.L., Schwartz, J.S., and Porter, S. 2003. Stream geomorphology, bank vegetation, and three-dimensional habitat hydraulics for fish in midwestern agricultural streams." *Water Resources Research* **39**(8), 1218, doi:10.1029/2003WR002294.

Roni, P. and Beechie, T. 2012. *Stream and Watershed Restoration: A Guide to Restoring Riverine Processes and Habitats*, John Wiley and Sons, Chichester, UK.

Roseman, E.F., Manny, B., Boase, J., Child, M., Kennedy, G., Craig, J., Soper, K., and Drouin, R. 2011. Lake sturgeon response to a spawning reef constructed in the Detroit river. *Journal of Applied Ichthyology* **27**(2), 66 – 76.

Rosgen. D. 1996. *Applied River Morphology*. Wildland Hydrology, Pagosa Springs, CO.

Roy, A.G., Buffin-Belanger, T., Lamarre, H., and Kirkbride, A.D. 2004. Size, shape, and dynamics of large-scale turbulent flow structures in a gravel-bed river. *Journal of Fluid Mechanics* **500**, 1 – 27.

Rutherford, J.C. 1994. *River Mixing*. John Wiley & Sons Inc., Chichester.

Sabater, S. 2008. Alterations of the global water cycle and their effects on river structure, function and services. *Freshwater Reviews* **1**, 75 – 88.

Sauer, V.B. Standards for the analysis and processing of surface-water data and information using using electronic methods. *Water Resources Investigations Report 01 – 4044, US Department of the Interior, US Geological Survey*, Reston, VA, 106 pp.

Schlosser, I.J. 1991. Stream fish ecology: A landscape perspective. *Bioscience* **41**, 704 – 712.

Schlosser, I.J. and Angermeier, P.L. 1995. Spatial variation in demographic processes in lotic fishes: Conceptual models, empirical evidence, and implications for conservation. *American Fisheries Society Symposium* **17**, 360 – 370.

Scott, W.B. and Crossman, E.J. 1998. *Freshwater Fishes of Canada*. Galt House Publications Ltd., Oakville, ON, 966 pp.

Seo, I.W. and Cheong, T.S. 1998. Predicting longitudinal dispersion coefficient in natural streams." *Journal of Hydraulic Engineering* **124**(1), 25 – 32.

Shamloo, H., Rajaratnam, R., and Katopodis, C. 2001. Hydraulics of simple habitat structures. *Journal of Hydraulic Research* **39**(4), 351 – 366.

Shen, C., Nui, J., Anderson, E.J., and Phanikumar, M.S. 2010. Estimating longitudinal dispersion in rivers using acoustic Doppler current profilers. *Advances in Water Resources* **33**, 615 – 623.

Shields Jr., F.D., Knight, S.S., Testa, S., and Cooper, C.M. 2003. Use of acoustic Doppler current profilers to describe velocity distributions at the reach scale. *Journal of the American Water Resources Association* **39** (6), 1397 – 1408.

Shields Jr., F.D. and Rigby, J.R. 2005. River habitat quality from river velocities measured using acoustic Doppler current profiler. *Environmental Management* **36**(4), 565 – 575.

Sime, L.C., Ferguson, R.I., and Church, M. 2007. Estimating shear stress from moving boat acoustic Doppler velocity measurements in a large gravel bed river. *Water Resources Research* **43**, W03418, doi: 10.1029/2006WR005069.

Simpson, M.R., and Oltmann, R.N. 1993. Discharge measurement system using an acoustic Doppler current profiler with applications to large rivers and estuaries. *US Geological Survey Water Supply Paper 2395*; 32 pp.

Simpson, M.R. 2001. Discharge measurements using a broad-band acoustic Doppler current profiler. *US Geological Survey Open-File Report 01-1*; 123 pp.

Smith, D.L., Brannon, E.I., and Odeh, M. 2005. Response of juvenile rainbow trout to turbulence produced by prismatoidal shapes. *Transactions of the American Fisheries Society* **134**, 741 – 753.

Smith, D.L. and Brannon, E.L. 2007. Influence of cover on mean column hydraulic characteristics in small pool riffle morphology streams. *River Research and Applications* **23**, 125 – 139.

SonTek 2011. *RiverSurveyor S5/M9 System Manual, Firmware Version 1.0*. SonTek/YSI Incorporated, San Diego, CA.

Stalnaker, C., Lamb, B.L., Henriksen, J., Bovee, K., and Bartholow, J. 1995. The Instream Flow Incremental Methodology: A primer for IFIM. *Biological Report 29, national Biological Service, U.S. Department of the Interior,* Washington, D.C., 53 pp.

Stamhuis, E. and Videler, J. 1995. Quantitative flow analysis around aquatic animals using laser sheet particle image velocimetry. *Journal of Experimental Biology* **198**, 283 – 294.

Statzner, B. and Muller, R. 1989. Standard hemispheres as indicators of flow characteristics in lotic benthos research. *Freshwater Biology* **21**, 445 – 459.

Statzner, B., Gore, J.A., and Resh, V.H. 1988. Hydraulic stream ecology: Observed patterns and potential applications. *Journal of the North American Benthological Society* **7**(4): 307 – 360.

Teledyne RD Instruments (RD Instruments) 2013. *WinRiver II Software User's Guide*. Teledyne RD Instruments Incorporated, Poway, CA, 292 pp.

Thoms, M.C. and Parsons, M. 2002. Eco-geomorphology: An interdisciplinary approach to river science. *International Association of Hydrological Sciences* **276**, 113 – 120.

Thompson, D.M. 2002. Long-term effect of instream habitat-improvement structures on channel morphology along the Blackledge and Salmon rivers, Connecticut, USA. *Environmental Management*, **29**(1), 250 – 265.

Thomson, J.R., Taylor, M.P., Fryirs, K.A., and Brierley, G.J. 2001. A geomorphological framework for river characterization and habitat assessment. *Aquatic Conaservation: Marine and Freshwater Ecosystems* **11**, 373 – 389.

Thorp, J.H., Thoms, M.C., and DeLong, M.D. 2006. The riverine ecosystem synthesis: Biocomplexity in river networks across space and time. *River Research and Applications* **22**, 123 – 147.

Topcon Positioning Systems Inc. (Topcon) 2010. *Sokkia GRX1 Operator's Manual*. Topcon Positioning Systems, Inc., Livermore, CA.

Tritico, H.M. and Hotchkiss, R.H. 2005. Unobstructed and obstructed turbulent flow in gravel bed rivers. *Journal of Hydraulic Engineering* **131**(8), 635 – 645.

US Army Corps of Engineers (USACE) 2007. *Control and topographic surveying*. Engineer Manual: Manual no. 1110-1-1005, Washington, DC.

US Army Corps of Engineers (USACE) 2010. HEC-RAS River Analysis System Hydraulic Reference Manual, Version 4.1. *Hydrologic Engineering Center, US Army Corps of Engineers*, Davis, CA, 417 pp.

Van Zyll de Jong, M.C., Cowx, I.G., and Scruton, D.A. 1997. An evaluation of instream habitat restoration techniques on salmonid populations in a Newfoundland stream. *Regulated Rivers: Research and Management* **13**, 603 – 614.

Videler, J.J., Muller, U.K., and Stamhuis, E.J. (1999). Aquatic vertebrate locomotion: Wakes from body waves. *Journal of Experimental Biology* **202**(23), 3423 – 3430.

Walpole, R.E., Myers, R.H., Myers, S.L., and Ye, K. 2007. *Probability and Statistics for Engineers and Scientists, 8th Edition.* Pearson Prentice-Hall, Upper Saddle River, NJ.

Wang, C., Kynard, B., Wei, Q., Du, H., and Zhang, H. 2013. Spatial distribution and habitat suitability indices for non-spawning and spawning adult Chinese Sturgeons below Gezhouba Dam, Yangtze River: effects of river alterations." *Journal of Applied Ichthyology* **29**, 31 – 40.

Ward, J.V. 1998. Riverine landscapes: Biodiversity patterns, disturbance regimes, and aquatic conservation. *Biological Conservation* **83**(3), 269 – 278.

Ward, J.V. and Standford, J.A. 1995. Ecological connectivity in alluvial river ecosystems and its disruption by flow regulation. *Regulated Rivers: Research & Management* **11**(1), 105 – 109.

Ward, J.V. and Tochner, K. 2001. Biodiversity: Towards a unifying theme for river ecology. *Freshwater Biology* **46**, 807 – 819.

Way, C.M., Burky, A.J., Bingham, C.R., and Miller, A.C. 1995. Substrate roughness, velocity refuges, and macroinvertebrate abundance on artificial substrates in the Lower Mississippi River. *Journal of the North American Benthological Society* **14**, 510 – 518.

Wei Q.W, Kynard B., Yang D. G., Chen X. H., Du1 H., Shen L. and Zhang H. 2009. Using drift nets to capture early life stages and monitor spawning of the Yangtze River Chinese sturgeon (*Acipenser sinensis*). *Journal of Applied Ichthyology* **25**(2), 100 – 106.

Wentworth, C.K. 1922. A scale of grade and class terms for clastic sediments. *Journal of Geology* **30**(5): 377 – 392.

Whiting, P.J. and Dietrich, W.E. 1990. Boundary shear stress and roughness over mobile alluvial beds. *Journal of Hydraulic Engineering* **116**(12), 1495 – 1511.

Wilcock, P.R. 1996. Estimating local bed shear stress from velocity observations. *Water Resources Research* **32** (11), 3361 – 3366.

Witzel, L.D. and MacCrimmon, H.R. 1983. Redd-site selection by brook trout and brown trout in southwestern Ontario streams. *Transactions of the American Fisheries Society* **112**, 760 – 771.

Wolman, M.G. 1954. A method of sampling coarse river-bed material. *Transactions of the American Geophysical Union* **35**(6), 951 – 956.

Wooldridge, C.L. and Hickin, E.J. 2002. Step-pool and cascade morphology, Mosquito Creek, British Columbia: a test of four analytical techniques. *Canadian Journal of Earth Science* **39**, 493 – 503.

Yorke, T.H. and Oberg, K.A. 2002. Measuring river velocity and discharge with acoustic Doppler profilers." *Flow Measurement and Instrumentation* **13**: 191 – 195.

Zimmer, M.P. and Power, M. 2006. Brown trout spawning habitat selection preferences and red characteristics in the Credit River, Ontario. *Journal of Fish Biology* **68**, 1333 – 1346.

Appendix A

Study Reach Hydrology

A.1 Methodology

Evaluating the flow regime under the 2000 Rule Curve is not the focus of this study; rather, it investigates linkages between physical habitat characteristics and spawning habitat. Nonetheless, a general investigation into hydrology in the study reach under the 2000 Rule Curve is warranted for scope purposes.

Environment Canada's Water Survey of Canada provided archived discharges of the Rainy River at Fort Frances (WSC Station 05PC019, located directly downstream of the IFD) from 1906 – 2010 inclusive (WSC, 2013). To examine overall hydrologic behaviour, Log Pearson Type III (LPIII) flow frequency analyses were performed over the entire 105 year period of record, as well as for the time periods corresponding to the different operation regimes of the IFD.

Further hydrologic investigations were limited to 2000 – present, as the 2000 Rule Curve which currently governs IFD discharges was implemented in 2000. Dam operators provided Rainy Lake WSE at the IFD as well as IFD discharge records from 2002 – 2013 (Medina, 2013).

Provided suitable spawning habitat is available, the main concern regarding river regulation is significant fluctuation causing either egg dessication or washout. Walleye and lake sturgeon spawning occurs anywhere during the months of April – June, depending on climatic conditions in the year of interest with an egg incubation period of approximately 3 weeks (COSEWIC, 2006). Considering this 3 week (21 day) period, Q_{IFD} was considered IFD discharge on day 1 (the day where eggs may be dispersed), with Q_{max} and Q_{min} being the maximum and minimum discharges observed within the 3 week window. The maximum and minimum deviation in IFD discharge from the day of egg dispersal were calculated as $Q_{max} - Q_{IFD}$, and $Q_{min} - Q_{IFD}$, respectively, and represented the fluctuation in flow experienced by eggs deposited on day 1. This calculation was performed for each day in a moving time window fashion for the potential spawning months (April, May, June) for 2000 – 2010.

Three HOBO U20 Water Level loggers (Onset Computer Corporation, 2013) were installed at three locations and obtained water levels over various portions of the period of study: 1) at the Fort Frances boat launch (XS07) from October 2011 – October 2013, 2) downstream of the major island/90^{o} bend (XS18) from October 2012 – October 2013, and 3) downstream of the confluence with Littlefork River (XS44) from October 2012 – October 2013. Rating curves were developed according to methods by

Sauer (2002) for these three locations using WSE obtained from HOBO U20 loggers and reported IFD discharges.

A.2 Results

Results of LPIII flow frequency analysis using flow records from Environment Canada are summarized in Table A.1 and Figure A.1.

Table A.1: Rainy River at Fort Frances LPIII Flow Frequency Analysis

Time Period	# of Years	IFD Operating Guideline	Discharge (m^3/s) for Return Period (years)								
			1.0101	1.5	2	5	10	25	50	100	200
1906 - 2010	105	All	136	440	642	942	1112	1297	1415	1519	1611
1906 - 1949	44	Unrestricted	122	320	473	765	981	1278	1515	1764	2027
1950 - 1970	21	1949 Order, 1957 Supplementary Order	219	610	849	1067	1153	1221	1253	1274	1289
1971 - 1999	29	1970 Supplementary Order	271	500	676	926	1089	1292	1440	1586	1733
2000 - 2010	11	2000 Rule Curve	241	510	743	1112	1373	1717	1983	2257	2542

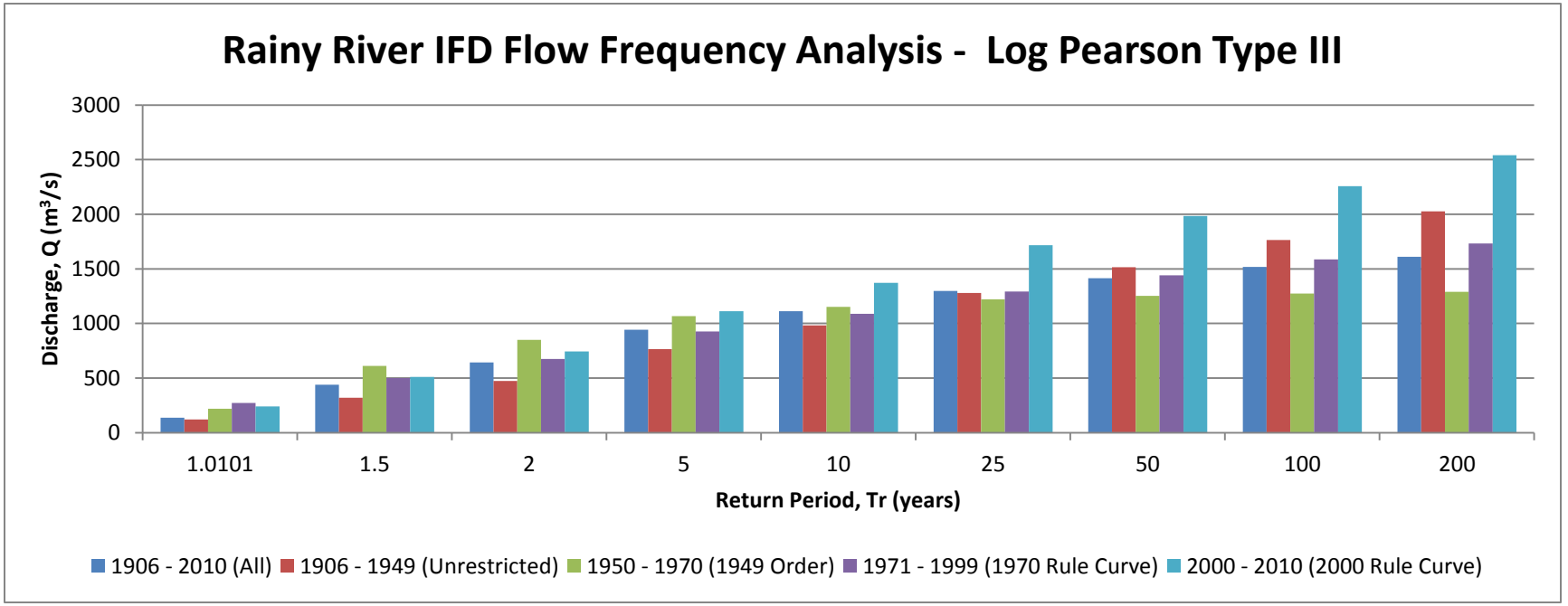

Figure A.1: Rainy River at Fort Frances LPIII Flow Frequency Analysis

Figure A.2 illustrates IFD discharges in comparison to water surface elevations (WSE) for each of the transducer locations. Rating curves and equations at the Fort Frances boat launch (XS07), downstream of the major island/90^{o} bend (XS18), and downstream of the confluence with Littlefork River (XS44) and are illustrated in Figure A.3, Figure A.4, and Figure A.5, respectively. While power curve equations demonstrated $R^2 > 0.9$, regions of outlier data highlight the variability in stage-discharge relationships in the study reach caused by backwater/routing and hysteresis effects.

Figure A.6 illustrates the maximum increase or decrease in IFD discharge in a 3-week floating window from a given day (corresponding to the maximum incubation time for Walleye and Lake Sturgeon eggs (COSEWIC 2006), within the spawning season (May – June) in years 2000 – 2010 (ie; under the 2000 Rule Curve). The observed historical fluctuations may introduce variability in hydraulics; the rate of these changes may be greater than fish would be naturally accustomed to. The fish would choose spawning locations based on the hydraulic habitat conditions present at the time – given the observed variability in hydraulics as a function of IFD discharge, it may be more effective to maintain consistency/slow alteration of flows rather than targeting a specific discharge rate for "optimal" conditions.

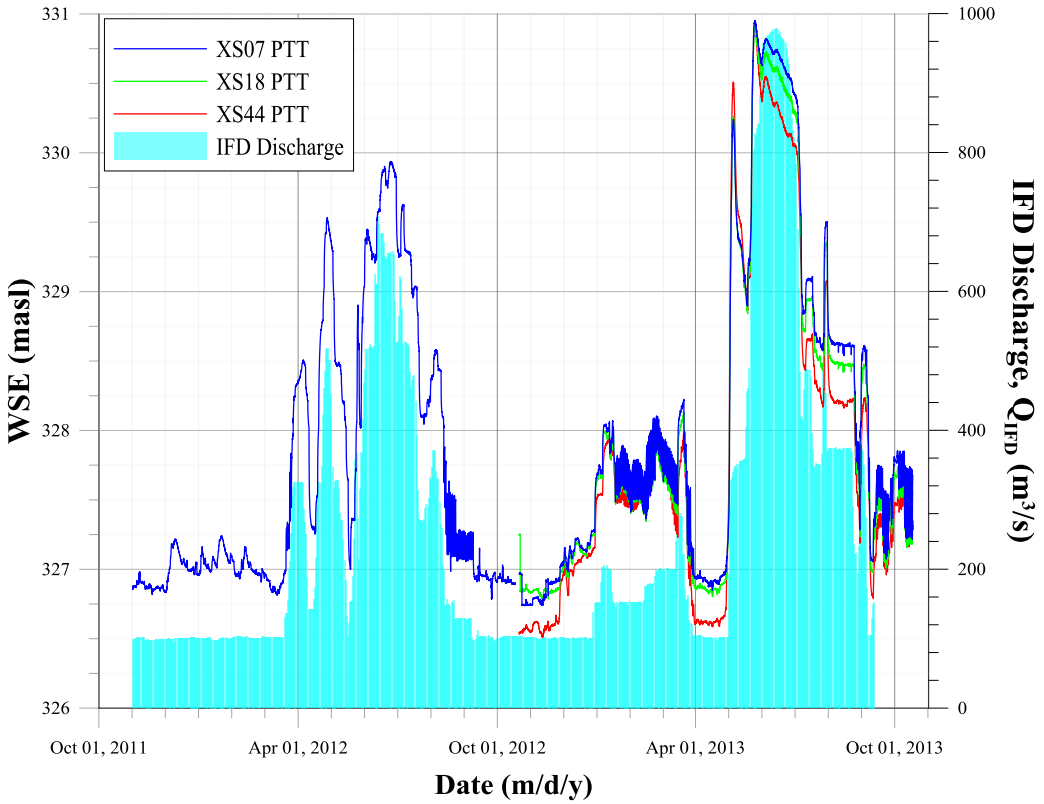

Figure A.2: Rainy River Hydrograph October 2011 – October 2013

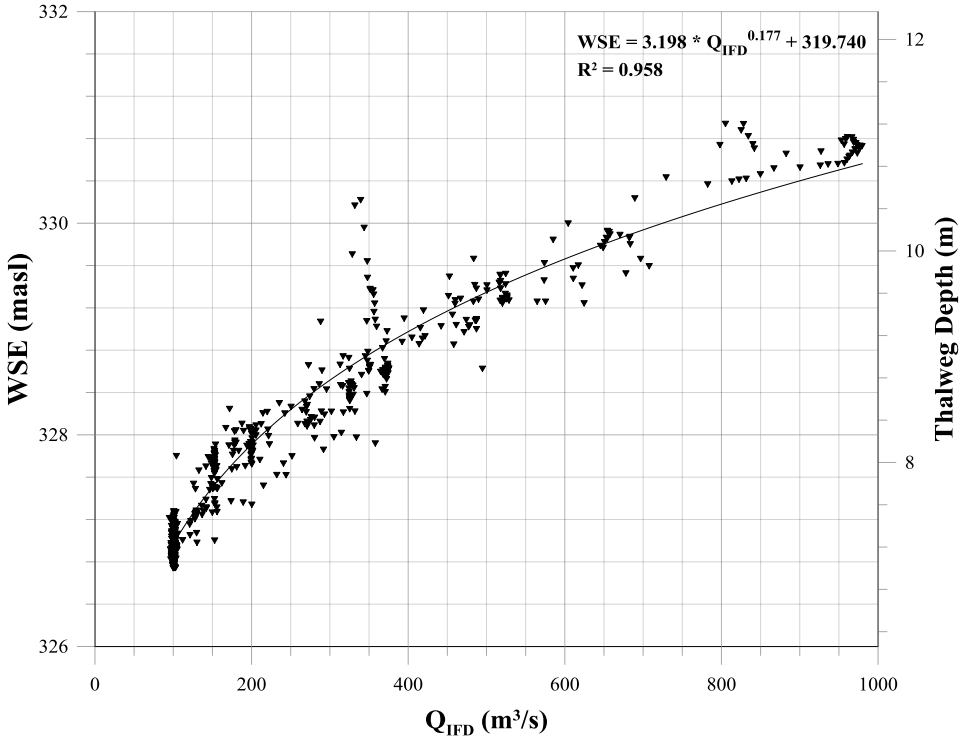

Figure A.3: Rating Curve at Fort Frances Boat Launch (XS07)

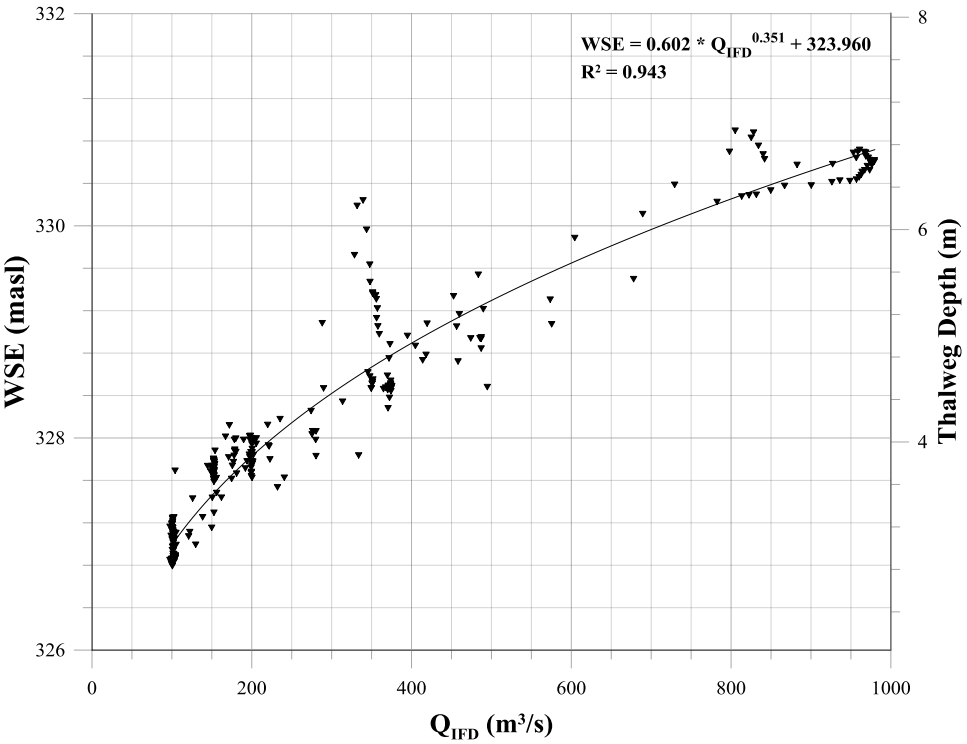

Figure A.4: Rating Curve Downstream of the Major Island/90^{o} Bend (XS18)

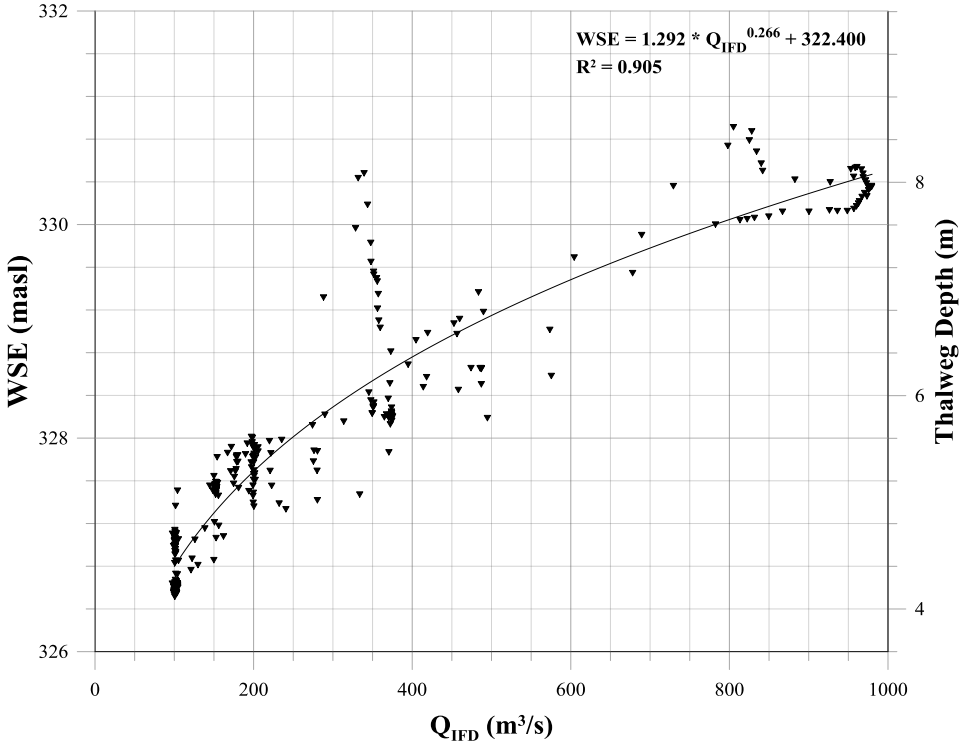

Figure A.5: Rating Curve Downstream of the Confluence with Littlefork River (XS44)

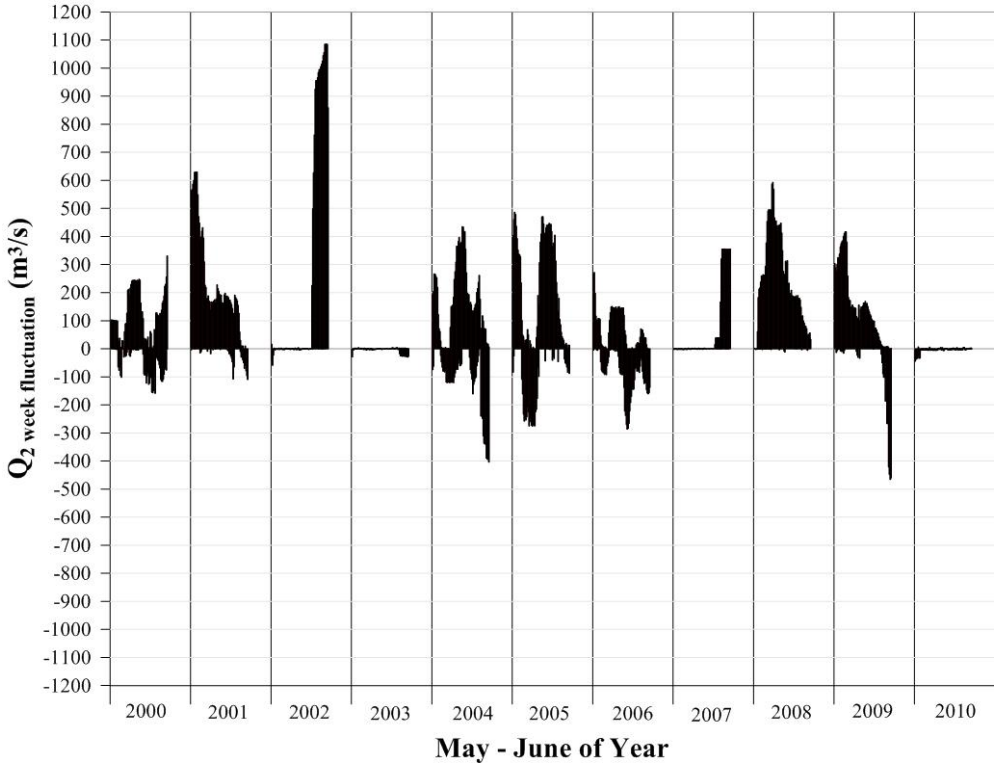

Figure A.6: IFD discharge fluctuations within 3-week floating windows during the spawning months (May – June) of 2000 – 2010

Rainy Lake WSE at the IFD are illustrated with the Rainy Lake 2000 Rule Curve along with Rainy River discharge hydrographs for each year from 2002 – 2013 inclusive are illustrated in Figure A.7 through Figure A.26. Manual inspection of records eliminated conspicuously outlying data resulting in the observed discontinuities. Plots for 2008 and 2009 are not shown due to poor quality data. The Rainy Lake WSE plots illustrate overall consistent satisfaction of the 2000 Rule Curve in the majority of the years. However, hydrograph patterns in the Rainy River fail to demonstrate the same degree of consistency, highlighting the unnatural seasonal flow patterns resulting from the lack of direct regulation of Rainy River flows.

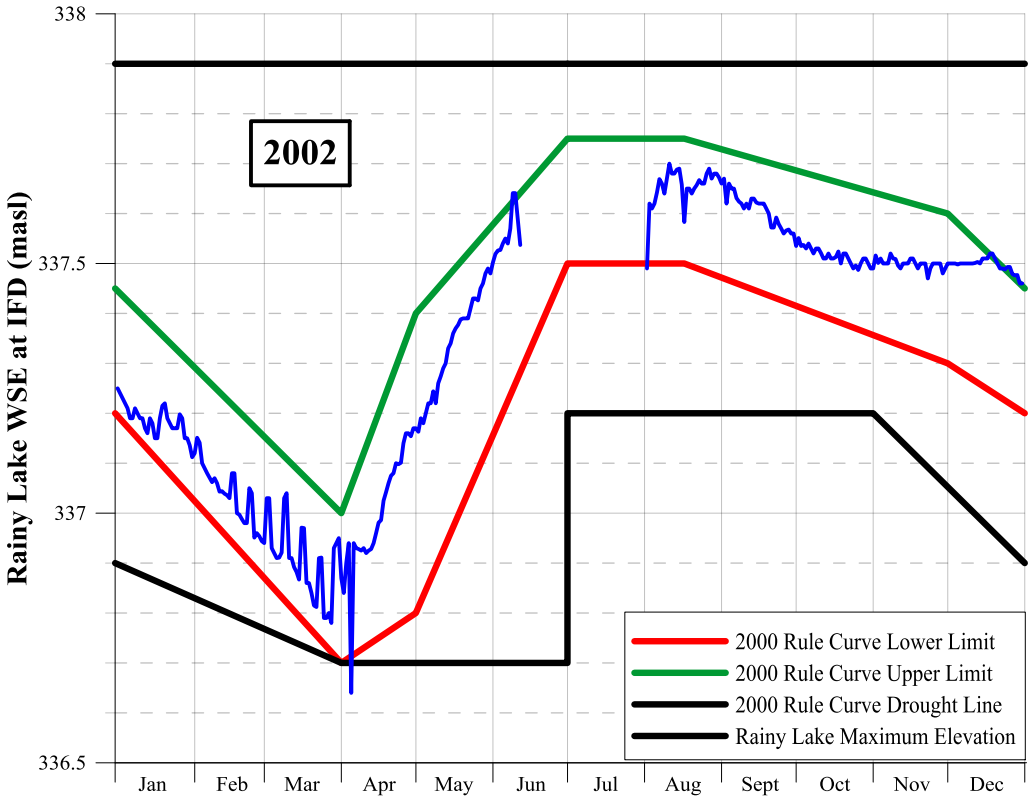

Figure A.7: 2002 Rainy Lake WSE at IFD and 2000 Rule Curve

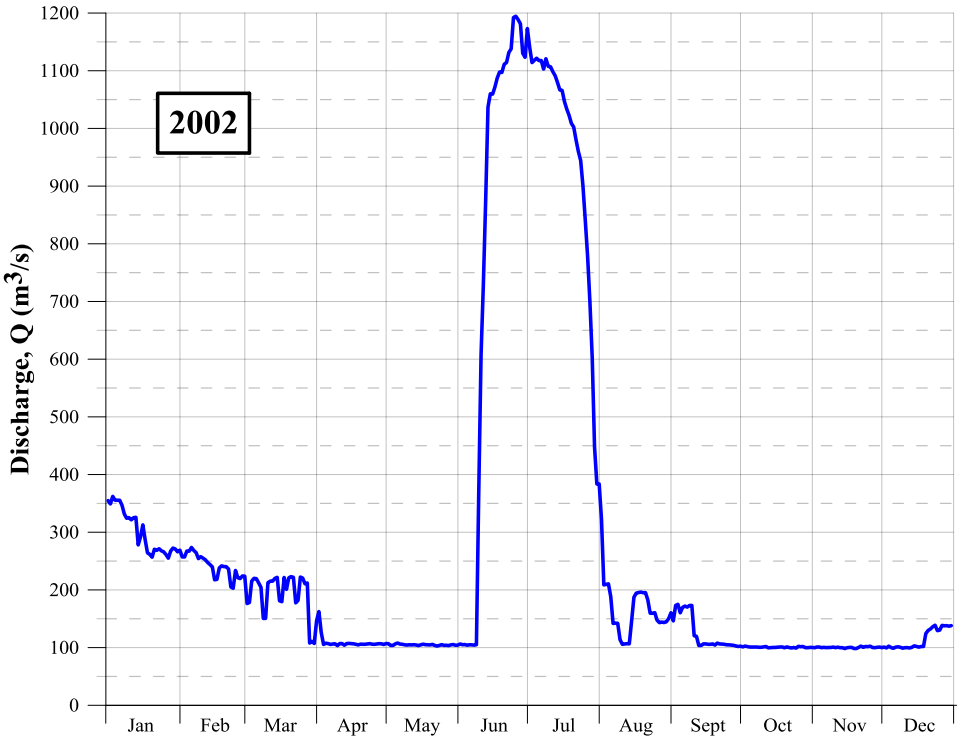

Figure A.8: 2002 Rainy River Hydrograph

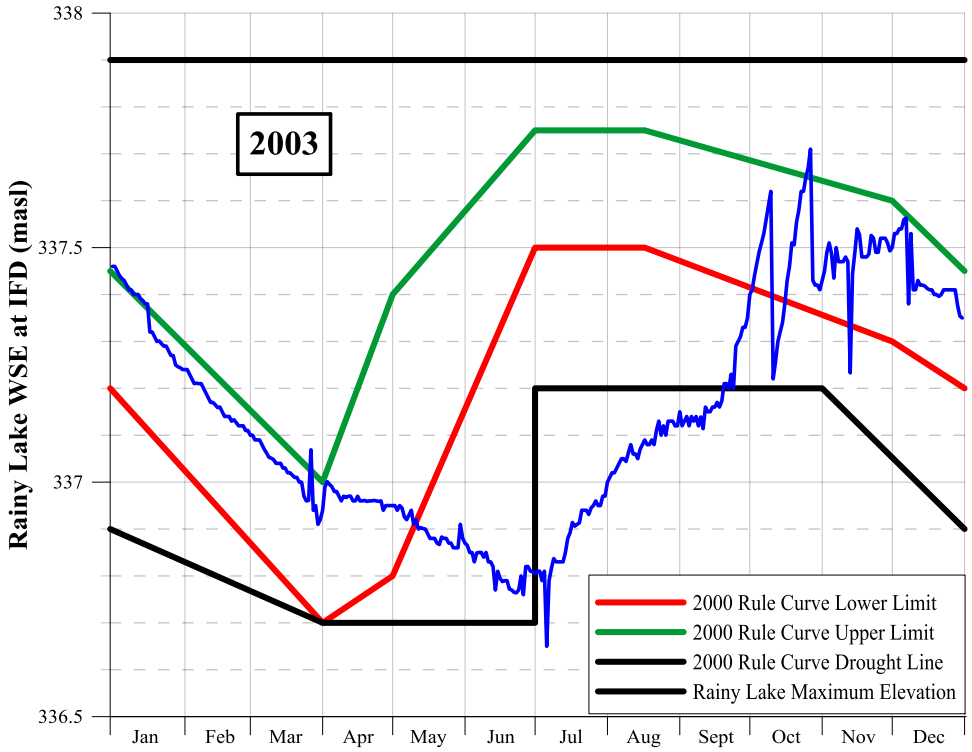

Figure A.9: 2003 Rainy Lake WSE at IFD and 2000 Rule Curve

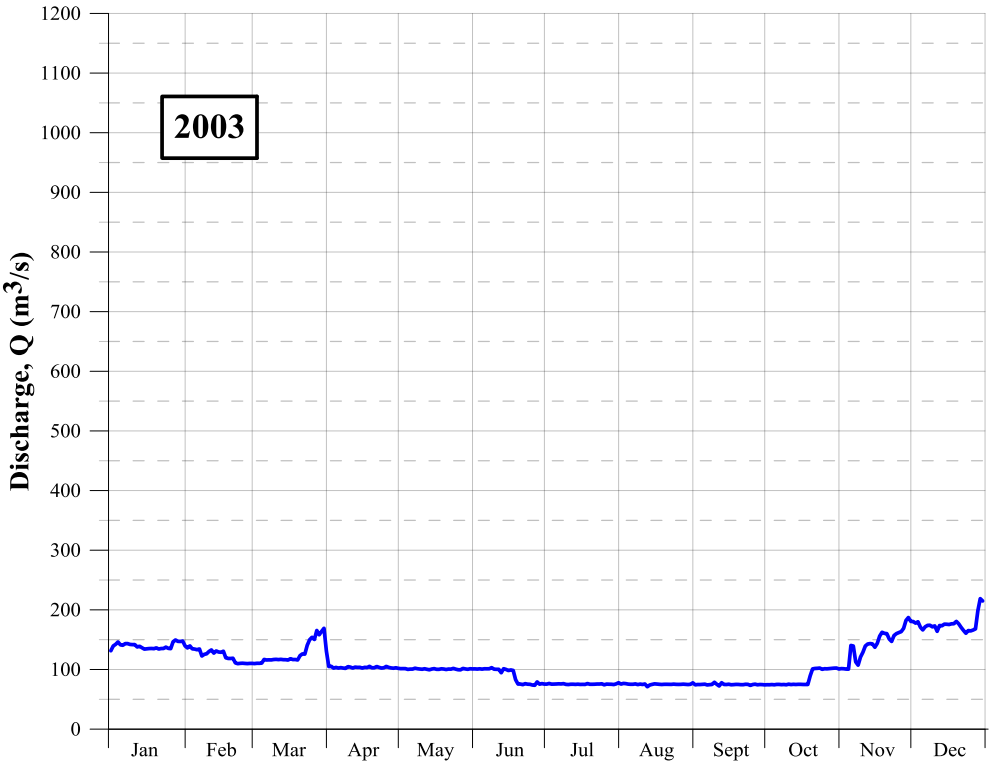

Figure A.10: 2003 Rainy River Hydrograph

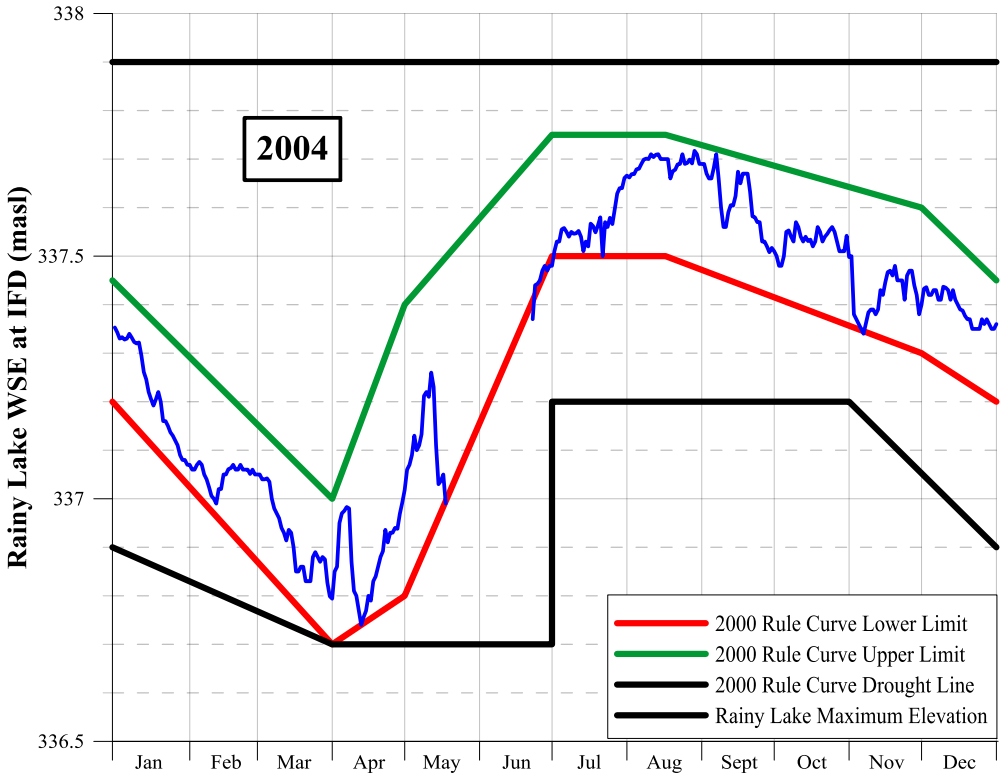

Figure A.11: 2004 Rainy Lake WSE at IFD and 2000 Rule Curve

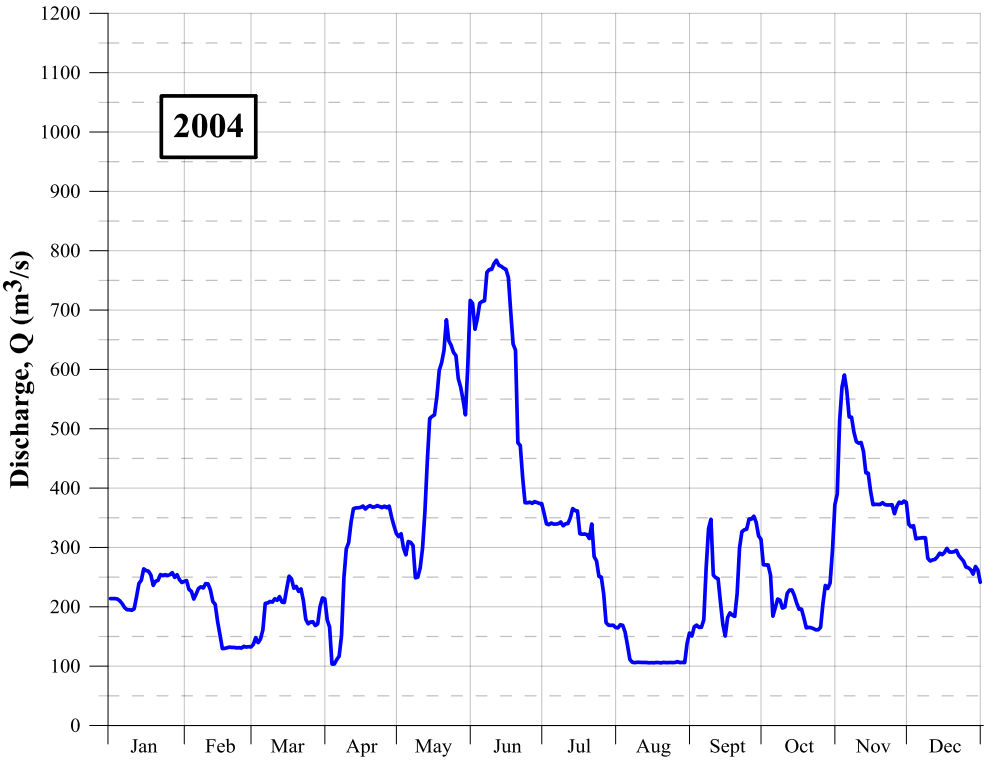

Figure A.12: 2004 Rainy River Hydrograph

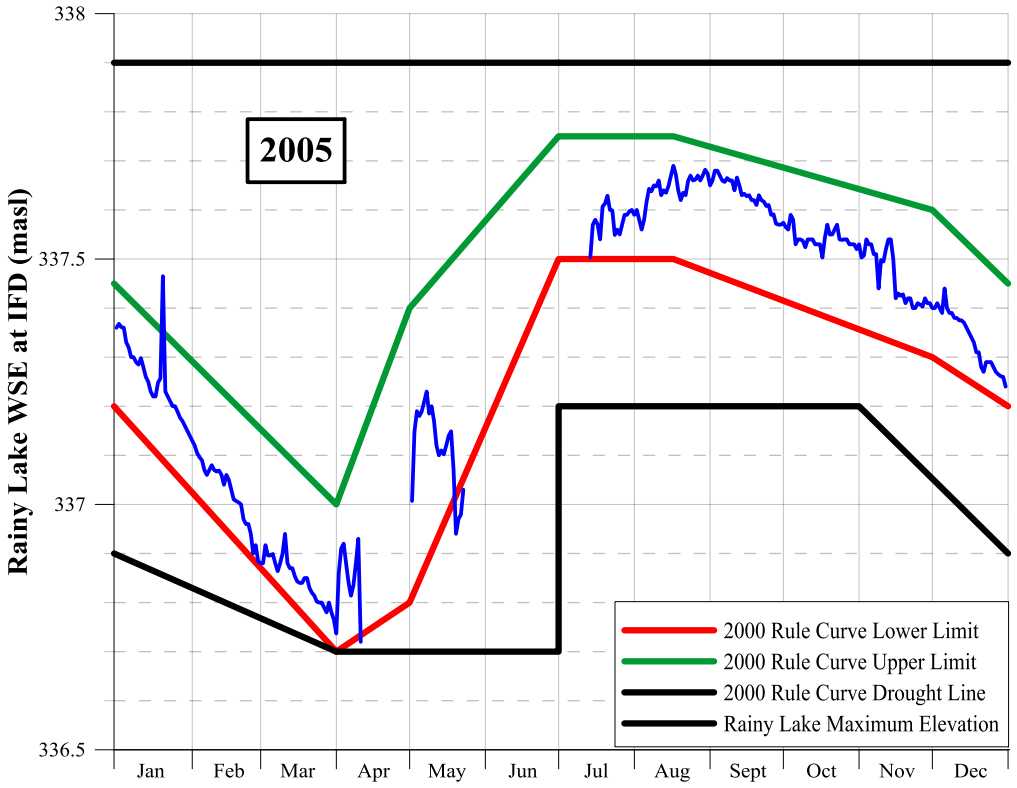

Figure A.13: 2005 Rainy Lake WSE at IFD and 2000 Rule Curve

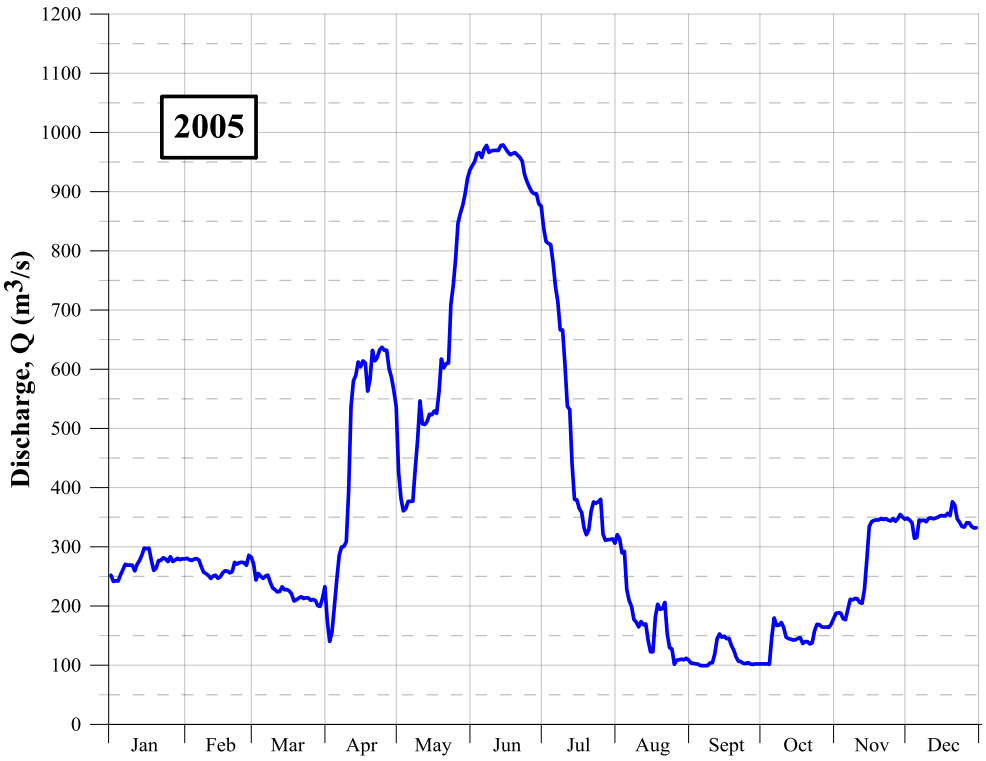

Figure A.14: 2005 Rainy River Hydrograph

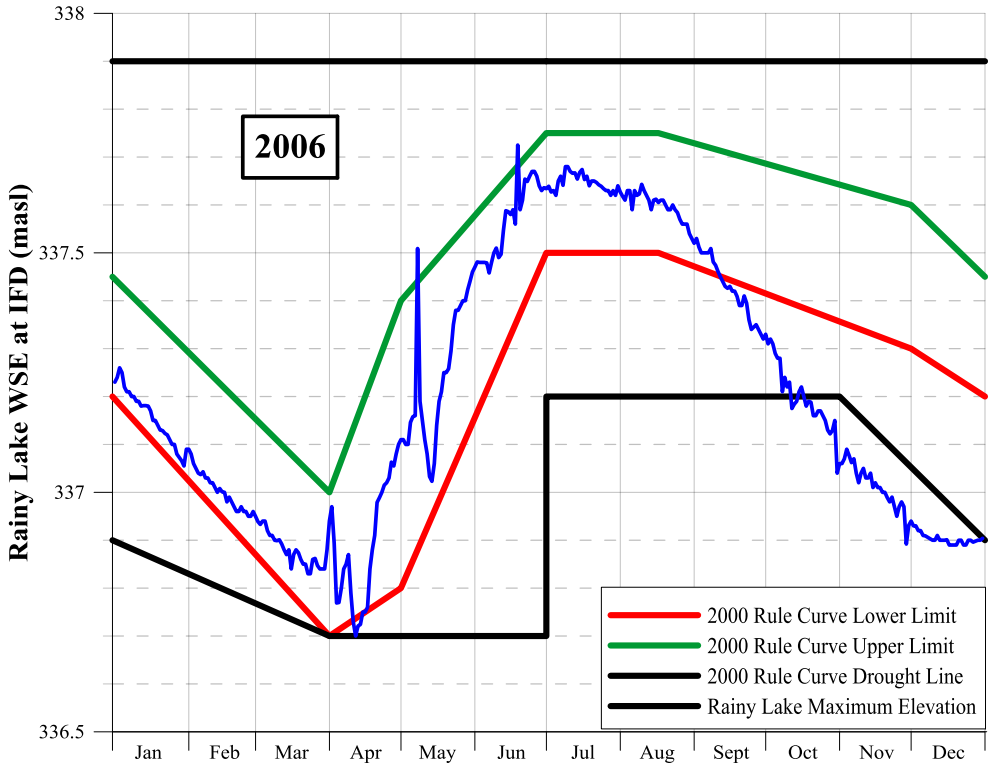

Figure A.15: 2006 Rainy Lake WSE at IFD and 2000 Rule Curve

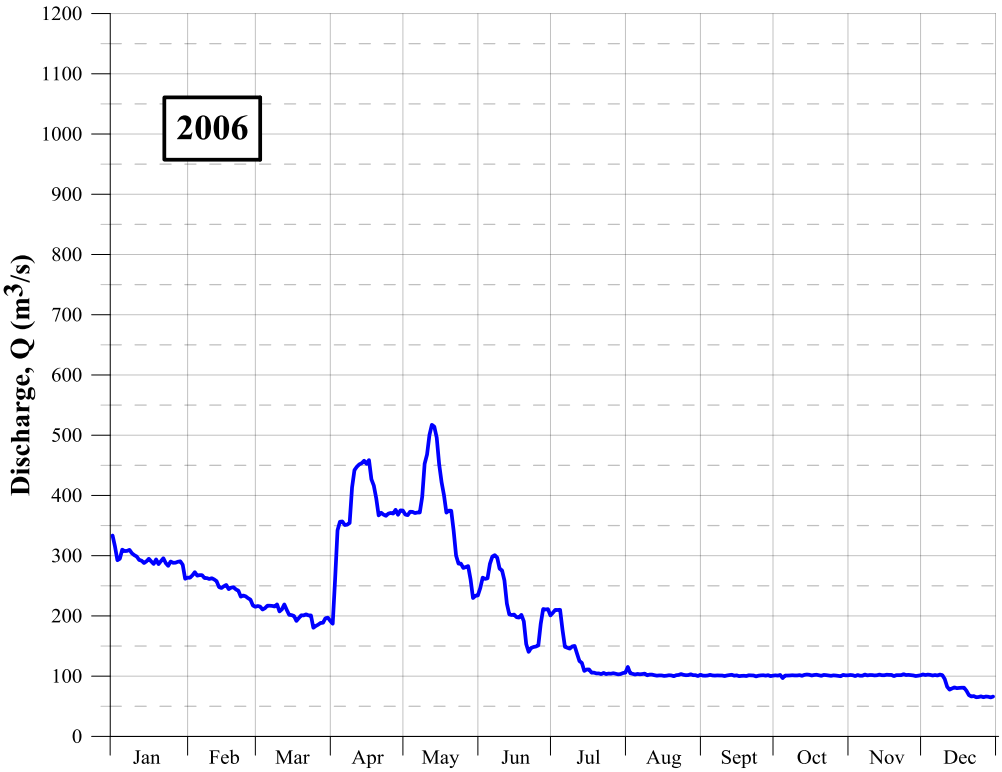

Figure A.16: 2006 Rainy River Hydrograph

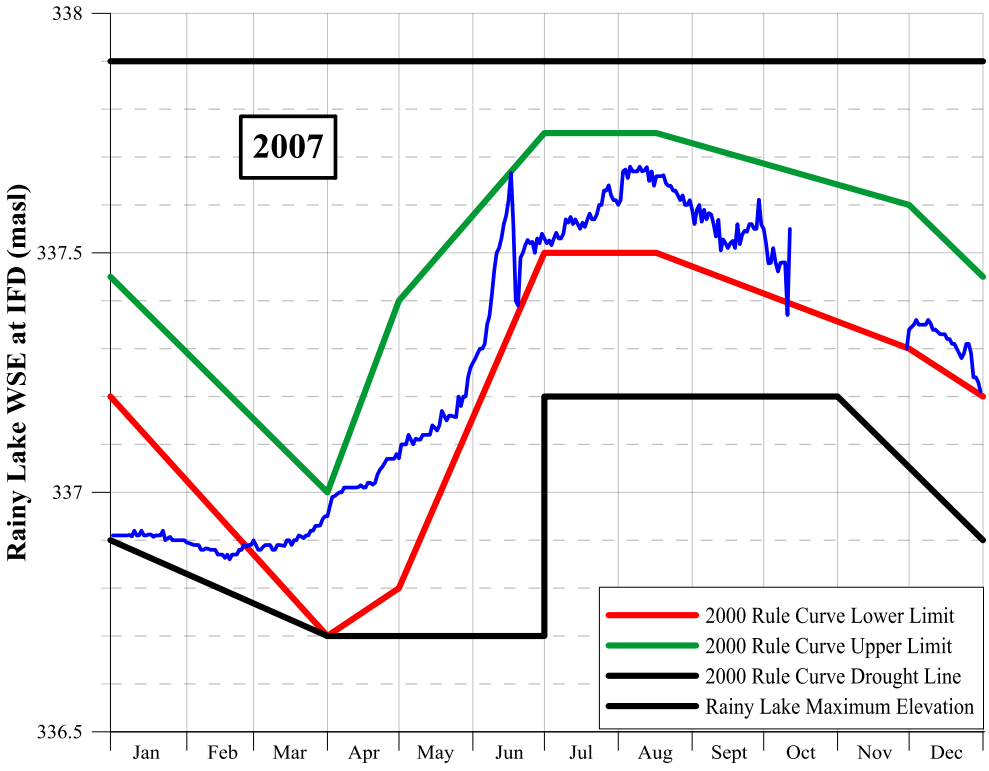

Figure A.17: 2007 Rainy Lake WSE at IFD and 2000 Rule Curve

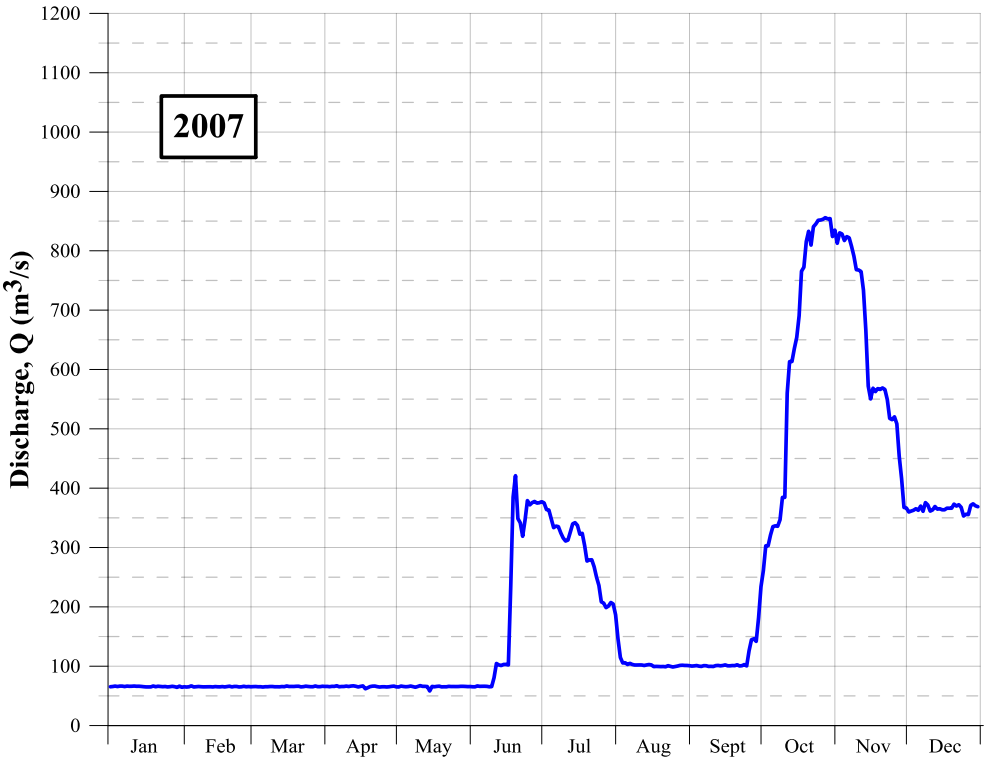

Figure A.18: 2007 Rainy River Hydrograph

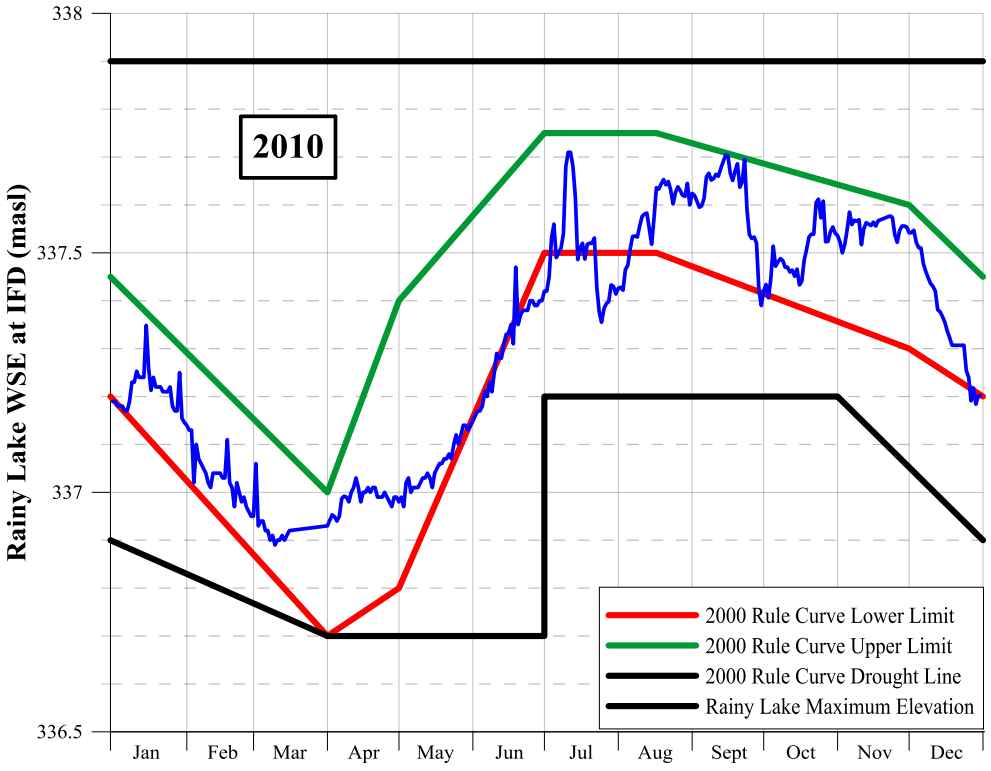

Figure A.19: 2010 Rainy Lake WSE at IFD and 2000 Rule Curve

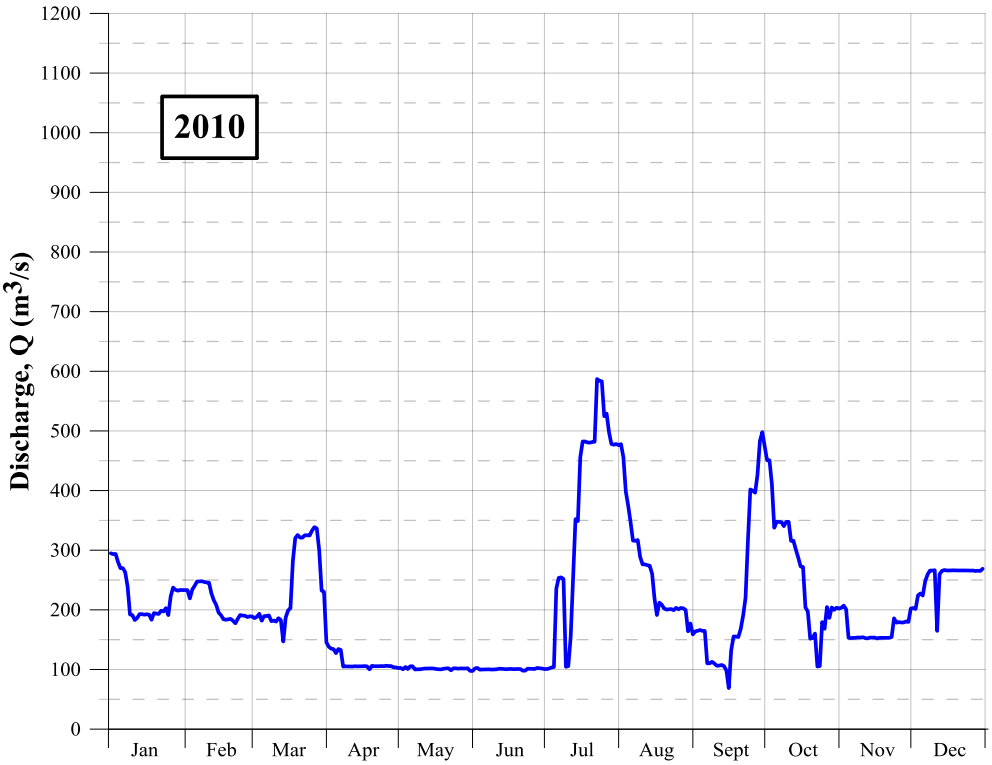

Figure A.20: 2010 Rainy River Hydrograph

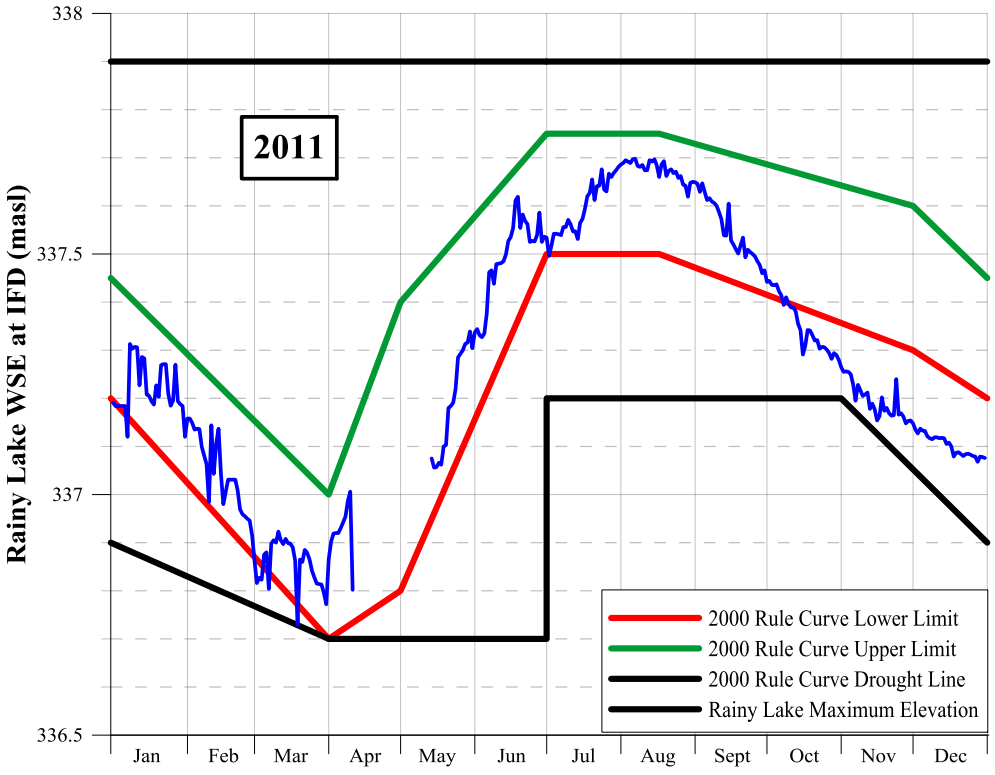

Figure A.21: 2011 Rainy Lake WSE at IFD and 2000 Rule Curve

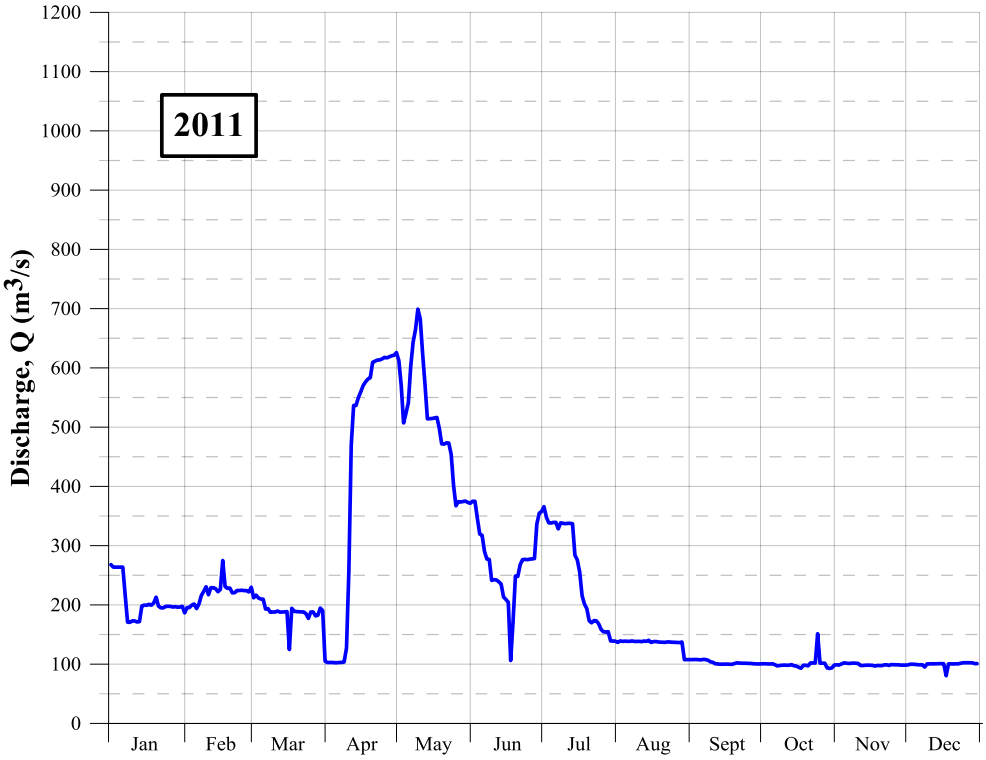

Figure A.22: 2011 Rainy River Hydrograph

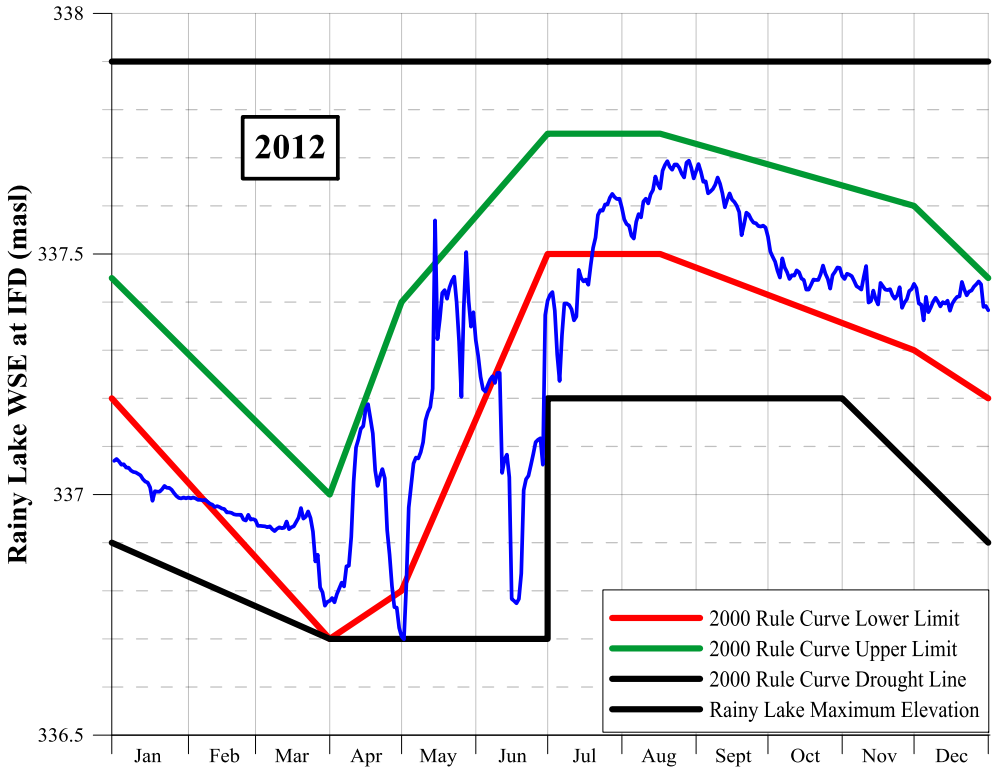

Figure A.23: 2012 Rainy Lake WSE at IFD and 2000 Rule Curve

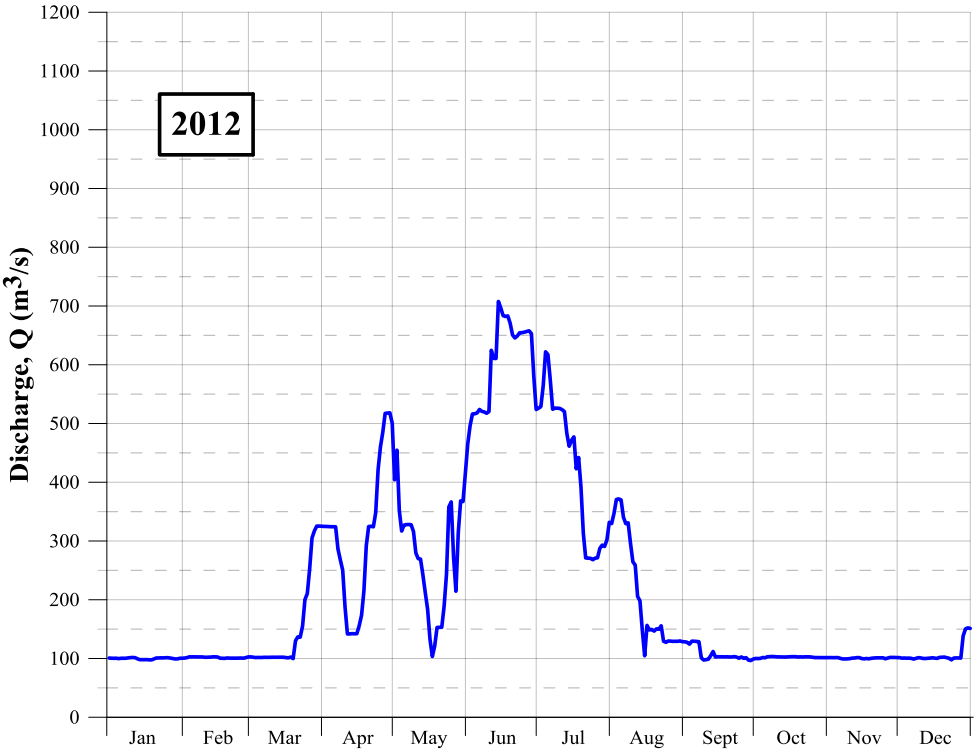

Figure A.24: 2012 Rainy River Hydrograph

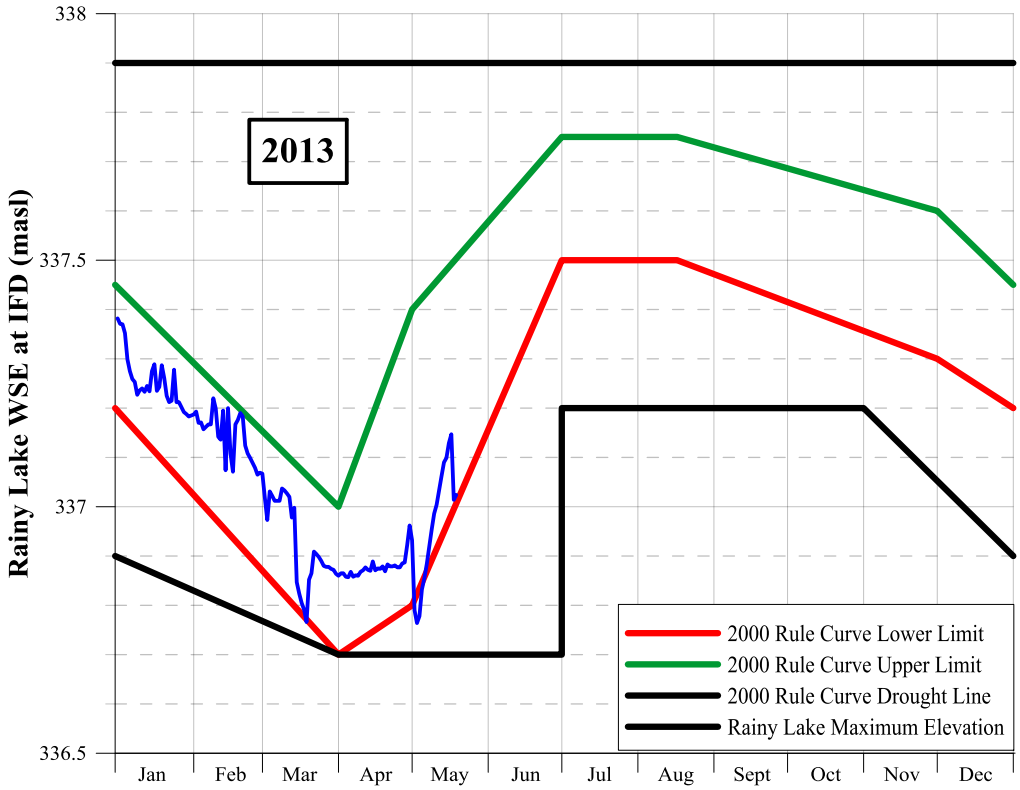

Figure A.25: 2013 Rainy Lake WSE at IFD and 2000 Rule Curve

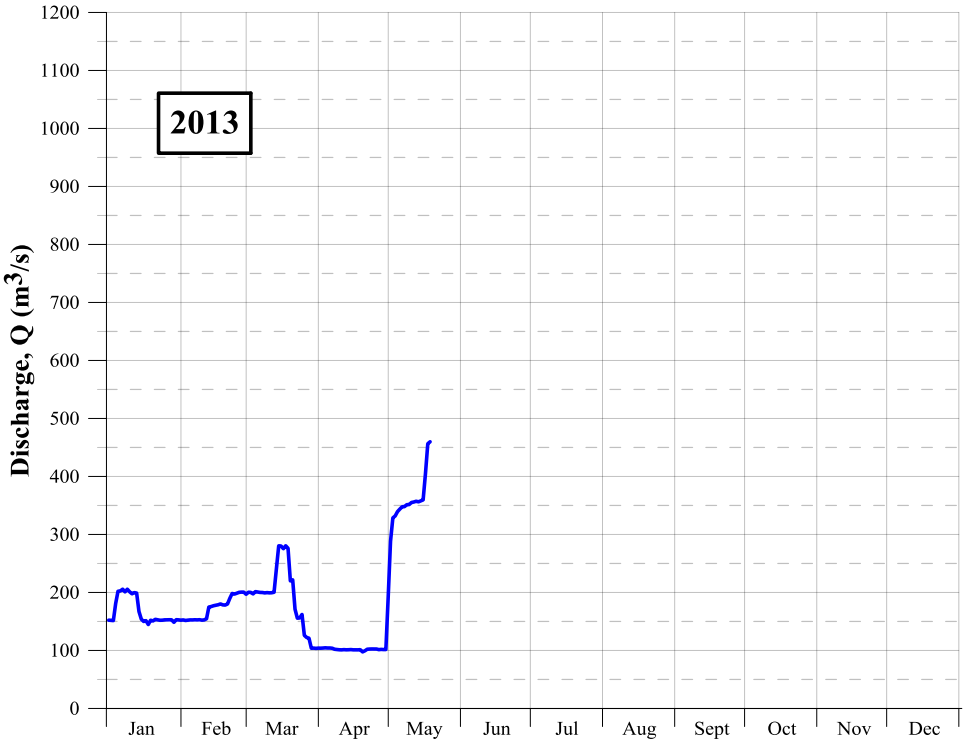

Figure A.26: 2013 Rainy River Hydrograph

Appendix B

Study Reach Water Temperature

B.1 Methodology

The three HOBO U20 Water Level loggers described in Appendix A obtained water temperature records at locations and time periods previously specified. Water temperature was also collected by the ADCP transducer during velocity profile surveying. The HOBO logger temperatures were obtained at the riverbed along river margins, whereas ADCP temperatures were obtained at the water's surface. Air temperature records were obtained from the Fort Frances Airport weather station. Analysis of study reach water temperatures addressed general temporal/seasonal patterns, inter-transect spatial mixing, and streamwise temperature trends.

B.2 Results

Figure B.1 illustrates water and air temperatures during October 2011 – October 2013.
Typical northwestern Ontario water temperature patterns are evident, generally following air temperature trends and consisting of low winter temperatures (1 – 2 ^{o}C) and warm summer temperatures (20 – 25 ^{o}C).

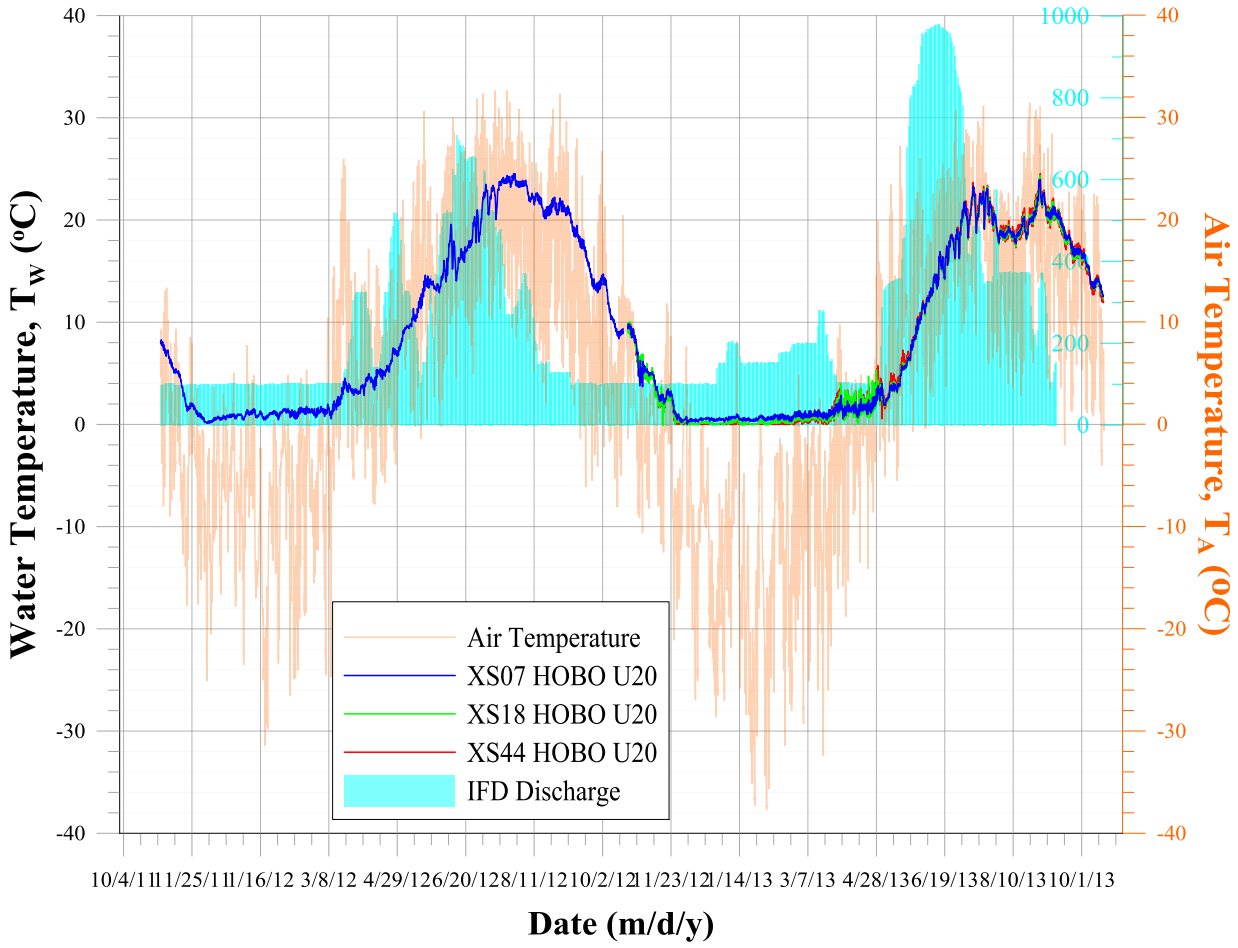

Figure B.1: Temporal Record of Water and Air Temperatures

Figure B.2 and Figure B.3 illustrate the temporal record of water and air temperatures over the 2012 and 2013 field seasons respectively, with water temperatures from HOBO loggers and ADCP surveys indicated. Water temperatures at the water surface (ADCP survey) were 0.64 °C greater on average than at the riverbed (HOBO loggers). Inspection of cross-transect water temperature patterns indicated greater temperatures typically present toward river margins corresponding to lower flow velocities and shallower depths.

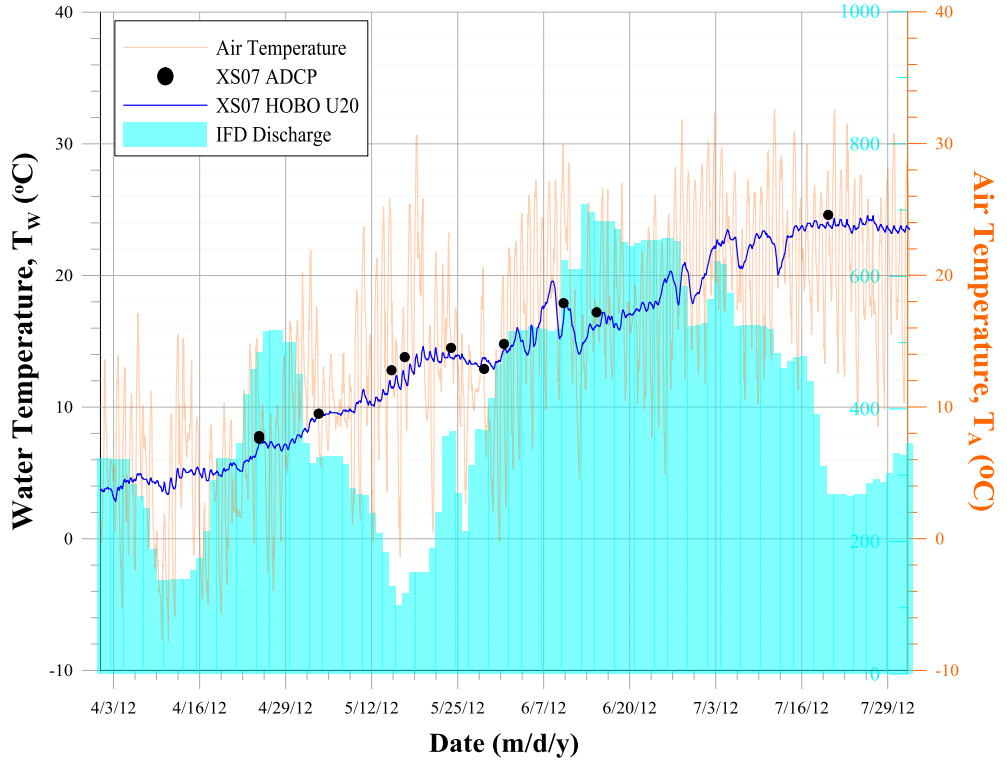

Figure B.2: Temporal Record of Water and Air Temperatures During 2012 Field Season

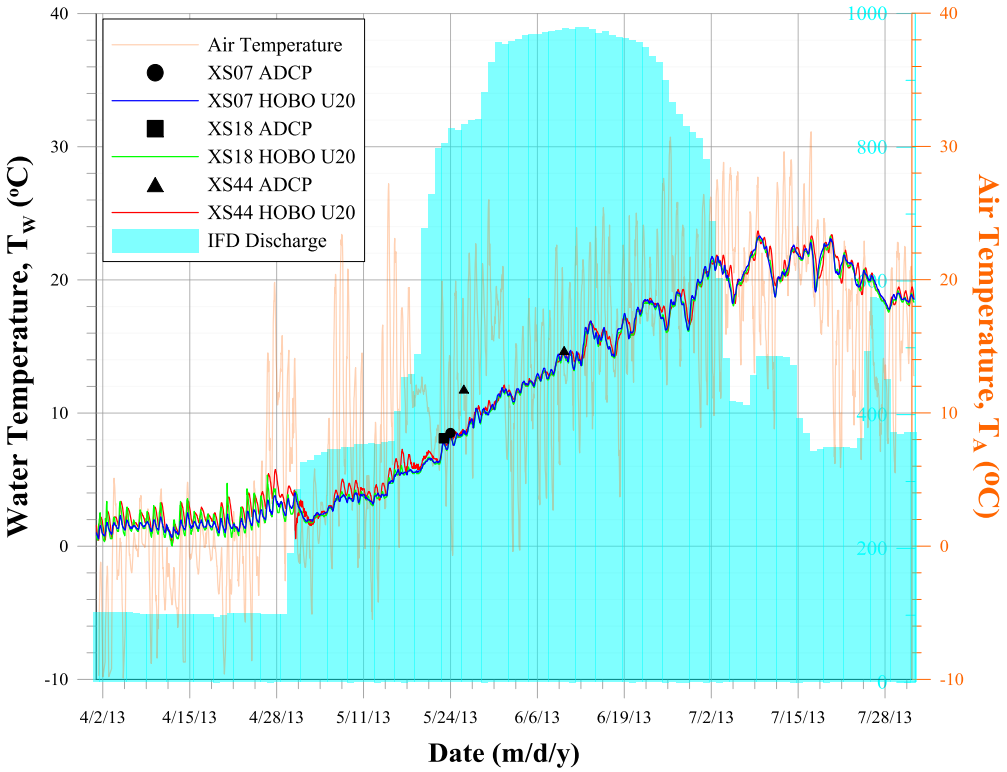

Figure B.3: Temporal Record of Water and Air Temperatures During 2013 Field Season

Figure B.4 illustrates four instances where water temperatures over the entire study reach were obtained within a 3 day period through ADCP survey, indicating patterns of longitudinal temperature change at a given point in time. Water temperatures did not exhibit substantial longitudinal change over the length of the study reach (maximum range of 3.7 ^{o}C), however spikes in water temperature were observed below confluence with the Littlefork River (~ 21 km downstream of the IFD) suggesting water in this unregulated major tributary is typically warmer than in the Rainy River.

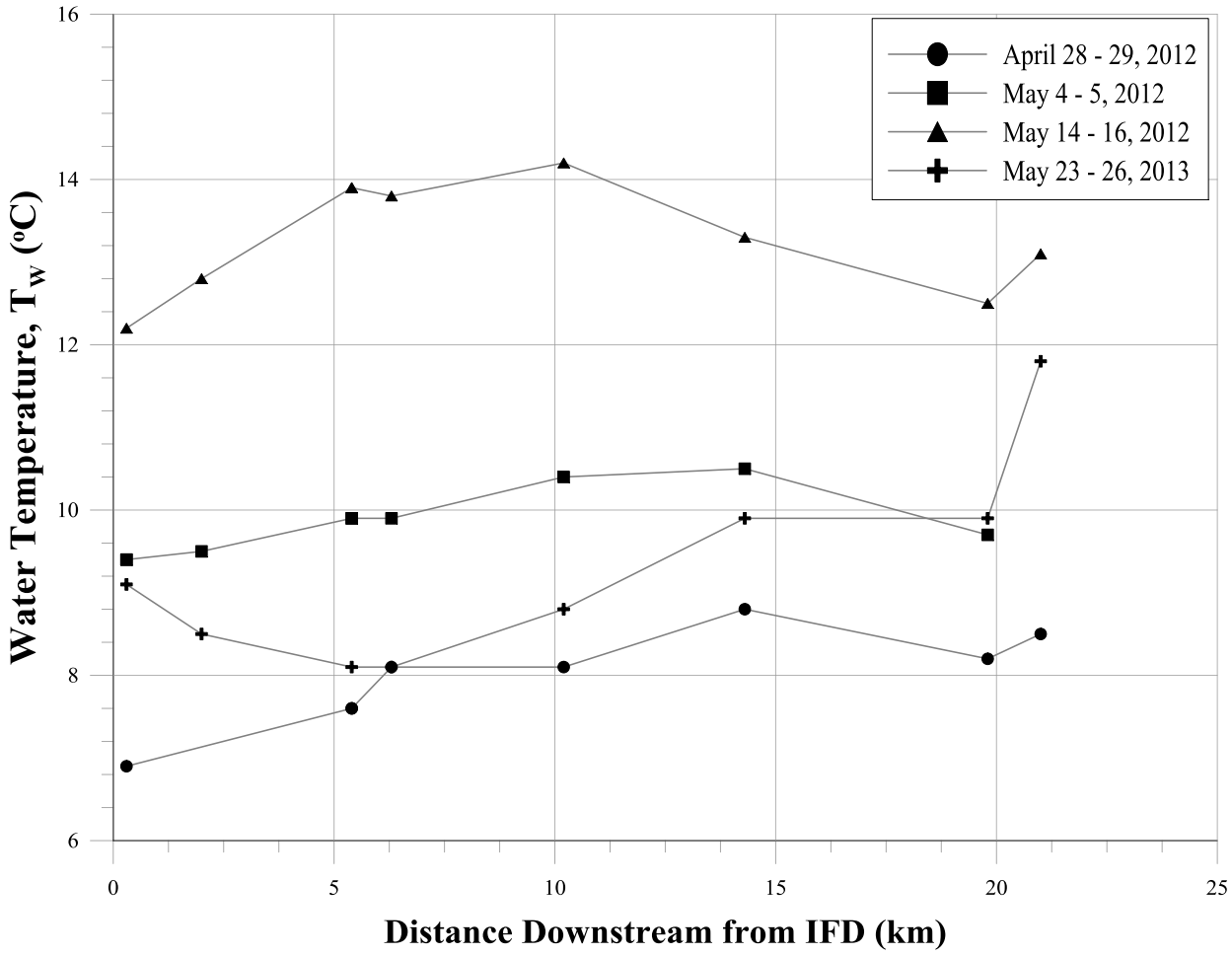

Figure B.4: Longitudinal Patterns of Water Temperature

Appendix C

Study Reach Substrate

C.1 Methods

Substrate survey consisted of delineation of zones of pavement layer sediment classes throughout the study reach. Analyses incorporating detailed sediment transport, fine-scale grain sizes, and characterization of sub-pavement sediment were not performed because a) the primary focus of this research is on the hydrodynamic impacts of dam discharges on fish spawning and nursery habitat (Kallemeyn et. al., 2009), b) detailed sediment transport analyses are not valid in the study reach as the IFD represents a longitudinal discontinuity in the system (Bunn and Arthington, 2002), c) temporally variable grain size distributions due to fluctuating flows and backwater effects made considering substrate samples at a fine quantitative scale inappropriate, and d) aquatic organisms interact primarily with pavement layer substrate.

Sediment sampling was performed during low flow conditions in October 2012 (WSE ~ 327 masl at XS07) with IFD discharges of approximately 100 m^3/s, allowing for sampling of the vast majority of littoral and shallow water areas deemed important for spawning and nursery habitat as identified in April – August 2012 and April – June 2013. Portions of the river inundated with water in October 2012 were not surveyed but were considered to be homogeneously composed of fines/sand and gravel based on preliminary Eckman and Ponar dredge substrate sampling attempts occurring in June 2012. Wetted portions of the river channel do not represent significant spawning or nursery habitat and thus, this generalist assumption is reasonable.

Sampling was performed at the right and left bank of each of the 47 standard cross sections in the study reach. The characteristics associated with the sampling location at each standard cross section was assumed to occur for a 10-15 m wide swath of riverbank and bounded by the points halfway to the upstream and downstream standard cross section sampling locations. Where features or areas between standard cross sections displayed sediment characteristics different from those at standard cross section sampling locations, intermediate sampling was performed and coordinates of extents/boundaries were noted for zone delineation during post processing.

A combination of qualitative and quantitative sampling methods was employed. Qualitative methods consisted of photographic documentation and detailed field notes. Detailed field notes were logged at each sampling site. Photographs of sediment were obtained using a 0.813 m x 0.610 m rectangle cutout (henceforth referred to as the "grid") with 0.35 m grid squares as a standard scaling reference. In an adapted method from Warrick et. al. (2009), photographs were taken at a consistent distance above

ground by ensuring the grid filled the entire photo window, thus guaranteeing photograph dimensions and scale were maintained throughout the sampling protocol. Where substrate was larger than grid dimensions, a stadia rod/tape measure was used as a scaling reference. Example grid and stadia rod photographs are provided in Figure C.1 and C.2.

Figure C.1: Example of a Grid Photograph

Figure C.2: Example of a Stadia Rod Photograph

Quantitative methods consisted of representative bulk samples (RBS) and pebble counts (PB). RBS's consisted of a representative collection of pavement layer sediment at the sampling location of interest. While exact location and quantity of sample was somewhat subjective, the best efforts were made to obtain equal portions of sediment over the extent of exposed area in an unbiased manner. Pebble counts

(PC's) were conducted over the sampling location of interest in accordance with methods of Leopold (1970) and Wolman (1954).

Sampling methods at each sampling location depended on the sediment characteristics present. As an example, Kellerhals and Bray (1971) and Adams (1979) identify sample sizes needed for statistically relevant sieve analysis of cobble and boulder areas could require RBS masses of hundreds of kilograms, making it implausible in certain situations (Warrick et. al 2009). Although alternative methods such as pebble counts described by Wolman (1954) and Leopold (1970) may be more suitable to characterizing larger grain sizes, these may still require significant time commitments for field surveys (Warrick et. al. 2009). Extracting substrate information from photographs represents a viable alternative given the scale and objectives of substrate survey in this study; early attempts by Kellerhals and Bray (1971) and Adams (1979) demonstrated comparable estimation of mean grain sizes from photograph and sieving, and more recently developed digital image processing methods involving directly measured individual particles (Buscombe and Masselink, 2009; Graham et al. 2005a, 2005b; Sime and Ferguson 2003; Butler et. al. 2001; Ibbeken and Schleyer 1986) or field calibrated grain size estimates based on photograph texture (Warrick et. al. 2009; Buscombe 2008; Verdu et. al. 2005; Carbonneau et. al 2004; Rubin 2004). In this study, macro-scale substrate characterization objectives are at a greater or equal scale to photographic method capabilities, therefore validating its application (Warrick et. al. 2009; Church et. al 1987; Kellerhals and Bray 1971) in an adapted framework using the grid photographs.

Qualitative characterization was performed at every sampling location: grid photographs were taken at every sampling location with particle sizes smaller than grid dimensions, with measurements and photographs using a stadia rod and/or tape measure as a scaling reference obtained where particle sizes were larger than grid dimensions. Quantitative measurements (RBS and PC) were obtained at regular intervals throughout the study reach (at least every 3 cross sections), as well as at locations where significant variation in substrate characteristics were noted. RBS's were obtained where sediment consisted of predominantly fines and gravels. PC's were performed where particle sizes were large enough that the manual measuring of particles involved with this method was appropriate. All RBS's and PC's were accompanied by a qualitative method (either grid or stadia rod/tape measure photo) such that quantitative results could be related to a visual representation of substrate available at each sampling location.

Grain size distributions for RBS's were obtained through the drying and mechanical sieving dried and mechanically sieved through a set of US Standard sieves (sizes provided in Table C.1) providing grain

size distributions. PC samples provided grain size distributions following methods of Bundte and Abt (2001). Substrate was categorized into classes based on functionally different particle diameter ranges (in an ecological sense) as specified in Table C.2. This approach is not uncommon in ecological frameworks; physical habitat models (PHM's) such as PHABSIM and associated Instream Flow Incremental Methodologies (IFIM's) consider sediment characteristics in discrete categories (Milhous et. al. 1989), and past studies on the study reach (O'Shea 2005) consider Habitat Suitability Criteria (HSC) (Aadland and Kuitunen, 2006) specifying habitat substrate in 9 separate groupings (detritus, silt, sand, gravel, cobble, rubble, small boulder, large boulder, and bedrock). Examples of photographs for each of the substrate categories are included in Figure C.3 through C.10.

Table C.1: US Standard Sieves

Sieve Size (mm)	Sieve No.	Sieve Size (mm)	Sieve No.
N/A	63	14	1.4
N/A	45	18	1
N/A	31.5	25	0.71
N/A	22.4	35	0.5
N/A	16	45	0.355
N/A	11.2	60	0.25
N/A	8	80	0.18
N/A	6.3	120	0.125
5	4	170	0.09
7	2.8	230	0.063
10	2	Pan	-

Table C.2: Substrate Classification Categories

Substrate Category	Code
Fines/Sand	FS
Predominantly Fines/Sand, with Gravel	FS-G
Predominantly Fines/Sand, with Cobbles/Boulders	FS-CB
Predominantly Gravel, with Fines/Sand	G-FS
Gravel	G

Predominantly Gravel, with Cobbles/Boulders	G-CB
Cobbles/Boulders	CB
Bedrock with Cobbles/Boulders	B-CB
Bedrock	B

Figure C.3: Example Grid Photograph – Fines/Sand (FS)

Figure C.4: Example Grid Photograph – Predominantly Fines/Sand, with Gravel (FS-G)

Figure C.5: Example Stadia Rod Photograph – Predominantly Fines/Sand, with Cobbles/Boulders (FS-CB)

Figure C.6: Example Grid Photograph – Predominantly Gravel, with Fines/Sand (G-FS)

Figure C.7: Example Grid Photograph – Predominantly Gravel, with Cobbles/Boulders (G-CB)

Figure C.8: Example Stadia Rod Photograph – Cobbles/Boulders (CB)

Figure C.9: Example Photograph – Bedrock with Cobbles/Boulders (B-CB)

Figure C.10: Example Photograph – Bedrock (B)

A numerically based protocol for quantitative sample classification was adapted from the Unified Soil Classification System as outlined in Das (2005), and is illustrated in Figure C.11 (considers fines/sand diameter < 2 mm, gravel diameter 2 – 64 mm, cobbles/boulders diameter > 64 mm). Comparison of grid and stadia rod photographs to corresponding substrate characterizations resulting from quantitative samples. Figure C.3 through Figure C.11 provided reference for the categorization of locations lacking quantitative samples. Substrate zones were delineated using the coordinates obtained during field survey.

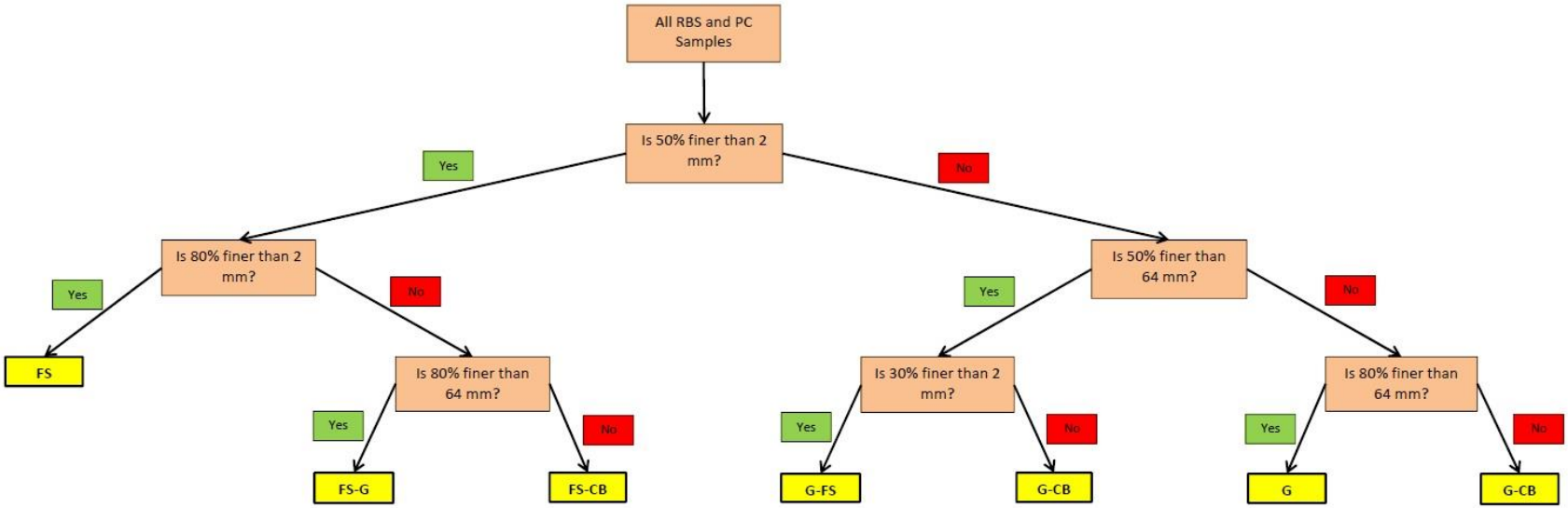

Figure C.11: Numerical Classification Protocol

C.2 Results

A total of 149 locations (with 29 RBS's and 20 PC's) were sampled throughout the study reach. Particle size distribution curves for RBS and PC samples with corresponding substrate categorizations are observed in Figure C.12. Sampling locations with corresponding sampling methods and substrate classifications are available in tabular format upon request. GIS shapefiles of substrate classification zones are available upon request. The vast majority of the study reach is characterized by either FS-G or another variant involving fines, sands, and gravels. Sporadic outcroppings of bedrock with cobbles or boulders are evident, specifically in the upper 7 km of the study reach.

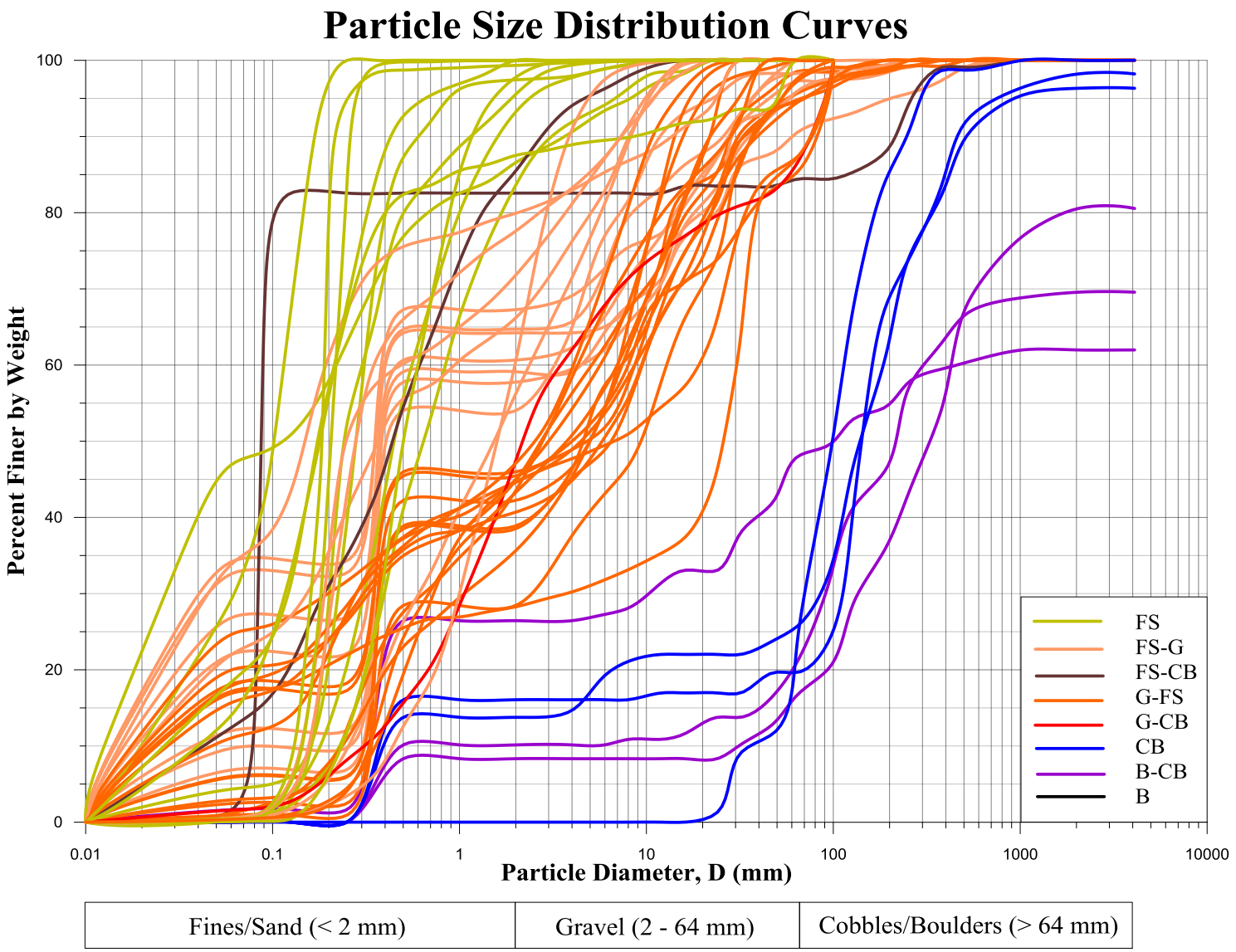

Figure C.12: Particle Size Distributions

Appendix D

Study Reach Bathymetry

D.1 Methods

Bathymetry maps of the study reach may prove to be of use in a) navigating the river, b) understanding flow and hydrodynamic patterns on a general scale, and c) eventual creation and calibration of a 2-D or 3-D integrative hydraulic/biological model (beyond the scope of this project). The SonTek M9 ADCP, Sokkia GRX1, and a Digital Elevation Model (DEM) were used to obtain necessary geospatial data.

Horizontally coordinate water depths acquired from the SonTek M9 ADCP were corrected using Sokkia GRX1 surveyed WSE providing a set of georeferenced riverbed elevations for wetted portions of the study reach. ADCP bathymetry survey coverage of the study reach consisted of 4 longitudinal traverses (close proximity to right and left banks, ¼ channel width from right and left banks) as well as zig-zag traverses (wavelength approximately 150-200 m) throughout. Where WSE dropped within a traverse, the riverbed corrections were made at Sokkia surveyed WSE intervals of 0.01 m. Increased survey resolution was acquired where channel features were complex or rapidly changing. The described degree of coverage was sufficient to create a set of smooth and accurate elevation contours.

The Sokkia GRX-1 acquired georectified elevations over the somewhat irregular bathymetry patterns of key river features emergent during low flow (islands, rock shoals, etc.). The high resolution of survey data over these hydraulically and biologically important features increased the accuracy of their bathymetric representation.

Spot elevations were extracted from a cross-boundary, fully merged DEM (created from a variety of DEM's provided by Canadian and American agencies in a 50 m by 50 m grid, for a buffer of approximately 250 m on either side of the river. While less accurate that the aforementioned survey elevation methods, the DEM spot elevations provided sufficient accuracy to characterize bank and above-river topography.

Golden Software Surfer 8 performed the topographical interpolation using the Kriging method, providing a .grd file as well as bathymetric contours at a 0.5 m interval. Due to the large number of data points and long, sinuous nature of the study reach, the study reach was partitioned into 14 sections and interpolation/contour formation performed for each. Upon completion, contours were exported to ArcMap where the sections were merged together creating a single continuous bathymetry map.

D.1 Results

A total of 29 829 georeferenced elevations were compiled over the course of the 2012-2013 field seasons using the SonTek M9 RiverSurveyor (n = 23 497), the Sokkia GRX1 (n = 2024), and DEM spot elevations (n = 4308). The full compilation of georeferenced elevations as well as bathymetry contour shapefiles are available upon request.